Intercomparison of global ground-level ozone datasets for health-relevant metrics

Hantao Wang[1], Kazuyuki Miyazaki[2], Haitong Zhe Sun[3], Zhen Qu[4], Xiang Liu[5], Antje Inness[6], Martin Schultz[7], Sabine Schröder[7], Marc Serre[1], J. Jason West[1]

[1]Department of Environmental Sciences and Engineering, University of North Carolina at Chapel Hill, Chapel Hill, 27599, USA
[2]Jet Propulsion Laboratory, California Institute of Technology, Pasadena, 91125, USA
[3]Department of Paediatrics, National University of Singapore, Singapore,117549, SG
[4]Department of Marine, Earth and Atmospheric Sciences, North Carolina State University, Raleigh, 27606, USA
[5]Department of Earth and Planetary Sciences, Harvard University, Cambridge, Massachusetts, 02138, USA
[6]ECMWF, Shinfield Park, Reading, RG2 9AX, UK
[7]Jülich Supercomputing Centre, Forschungszentrum Jülich, Jülich, 52428, Germany

Correspondence to: J. Jason West (jasonwest@unc.edu)

SUPPLEMENTARY INFORMATION

Text S1. Grouping method used in pairwise spatial similarity comparison

The Grouping method is based on the pairwise correlation between each dataset. Initially, all datasets are re-gridded to a resolution of 0.1° by 0.1°. Subsequently, the pairwise correlation coefficient (R) is computed for each pair of datasets spanning the period from 2006 to 2016. The mean pairwise correlation for each grouping over the same timeframe is then calculated to construct Figure 5(a). Then, we generate a random groups table. For this comparison, involving 6 datasets, there are 203 possible combinations for grouping. For each grouping combination, 4 variables are computed: the sum of pairwise correlations within groups (C_i), the sum of pairwise correlations outside the groups (C_o), the number of dataset pairs within groups (N_i), and the number of dataset pairs outside the groups (N_o). The objective is to ascertain the grouping combination that maximizes the difference between $\frac{Ci}{Ni}$ and $\frac{Co}{No}$.

For example, consider a grouping scenario where:
Group A: BME, NJML, UKML
Group B: CAMS, GEOS, TCR-2.

"pwcorr" denotes the operation to compute the pairwise correlation between two datasets. The calculations proceed as follows:
C_i = pwcorr(BME, NJML)+ pwcorr(BME, UKML)+ pwcorr(NJML, UKML)+ pwcorr(CAMS, GEOS)+ pwcorr(CAMS, TCR-2)+ pwcorr(TCR-2, GEOS)
C_o = pwcorr(BME, GEOS)+ pwcorr(BME, TCR-2)+ pwcorr(BME, CAMS)+ pwcorr(NJML, GEOS)+ pwcorr(NJML, TCR-2)+ pwcorr(NJML, CAMS)+ pwcorr(UKML, GEOS)+ pwcorr(UKML, TCR-2)+ pwcorr(UKML, CAMS)
$N_i = 6$
$N_o = 9$
Difference = $\frac{Ci}{Ni} - \frac{Co}{No}$

This analysis is conducted for all 203 combinations, identifying the optimal grouping that maximizes the difference.
Group A: BME, UKML, CAMS, GEOS, TCR-2
Group B: NJML

We also use the hierarchical clustering method to group 6 datasets based on pairwise correlation (R) and get the same result. The hierarchical clustering is typically used with a dissimilarity (distance) matrix, where the elements represent the distances or dissimilarities between data (Bishop, 2006).

Table S1. Inputs to the BME dataset include nine chemistry models and observations from TOAR-I and CNEMC. Table based on DeLang et al. (2021)

Model/Observation	Years	Resolution	Experiment	Reference
TOAR-I	1990-2017	7269 monitoring stations	Tropospheric Ozone Assessment Report	(Schultz et al., 2017)
CNEMC	2014-2017	1565 monitoring stations	the Chinese National Environmental Monitoring Center Network	(Lu et al., 2018)
CESM1 CAM4-CHEM	1990-2010	1.9° × 2.5°	CCMI REF-C1SD	(Tilmes et al., 2015)
CESMI WACCM	1990-2010	1.9° × 2.5°	CCMI REF-C1SD	(Marsh et al., 2013; Garcia et al., 2017)
CHASER	1990-2010	2.8° × 2.8°	CCMI REF-C1SD	(Sudo et al., 2002; Watanabe et al., 2011)
GFDL AM3	1990-2014	2° × 2.5°	CCMI REF-C1SD	(Lin et al., 2017)
GFDL AM4	2010-2016	1° × 1.25°	CMIP6 nudged to NCEP wind	(Zhang et al., 2020; Horowitz et al., 2020)
MERRA2-GMI	1990-2017	0.5° × 0.625°	MACCity and GFED-4s emissions	(Ziemke et al., 2019; Strode et al., 2019)
MOCAGE	1990-2016	2° × 2°	CCMI REF-C1SD	(Josse et al., 2004; Teyssèdre et al., 2007)
MRI-ESM1r1	1990-2010	2.8° × 2.8°	CCMI REF-C1SD	(Adachi et al., 2013)
MRI-ESM2.0	2011-2017	2.8° × 2.8°	CMIP6 historical and ssp370	(Yukimoto et al., 2019c)

Table S2. Inputs to the NJML dataset include meteorology terms, chemical models, landcover and satellite observations. Ground observation from TOAR-I (2003–2019) are used as labels for training. Table based on Liu et al. (2022)

Variable	Years	Resolution	Source	Reference
10m wind speed	2003-2019	30 km/0.25 °	ERA5	(Hersbach et al., 2020)
2m temperature	2003-2019	30 km/0.25 °	ERA5	
Boundary layer height	2003-2019	30 km/0.25 °	ERA5	
Forecast surface roughness	2003-2019	30 km/0.25 °	ERA5	
Mean sea level pressure	2003-2019	30 km/0.25 °	ERA5	
Mean surface downward short-wave radiation flux	2003-2019	30 km/0.25 °	ERA5	
Mean surface downward UV radiation flux	2003-2019	30 km/0.25 °	ERA5	
Total precipitation	2003-2019	30 km/0.25 °	ERA5	
Soil temperature level 1	2003-2019	30 km/0.25 °	ERA5	
Surface latent heat flux	2003-2019	30 km/0.25 °	ERA5	
Surface sensible heat flux	2003-2019	30 km/0.25 °	ERA5	
Total cloud cover	2003-2019	30 km/0.25 °	ERA5	
Total column ozone	2003-2019	30 km/0.25 °	ERA5	
Forecast albedo	2003-2019	30 km/0.25 °	ERA5	
Evaporation	2003-2019	30 km/0.25 °	ERA5	
2m dewpoint temperature	2003-2019	30 km/0.25 °	ERA5	
Volumetric soil water layer 1	2003-2019	30 km/0.25 °	ERA5	
2m temperature one month lag	2003-2019	30 km/0.25 °	ERA5	
2m dewpoint temperature one month lag	2003-2019	30 km/0.25 °	ERA5	
Total precipitation one month lag	2003-2019	30 km/0.25 °	ERA5	
Mean sea level pressure one month lag	2003-2019	30 km/0.25 °	ERA5	
Total aerosol optical depth at 550 nm	2003-2019	80 km/0.75 °	CAMS	(Inness et al., 2019)
Total column hydroxyl radical	2003-2019	80 km/0.75 °	CAMS	
Total column methane	2003-2019	80 km/0.75 °	CAMS	
Total column nitrogen dioxide	2003-2019	80 km/0.75 °	CAMS	
Total column ozone/GEMS Total column ozone	2003-2019	80 km/0.75 °	CAMS	
Particulate matter d < 2.5 µm (PM2.5)	2003-2019	80 km/0.75 °	CAMS	
Total column carbon monoxide	2003-2019	80 km/0.75 °	CAMS	
Total column formaldehyde	2003-2019	80 km/0.75 °	CAMS	
Total column nitrogen monoxide	2003-2019	80 km/0.75 °	CAMS	
Carbon monoxide	2003-2019	80 km/0.75 °	CAMS	
Dust aerosol (0.55 - 0.9 µm) mixing ratio	2003-2019	80 km/0.75 °	CAMS	
Dust aerosol (0.03 - 0.55 µm) mixing ratio	2003-2019	80 km/0.75 °	CAMS	
Dust aerosol (0.9 - 20 µm) mixing ratio	2003-2019	80 km/0.75 °	CAMS	
Hydrophilic organic matter aerosol mixing ratio	2003-2019	80 km/0.75 °	CAMS	
Hydrophobic organic matter aerosol mixing ratio	2003-2019	80 km/0.75 °	CAMS	

Nitrogen monoxide	2003-2019	80 km/0.75 °	CAMS	
SO2 precursor mixing ratio	2003-2019	80 km/0.75 °	CAMS	
Sea salt aerosol (0.5 - 5 μm) mixing ratio	2003-2019	80 km/0.75 °	CAMS	
Sulphur dioxide	2003-2019	80 km/0.75 °	CAMS	
Formaldehyde	2003-2019	80 km/0.75 °	CAMS	
Hydrophilic black carbon aerosol mixing ratio	2003-2019	80 km/0.75 °	CAMS	
Hydrophobic black carbon aerosol mixing ratio	2003-2019	80 km/0.75 °	CAMS	
Hydroxyl radical	2003-2019	80 km/0.75 °	CAMS	
Methane (chemistry)	2003-2019	80 km/0.75 °	CAMS	
Nitrogen dioxide	2003-2019	80 km/0.75 °	CAMS	
Ozone/GEMS Ozone	2003-2019	80 km/0.75 °	CAMS	
Sea salt aerosol (0.03 - 0.5 μm) mixing ratio	2003-2019	80 km/0.75 °	CAMS	
Sea salt aerosol (5 - 20 μm) mixing ratio	2003-2019	80 km/0.75 °	CAMS	
Sulphate aerosol mixing ratio	2003-2019	80 km/0.75 °	CAMS	
Black Carbon Surface Mass Concentration	2003-2019	0.5 °×0.625 °	MERRA2	Global Modeling and Assimilation Office (GMAO) (2015)
Dust Surface Mass Concentration	2003-2019	0.5 °×0.625 °	MERRA2	
Organic Carbon Surface Mass Concentration	2003-2019	0.5 °×0.625 °	MERRA2	
Sea Salt Surface Mass Concentration	2003-2019	0.5 °×0.625 °	MERRA2	
SO4 Surface Mass Concentration	2003-2019	0.5 °×0.625 °	MERRA2	
SO2 Surface Mass Concentration	2003-2019	0.5 °×0.625 °	MERRA2	
Total Aerosol Extinction AOT [550 nm]	2003-2019	0.5 °×0.625 °	MERRA2	
CO Column Burden	2003-2019	0.5 °×0.625 °	MERRA2	
CO Surface Concentration in ppbv	2003-2019	0.5 °×0.625 °	MERRA2	
total_column_ozone	2003-2019	0.5 °×0.625 °	MERRA2	
Nitrogen dioxide	2003-2019	0.9 °×1.25 °	CAM_CHEM	Atmospheric Chemistry Observations & Modeling, National Center for Atmospheric Research, University Corporation for Atmospheric Research (2020)
Ozone	2003-2019	0.9 °×1.25 °	CAM_CHEM	
Nitrogen monoxide	2003-2019	0.9 °×1.25 °	CAM_CHEM	
Population	2003-2019	1 km	Worldpop	(Lloyd et al., 2019)
Elevation mean	2003-2019	1 arc-minute	NOAA/NGDC/ETOPO1	(Amante and Eakins, 2009)
Elevation sd	2003-2019	1 arc-minute	NOAA/NGDC/ETOPO1	
Water percentage	2003-2019	0.05 °	MODIS	(Friedl, 2015)
Shrublands percentage	2003-2019	0.05 °	MODIS	

Savannas percentage	2003-2019	0.05 °	MODIS	
Non Vegetated percentage	2003-2019	0.05 °	MODIS	
Grasslands percentage	2003-2019	0.05 °	MODIS	
Croplands percentage	2003-2019	0.05 °	MODIS	
Forests percentage	2003-2019	0.05 °	MODIS	
Urban percentage	2003-2019	0.05 °	MODIS	
Dark Target and Deep Blue AOD @ 0.55 micron	2003-2019	1 °	CERES	(Doelling et al., 2016)
Tropospheric vertical column densities (VCDs) of NO2	2004-2019	0.25 °	OMI/Aura	(Krotkov et al., 2017)
tropospheric ozone	2004-2019	1 °	OMI/Aura	
Total ozone column	2003-2019	1.25 °×1 °	TCO	(Greg E. Bodeker, 2022)
Total ozone column uncertainty	2003-2019	1.25 °×1 °	TCO	
Leaf area index	2003-2019	0.5 °	MODIS	(Lin et al., 2023)
bc emission	2003-2019	0.5 °	CEDS	DOI：10.5281/zenodo.3592072
nox emission	2003-2019	0.5 °	CEDS	
co emission	2003-2019	0.5 °	CEDS	
nmvoc emission	2003-2019	0.5 °	CEDS	
ch4 emission	2003-2019	0.5 °	CEDS	
so2 emission	2003-2019	0.5 °	CEDS	
oc emission	2003-2019	0.5 °	CEDS	

Table S3. Inputs to the UKML dataset include multiple CMIP6 Chemistry−Climate Models. In situ observations from TOAR-I (1990−2014) and CNEMC (2015−2019) are used as labels for supervised learning. Table based on Sun et al. (2022)

Model[a]	Grids[b]	Hist[c]	Ssp245[d]	Reference
BCC-ESM1	128×64	3		(Wu et al., 2020; Zhang et al., 2018)
MPI-ESM1.2-HAM	192×96	3		(Neubauer et al., 2019)
MPI-ESM1.2-HR	384×192	19	3	(Von Storch et al., 2017; Gutjahr et al., 2019; Schupfner et al., 2019)
UKESM1-0-LL	192×144	3		(Tang et al., 2019; Good et al., 2019; Yool et al., 2020; Sellar et al., 2020; Sellar et al., 2019; Mulcahy et al., 2018; Archibald et al., 2020)
MRI-ESM2.0	128×64	5	5	(Yukimoto et al., 2019a; Yukimoto et al., 2012; Yukimoto et al., 2019b)
NASA-GISS-E2.1-G	144×90	19	20	(Studies, 2018b, a, 2020; Shindell et al., 2013)
NASA-GISS-E2.1-H	144×90	10		
NCAR-CESM2-WACCM	288×192	3		(Danabasoglu, 2019; Gettelman et al., 2019)
NCC-NorESM-MM	288×192	3	2	(Seland et al., 2019; Bentsen et al., 2019)
NOAA-GFDL-ESM4	288×180	1	1	(John et al., 2018; Horowitz et al., 2018; Krasting et al., 2018)
EC-Earth3	120×90	2		(Consortium, 2020)
BCC-CSM2	320×160	1		(Hegglin et al., 2016; Wu et al., 2021)

[a]The names of coupled earth system models are abbreviated.

[b]The planar dimensional spatial resolutions are presented in longitudinal latitudinal grids.

[c]Numbers of simulation ensembles for historical period (1990−2014, using historical experiments)

[d]Numbers of simulation ensembles for recent years (2015−2019, using ssp245 experiments)

Table S4. Satellite observations used for ozone assimilation in CAMS (CAMS global ECMWF Atmospheric Composition Reanalysis 4). Table based on Inness et al. (2019)

Species	Instrument	Period	Data typea	Reference
Ozone, NO2	SCIAMACHY (Envisat)	2003-2012	TC for Ozone, TRC for NO2	(Lerot et al., 2009)
Ozone	MIPAS (Envisat)	2003-2012	PROF	(Von Clarmann et al., 2009)
Ozone	MLS (Aura)	2004-2016	PROF	(Schwartz, 2015)
Ozone, NO2	OMI (Aura)	2004-2020	TC for Ozone, TRC for NO2	(Liu et al., 2010)
Ozone, NO2	GOME-2 (Metop-A)	2007-2020	TC for Ozone, TRC for NO2	(Hao et al., 2014)
Ozone, NO2	GOME-2 (Metop-B)	2013-2020	TC for Ozone, TRC for NO2	
Ozone	SBUV/2 (NOAA-14–NOAA-19)	2003-2020	PC	(Bhartia et al., 1996; Mcpeters et al., 2013)
CO	MOPITT (Terra)	2002-2020	TC	(Deeter et al., 2014)

[a]Satellite retrievals of atmospheric composition that were assimilated in the chemistry reanalysis. TC is total column, TRC is tropospheric column, PROF is profiles, PC is partial columns.

Table S5. Inputs used for ozone assimilation in GEOS. Table based on Qu et al. (2020)

Variable	Years	Source	Reference
NO_2 tropospheric column	2005-2016	OMNO2	(Qu et al., 2020b)
NO_2 tropospheric column	2005-2016	DOMINO	(Qu et al., 2020a)
Meteorological fields	2005-2016	MERRA-2	Global Modeling and Assimilation Office (GMAO) (2015)
Anthropogenic emissionsa	2005-2016	HTAP 2010 inventory version 2	(Janssens-Maenhout et al., 2015)
Anthropogenic emissions	2005-2016	CEDS	(Hoesly et al., 2018)
Nonanthropogenic emissionsb	2005-2016	Follows Qu et al. 2017	(Qu et al., 2017)

[a]Anthropogenic emissions include NO_x, SO_2, NH_3, CO, $NMVOC_S$ (non-methane volatile organic compounds), and primary aerosols.

[b]Nonanthropogenic emissions include biomass burning emissions, NO_x emissions from lightning, and soil NO_x emissions.

Table S6. Satellite observations used for ozone assimilation in TCR-2. Table based on Miyazaki et al. (2020)

Species	Instrument	Period	Data typea	Reference
NO_2 , SO_2	OMI (Aura)	2005-2020	TrC for NO2, PBL for SO2	(Boersma et al., 2011; Boersma et al., 2017; Krotkov et al., 2016; Li et al., 2013)
NO_2	SCIAMACHY (Envisat)	2005-2012	TrC	(Boersma et al., 2004)
NO_2	GOME-2 (Metop-A)	2007-2020	TrC	
Ozone	TES (Aura)	2005-2011	PROF	(Bowman et al., 2006; Herman and Kulawik, 2013)
Ozone, HNO_3	MLS (Aura)	2005-2020	PROF	(Livesey et al., 2017)
CO	MOPITT (Terra)	2005-2020	PROF	(Deeter et al., 2017; Deeter et al., 2013)

[a]Satellite retrievals of atmospheric composition that were assimilated in the chemistry reanalysis. TC is total column, TRC is tropospheric column, PROF is profiles, PC is partial columns. PBL is planetary boundary layer.

Table S7. The regions defined by Hemispheric Transport Air Pollution(HTAP)2 (Koffi et al., 2016)

	Tier 1		Tier 2
01	**GLO***	World	
02	OCN	Non-arctic/Antarctic Ocean	020 Baltic Sea 021 North Atlantic 022 South Atlantic 023 North Pacific 024 South Pacific 025 Indian Ocean 026 Hudson Bay 027 Mediterranean Sea 028 Black and Caspian Sea
03	**NAM***	US+Canada (upto 66 N; polar circle)	031 NE US (all divided on state or provincial lines) 032 SE US 033 NW US 034 SW US 035 E. Canada 036 W. Canada + Alaska up to 66 N.
04	**EUR***	Western + Eastern EU+Turkey (upto 66 N polar circle)	041 NW Europe 042 SW Europe (France follows provinces level at ca. 46 N). 043 Eastern Europe 044 Greece+Turkey+Cyprus
05	**SAS***	South Asia: India, Pakistan, Nepal, Bangadesh, Sri Lanka	051 North India+Pakistan+Nepal+Bangladesh 052 South India+Sri Lanka 053 Indian Himalaya (above an elevation of 1500 m)
06	**EAS***	E Asia: China, Korea, Japan	061 North East China 062 South East China 063 West China +Mongolia (excl. Himalaya) 064 North/South Korea 065 Japan 066 China/Tibet Himalaya (above an elevation of 1500 m)
07	**SEA***	South East Asia	071 Indonesia+Malaysia+Singapore 072 Thailand+Myanmar+Vietnam
08	PAN	Pacific, Australia+ New Zealand	081 Pacific 082 Australia 083 New Zealand
09	NAF	Northern Africa	091 Egypt 092 Rest of Northern Africa
10	**SAF***	Sub Saharan Africa	101 West and Central Africa: Côte d'Ivoire, Angola, Benin, Burkina Faso, Cameroon, Cape Verde, Chad, Congo Brazzaville, Democratic Republic of Congo, Equatorial Guinea, Gambia, Ghana, Guinea, Guinea Bissau, Liberia, Mali, Niger, Nigeria, Senegal, Sierra Leone and Togo 102 East Africa: Burundi, Djibouti, Eritrea, Ethiopia, Kenya, Sudan, Rwanda, Uganda, Somalia and Tanzania. 103 Southern Africa: Angola, Botswana, Lesotho, Madagascar, Malawi, Mauritius, Mozambique, Namibia, South Africa, Swaziland, Tanzania, Zambia, and Zimbabwe
11	**MDE***	Middle East; S. Arabia etc, Iran, Iraq	111 Middle East 112 S.Arabia; Yemen; Oman; etc 113 Iran, Iraq
12	MCA	Mexico, Central America, Caribbean,	121 Mexico 122 Central America 123 Caribbean

		Guyanas, Venezuela, Columbia	124 Guyanas, Columbia, Venezuela
13	SAM	S. America	131 South Brazil 132 Rest of Brazil 133 Uruguay, Paraguay, Argentina, Chile 134 Peru, Ecuador
14	RBU	Russia, Belarussia, Ukraine, Central Asia	141 Russia West 142 Russia East 143 Belarussia+Ukraine
15	CAS	Central Asia	144 Uzbekistan, Kazakhstan, Kyrgyzstan, Tajikistan, Turkmenistan
16	NPO	Arctic Circle (North of 66 N)+Greenland	150 Arctic (includes ocean and all of Greenland)
17	SPO	Antarctic	160 Antarctic 161 Southern Ocean, south of 60S

*Regions in bold characters defined as priority regions in this paper.

Table S8. The share of population exposed to ozone above particular thresholds in each world region for each year (from 2006 to 2016). The unit of thresholds is ppb and unit of share is percentage (%).

2006	Region	EAS	EUR	MDE	NAM	SAF	SAS	SEA	GLO
BME	>30	100	99.5	100	99.8	92.5	100	77.3	95.1
	>50	57.7	18.6	73.8	47.3	10	79.8	0.5	42.2
	>70	0	0.3	0	0.8	0	0	0	0.1
NJML	>30	100	100	100	100	100	100	93.5	99.4
	>50	79.3	92.3	99.5	91.1	35.2	98.5	31.8	73.7
	>70	3	2.5	17.4	9.5	0	13.7	0	6
UKML	>30	100	100	100	100	95.8	100	97.7	97.2
	>50	99.7	87.7	90.9	89.4	11.4	96	29.5	68.7
	>70	20.5	0	0	0	0	6.8	0	6
CAMS	>30	100	97.7	100	99.9	85.7	100	90.8	93.5
	>50	71	20.8	91.4	61.7	7.3	94.8	28.7	51.9
	>70	3.3	0	9.4	3.6	0.1	13.2	7.1	5
GEOS	>30	100	100	100	100	98.7	100	93.7	97.8
	>50	95.4	54.6	99.5	71.4	13.2	92	5.5	60.6
	>70	4.8	0	4.2	0	0	0.2	0	1.3
TCR-2	>30	100	100	100	100	97.5	100	86.5	97.1
	>50	94.1	78.9	92.5	88.6	18.3	87.3	19.5	64.9
	>70	37.2	0.1	33.5	3.1	1.3	2.8	0	11.1
2007	Region	EAS	EUR	MDE	NAM	SAF	SAS	SEA	GLO
BME	>30	100	97.2	100	99.4	96.8	100	86.1	96.4
	>50	76.7	19.9	80.5	42.1	12.7	85.8	0.7	48.5
	>70	17.4	0	0	0.6	0	0	0	3.7
NJML	>30	100	100	100	100	100	100	85.3	99
	>50	78.8	79.6	99.5	91.4	38.7	98.5	31.3	73.2
	>70	3.6	0	17.9	12.2	0	10.2	0	5
UKML	>30	100	100	100	100	97.6	100	96.5	97.8
	>50	99.9	81.4	92.2	90.1	10.7	97.3	35.9	69.3
	>70	23.8	0	0	0	0	14.9	0	8.6
CAMS	>30	100	92.5	100	100	91.5	100	86.9	94.6
	>50	77.2	19.6	88.2	52.2	12.6	94.7	28.3	53
	>70	0	0	8.1	4.2	0	8.4	6.6	3.1
GEOS	>30	100	100	100	100	98.5	100	83.6	97.1
	>50	97.1	40.3	99.5	58.3	11	94.3	2.6	59.5
	>70	2.9	0	3.6	0	0	0.3	0	0.8
TCR-2	>30	100	100	100	100	98.7	100	78.9	96.9
	>50	93.2	70.7	93.4	86.9	20.3	85.3	6.5	62.8
	>70	37.5	0.2	34.1	1.7	0.3	2.8	0	10.7
2008	Region	EAS	EUR	MDE	NAM	SAF	SAS	SEA	GLO
BME	>30	100	100	100	99.5	88.6	100	76.1	93.9
	>50	76.5	77.7	84	30.3	4	87.5	0.1	46.4
	>70	0.6	0	4.5	0.9	0	0.9	0	0.5
NJML	>30	100	100	100	100	100	100	85.6	99
	>50	76.8	75.8	99.5	89.3	38.6	98.4	25.1	71.4
	>70	3.2	0	9.1	4	0	8.4	0	3.8
UKML	>30	100	97.4	100	100	97.8	100	96.5	97.9
	>50	99.9	1.9	89.3	87.4	10.2	98.4	29.9	68.5
	>70	32.6	0	0	0	0	28.3	0	13.6
CAMS	>30	100	100	100	100	77.7	100	84.4	90.6
	>50	66.1	36	79.9	14	9.1	93.8	21	44.5
	>70	0.1	0	5.1	0	0	4	5.5	1.6

GEOS	>30	100	100	100	100	98.3	100	83.6	97
	>50	93.9	70.4	99.4	46.5	15.8	93.1	0.2	57.7
	>70	2.1	0.1	0.4	0	0	0	0	0.5
TCR-2	>30	100	100	100	100	96	100	76.2	95.5
	>50	89.3	77.7	93.2	81.8	19.5	86.7	3.7	61.3
	>70	31.5	0	32.5	0.8	0.3	5.5	0	9.7
2009	Region	EAS	EUR	MDE	NAM	SAF	SAS	SEA	GLO
BME	>30	100	98.3	99.8	99.8	69.7	99.4	80.2	90.5
	>50	76.8	18.3	79.3	13.4	0.8	84.7	0.4	44.7
	>70	6.2	0	0.1	0.5	0	0	0	1.3
NJML	>30	100	100	100	100	99.9	100	89.9	99.3
	>50	79.2	77.2	99.2	88.5	36.2	99.1	32.8	71.8
	>70	3.5	0	5.4	3.4	0	19	0	6.6
UKML	>30	100	100	100	100	98	100	97	97.4
	>50	99.8	79	92	85.5	9.9	98.2	34	68.4
	>70	20.4	0	0	0	0	29.6	0	11.3
CAMS	>30	100	91.6	100	100	90.8	100	88.1	93.7
	>50	72.9	15.4	87.8	28.7	6.8	95.2	30.9	50
	>70	0.1	0	6.5	3.6	0.1	9.5	6.6	3.4
GEOS	>30	100	100	100	100	97.9	100	91.7	97.3
	>50	96.4	44.3	97.9	36.9	11.4	97.1	2	58.8
	>70	3.5	0	2.7	0	0	1.4	0	1.2
TCR-2	>30	100	100	100	100	97.5	100	82.9	97.1
	>50	93	74.9	93.3	85.6	15.9	88.9	13	63.5
	>70	36.1	0.1	34.3	0	0.6	9.5	0	11.6
2010	Region	EAS	EUR	MDE	NAM	SAF	SAS	SEA	GLO
BME	>30	100	97.4	98.7	99.2	80.8	99.1	71.8	91.7
	>50	65.6	11.1	62.4	27.3	1.4	74.1	0	38.5
	>70	0	0	0	0.3	0	0	0	0
NJML	>30	100	100	100	100	100	100	82	98.9
	>50	62.9	73.1	99.5	87.7	34.1	98.3	21.4	67.8
	>70	3.1	0	8.2	2.5	0	8.9	0	3.6
UKML	>30	100	100	100	100	97.3	100	96.4	97.8
	>50	98.4	79.8	93.4	81.9	8.3	98.2	27.9	67.3
	>70	31.6	0	0	0	0	29.3	0	13.7
CAMS	>30	100	88.2	100	100	73.5	100	84.4	89.5
	>50	32.2	2	76.2	15	4.5	95.9	23.5	37.4
	>70	0	0	5.6	0	0	24.7	4.9	6.4
GEOS	>30	100	100	100	100	99.1	100	81.3	97.1
	>50	88.3	35.2	99.7	50.6	17.5	94.8	1.9	57.9
	>70	3.5	0	4.4	0	0	0.2	0	0.9
TCR-2	>30	100	100	100	100	98	99.8	75.7	96.3
	>50	93.5	64.5	92.4	84.7	18.2	86.1	14.2	62.9
	>70	37.7	0.3	40.7	0	1.1	6.6	0	11.9
2011	Region	EAS	EUR	MDE	NAM	SAF	SAS	SEA	GLO
BME	>30	100	98.9	99.3	99.4	94.1	100	81.3	95.8
	>50	68.5	15.5	72.6	26.6	8.6	89.8	7.9	46
	>70	0.3	0	0	0.4	0	2.1	0	0.6
NJML	>30	100	100	100	100	100	100	88.1	99
	>50	73.5	75.6	99.4	87.6	37.6	98.6	24.6	70.2
	>70	3.4	0.3	5	4.5	0	9.3	0	4
UKML	>30	100	100	100	100	97.3	100	96.6	97.6
	>50	99.9	75.5	93.6	85.2	12.5	98.9	43.5	69.5

	>70	29.1	0	0	0	0	35.5	0	14.6
CAMS	>30	100	92	100	99.9	92.3	100	88.6	94.3
	>50	66.5	14.5	91.7	54.6	11.7	97.2	27.7	51
	>70	2.9	0	10.4	0	0.2	9.2	6.6	3.8
GEOS	>30	100	100	100	100	99.2	100	90	97.6
	>50	97	38.6	99.7	55.2	15	95.1	0.1	59.4
	>70	2.4	0	2.3	0	0	0.6	0	0.7
TCR-2	>30	100	100	100	100	97.6	100	81.7	96.5
	>50	94.1	69.4	96.1	86.1	19.6	89.7	11.3	64.2
	>70	40.2	0.1	35.3	0	0.4	17.4	0	14.4
2012	Region	EAS	EUR	MDE	NAM	SAF	SAS	SEA	GLO
BME	>30	99.8	97.7	100	99.5	92.9	100	82.6	96.3
	>50	60.8	21.4	80.9	35.5	0.8	92.8	9	45.1
	>70	0.1	0	0	0.4	0	1.3	0	0.3
NJML	>30	100	100	100	100	100	100	88.7	99.1
	>50	69.5	73.1	99.5	90.6	30.2	98.7	31.4	68.7
	>70	3.4	0	8.4	3.2	0	8.1	0	3.5
UKML	>30	100	100	100	100	95.8	100	97.6	97.5
	>50	99.9	74.6	93.2	83.1	10	98.5	42.8	68.7
	>70	33.3	0	0	0	0	35	0	15.4
CAMS	>30	100	90.1	100	100	76.3	100	84.1	89.5
	>50	33.7	1	83.1	13.9	5.3	96.3	22.1	38.1
	>70	0.1	0	5.1	0	0	15.2	5.4	4.2
GEOS	>30	100	100	100	100	97.9	100	89.3	97.6
	>50	96	46.9	100	79.8	13.8	97.5	1	62
	>70	6	0	13.4	0	0	2.6	0	2.4
TCR-2	>30	100	100	100	100	96.9	100	86.6	97.3
	>50	94.6	67.7	96.4	83.7	16.8	92.5	15.8	64.6
	>70	42.7	0.1	45.1	0	0.4	15.4	0	15.1
2013	Region	EAS	EUR	MDE	NAM	SAF	SAS	SEA	GLO
BME	>30	98.6	99.6	99.5	99.1	93.2	100	79.1	96
	>50	35.2	22.1	74.2	12.4	1.9	84.6	0.2	35.7
	>70	0.1	0	0	0.3	0	0	0	0
NJML	>30	100	100	100	100	100	100	88.8	99.1
	>50	72.6	73.5	98.9	85	32.8	98.5	26.1	68.6
	>70	3	0	4.7	2.5	0	4.7	0	2.4
UKML	>30	100	100	100	100	96.1	100	96.9	97.5
	>50	99.9	69.5	92.4	84.7	12.7	99.8	43.5	69.3
	>70	34.8	0	0	0	0	34.8	0	15.6
CAMS	>30	100	99.6	100	100	86.2	100	88.6	93.5
	>50	73.9	11.5	86.8	45	6.3	97.4	19.4	50.3
	>70	1	0	10.4	0	0.1	14.3	5.9	4.4
GEOS	>30	100	100	100	100	98.7	100	88.3	97.5
	>50	92.2	42.8	99.7	45.9	14.5	94.9	0.5	58.5
	>70	1.2	0	6.6	0	0	0.3	0	0.6
TCR-2	>30	100	100	100	100	97.1	100	86.7	97.3
	>50	94.5	71.3	96.4	83.4	17.3	90.4	19	64.8
	>70	39.8	0.1	40.2	0	1.2	13.2	0	13.4
2014	Region	EAS	EUR	MDE	NAM	SAF	SAS	SEA	GLO
BME	>30	98.9	99.3	99.8	99.4	100	100	86.8	96
	>50	45.5	20.4	79.8	11.4	27.1	96.3	7.5	45.7
	>70	0.6	0	0	0.2	0	8.1	0	2
NJML	>30	100	100	100	100	99.9	100	91.5	99.2

	>50	64.8	65.1	98.8	83.1	28.9	98.7	31.2	65.9
	>70	3.7	0	3.9	2.5	0	8.8	0	3.5
UKML	>30	100	100	100	100	98.6	100	97.7	98.3
	>50	99.9	71.9	94.5	83.3	10.8	99.6	46.1	69.1
	>70	31.6	0	0	0	0	41.4	0	16.5
CAMS	>30	100	99.2	100	100	83.1	100	91.3	93.2
	>50	68.9	9	89	39.3	6.8	92	26.8	48
	>70	0.1	0	9.5	0	0.1	12.4	6.3	3.8
GEOS	>30	100	100	100	100	98.5	100	90	97.6
	>50	94.5	47.1	99.9	44	13.2	96.1	1.6	59
	>70	23.5	0	5.6	0	0	0.3	0	5.2
TCR-2	>30	100	100	100	100	97.2	100	91.3	97.7
	>50	94.7	69.8	93.8	81.4	16.3	91.4	21.7	64.4
	>70	48.4	0	41.1	0	0.9	14.9	0	15.7
2015	Region	EAS	EUR	MDE	NAM	SAF	SAS	SEA	GLO
BME	>30	99.4	97.2	100	99.5	91.1	99.9	84.6	95.6
	>50	46.7	19.5	81.7	13.9	2.4	92.9	7.1	40.5
	>70	0.3	0	0	0	0	0.1	0.7	0.1
NJML	>30	100	100	100	100	100	100	95	99.6
	>50	64.8	70.4	99	80.9	38	96.8	29.6	67.1
	>70	3.2	0.1	3.5	1.9	0	6.2	0	2.6
UKML	>30	100	100	100	100	99.1	100	97.6	98.1
	>50	99.9	81.2	96.4	63.2	12.9	99	46	69.5
	>70	33.7	0	0.9	0	0.8	44.5	0	17.8
CAMS	>30	100	100	100	100	85.2	100	91.3	93.4
	>50	72.1	13.6	90.8	40.1	5.1	94.6	34.6	50.1
	>70	1.2	0	12.2	0	0.1	12.4	7.9	4.4
GEOS	>30	100	100	100	100	98.8	100	90.6	97.6
	>50	92.3	50.5	99.9	43.2	15.7	92.1	0.9	58.1
	>70	14.1	0	2.5	0	0	0.5	0	3.2
TCR-2	>30	100	100	100	100	98.5	100	90.5	97.9
	>50	94.5	71.2	93.4	80.2	20.7	91.2	20.2	64.7
	>70	42.3	0.1	37.1	0	1.5	29.9	0.6	17.7
2016	Region	EAS	EUR	MDE	NAM	SAF	SAS	SEA	GLO
BME	>30	100	97.4	100	99.5	95.7	100	67.3	95.1
	>50	53.9	13.5	82.3	12.4	7.9	97.2	2.5	43.5
	>70	0.6	0	0.2	0	0	2.3	0	0.7
NJML	>30	100	100	100	100	100	100	84.3	99
	>50	53.9	64.2	97.7	15.5	39.7	97.1	19.1	63.2
	>70	0.6	0	3.1	0	0	7.1	0	2.8
UKML	>30	100	100	100	100	98.9	100	97.6	98.1
	>50	99.9	81.1	95.9	62.8	13.2	98.4	47.6	69.5
	>70	33.3	0	0.5	0	0.9	50.6	0	19.2
CAMS	>30	100	98.8	100	100	84.3	100	85.6	93.2
	>50	68.3	11.5	88.9	42.3	12.7	96.7	20.9	50
	>70	1.2	0	14.7	0.4	0	26.4	5.6	7.5
GEOS	>30	100	100	100	100	99.1	100	82.9	96.8
	>50	86.5	49.9	99.9	46.2	13.9	97.4	0.2	58.1
	>70	1.6	0	9	0	0	0.4	0	0.8
TCR-2	>30	100	100	100	100	98.2	100	84.1	97.3
	>50	93.5	67.4	96.4	84.1	22.7	93.8	18.4	65.9
	>70	40.2	0	40.6	0	1	33.4	0	18.6

Table S9. Different quantiles of TOAR-II observations for 2006 to 2015. The unit of TOAR-II observations is ppb.

Year	2006	2007	2008	2009	2010	2011	2012	2013	2014	2015
0%	12.52	15.74	15.32	13.25	12.28	8.25	12.01	9.07	8.76	12.24
10%	37.73	36.42	37.29	37.16	36.35	36.00	36.01	37.00	36.52	36.85
20%	41.58	39.46	40.32	40.14	39.35	38.83	38.79	39.52	39.25	39.92
30%	43.69	41.75	42.32	42.19	41.16	40.77	40.67	41.42	41.09	42.02
40%	45.56	43.96	44.13	44.06	42.64	42.49	42.29	42.96	42.74	43.89
50%	47.24	46.03	45.93	45.92	43.97	43.92	43.90	44.43	44.20	45.63
60%	48.87	48.08	47.76	48.13	45.28	45.28	45.53	45.71	45.59	47.44
70%	50.63	50.40	49.78	50.10	46.92	46.99	47.58	47.29	47.14	49.60
80%	52.81	52.96	52.18	52.45	49.07	49.61	49.91	49.33	48.87	52.58
90%	55.82	56.31	55.51	55.50	52.57	53.50	53.29	52.60	51.98	57.07
100%	78.83	79.95	79.33	80.38	72.17	82.24	80.63	83.21	75.16	92.03

Table S10. Performance evaluation of six datasets for countries (unions) with the most monitors from 2006 to 2015 against TOAR-II observations of OSDMA8. Number is the number of the TOAR-II monitor stations in each country. Density (per km2) is the density of the TOAR-II monitors in each country based on land area. Estimate is the average of the grid estimates for each dataset at the TOAR-II monitor locations in each country. Linear regression R2 and root mean squared error (RMSE) against TOAR-II observations in each country are presented. Country names are in ISO 3166-1 alpha-3, United States of America (USA), Japan (JPN), China (CHN), South Korea (KOR), Canada (CAN), United Kingdom of Great Britain and Northern Ireland (GBR). EU-27 includes Austria, Belgium, Bulgaria, Croatia, Cyprus, Czech Republic, Denmark, Estonia, Finland, France, Germany, Greece, Hungary, Ireland, Italy, Latvia, Lithuania, Luxembourg, Malta, Netherlands, Poland, Portugal, Romania, Slovakia, Slovenia, Spain, Sweden. "Others" is all other countries apart from those listed. The order of countries or regions is determined based on the number of ground monitoring stations.

2006	Country	EU-27	USA	JPN	KOR	CAN	GBR	Others
	Number	1755	717	643	226	198	82	94
	Density	4.39E-04	7.84E-05	1.76E-03	2.32E-03	2.25E-05	3.39E-04	4.53E-06
	TOAR	46.66	51.15	49.33	41.21	39.16	39.38	44.56
BME	Estimate	46.36	51.31	47.92	41.52	39.05	38.99	44.06
	R^2	0.55	0.77	0.21	0.11	0.73	0.46	0.63
	RMSE	4.90	3.67	5.00	6.97	2.67	4.38	6.24
NJML	Estimate	58.69	63.74	50.52	46.10	50.44	49.54	54.29
	R^2	0.33	0.47	0.01	0.02	0.45	0.16	0.46
	RMSE	13.47	13.88	6.35	8.64	11.98	11.51	12.45
UKML	Estimate	55.43	57.53	62.36	65.09	48.08	48.86	50.29
	R^2	0.11	0.26	0.09	0.00	0.27	0.09	0.47
	RMSE	11.29	9.19	13.94	24.87	10.34	11.12	9.94
CAMS	Estimate	44.14	54.13	42.56	49.61	40.28	31.65	43.49
	R^2	0.17	0.31	0.00	0.00	0.20	0.00	0.30
	RMSE	7.59	7.93	9.41	11.00	4.93	10.03	8.79
GEOS	Estimate	50.17	53.00	56.77	62.23	45.57	43.95	46.08
	R^2	0.15	0.28	0.03	0.01	0.24	0.04	0.44
	RMSE	7.62	6.70	9.21	22.12	7.83	7.34	7.89
TCR-2	Estimate	54.17	59.30	58.89	63.89	47.52	45.29	47.86
	R^2	0.16	0.23	0.01	0.03	0.23	0.04	0.35
	RMSE	10.20	10.95	11.94	24.02	9.83	8.37	10.07
2007	Country	EU-27	JPN	USA	KOR	CAN	GBR	Others
	Number	1840	751	745	237	197	50	95
	Density	4.67E-04	2.06E-03	8.14E-05	2.43E-03	2.24E-05	2.07E-04	4.18E-06
	TOAR	44.01	51.22	50.23	42.83	38.13	35.36	42.73
BME	Estimate	43.80	50.07	50.31	41.63	37.87	34.81	41.00
	R^2	0.58	0.28	0.81	0.26	0.83	0.30	0.70
	RMSE	4.46	5.28	3.40	6.58	2.32	4.65	6.17
NJML	Estimate	56.16	53.14	63.01	46.84	50.59	43.61	53.50
	R^2	0.43	0.01	0.54	0.06	0.60	0.11	0.52
	RMSE	13.28	7.11	13.99	8.24	13.10	9.80	13.29
UKML	Estimate	54.81	61.35	57.68	65.75	48.38	47.98	49.42
	R^2	0.21	0.03	0.40	0.01	0.42	0.03	0.51
	RMSE	12.57	11.77	9.64	24.18	11.27	13.93	10.55
CAMS	Estimate	41.22	44.96	52.41	51.29	39.42	30.88	41.48
	R^2	0.31	0.02	0.45	0.00	0.42	0.02	0.48
	RMSE	6.84	9.08	7.21	11.38	4.41	7.55	7.92
GEOS	Estimate	47.89	57.09	51.39	62.07	44.93	41.19	44.32
	R^2	0.24	0.08	0.36	0.04	0.55	0.02	0.50
	RMSE	7.18	8.30	6.40	20.59	7.89	8.01	7.82
TCR-2	Estimate	52.38	58.75	58.43	61.19	47.30	42.86	47.46

	R^2	0.29	0.03	0.42	0.05	0.43	0.00	0.40
	RMSE	10.25	10.59	10.34	20.01	10.35	9.45	10.20
2008	Country	EU-27	JPN	USA	KOR	CAN	GBR	Others
	Number	1962	808	746	255	197	87	113
	Density	4.91E-04	2.22E-03	8.16E-05	2.61E-03	2.24E-05	3.60E-04	4.74E-06
	TOAR	44.20	51.58	49.18	45.17	39.11	37.61	41.39
BME	Estimate	43.89	51.27	49.31	44.21	38.81	37.08	40.51
	R^2	0.47	0.34	0.85	0.19	0.80	0.42	0.75
	RMSE	4.56	4.66	3.16	6.37	2.28	4.38	5.47
NJML	Estimate	54.64	52.46	61.23	49.09	49.21	45.07	50.87
	R^2	0.33	0.04	0.59	0.03	0.46	0.15	0.56
	RMSE	11.70	6.09	13.17	7.84	10.81	9.12	11.92
UKML	Estimate	54.40	63.81	57.53	69.97	48.23	47.27	47.53
	R^2	0.17	0.13	0.45	0.02	0.25	0.10	0.53
	RMSE	11.92	13.32	10.28	25.90	10.49	11.15	9.94
CAMS	Estimate	38.41	44.82	46.32	51.48	37.82	32.06	38.30
	R^2	0.19	0.02	0.47	0.01	0.12	0.02	0.41
	RMSE	8.15	9.22	6.58	9.70	4.94	8.21	8.83
GEOS	Estimate	48.38	57.33	50.83	63.49	44.64	43.31	42.95
	R^2	0.17	0.06	0.42	0.00	0.26	0.04	0.57
	RMSE	7.10	7.96	6.41	19.55	7.07	7.97	7.24
TCR-2	Estimate	52.12	55.24	57.08	62.36	45.28	43.78	44.57
	R^2	0.18	0.03	0.30	0.07	0.29	0.00	0.41
	RMSE	10.11	8.26	10.62	18.97	8.05	8.83	9.75
2009	Country	EU-27	JPN	USA	KOR	CAN	GBR	Others
	Number	2056	1115	767	262	195	87	128
	Density	5.14E-04	3.06E-03	8.38E-05	2.68E-03	2.22E-05	3.60E-04	5.15E-06
	TOAR	44.34	51.37	46.77	48.14	38.08	35.65	40.39
BME	Estimate	44.10	50.16	47.07	47.77	37.87	34.82	39.21
	R^2	0.54	0.11	0.81	0.18	0.70	0.50	0.66
	RMSE	4.55	6.08	3.11	6.01	2.30	4.48	6.04
NJML	Estimate	55.24	51.31	58.31	51.09	48.47	42.54	50.48
	R^2	0.39	0.00	0.58	0.02	0.34	0.28	0.53
	RMSE	12.14	6.21	12.54	7.17	11.02	8.65	12.34
UKML	Estimate	54.28	60.79	56.41	64.69	46.28	47.72	45.93
	R^2	0.27	0.02	0.39	0.08	0.15	0.15	0.57
	RMSE	11.52	10.89	11.15	17.72	9.77	13.35	9.13
CAMS	Estimate	42.58	43.14	48.94	58.00	38.04	40.35	29.96
	R^2	0.31	0.08	0.46	0.01	0.01	0.41	0.02
	RMSE	6.41	10.11	6.38	13.47	4.46	7.88	8.55
GEOS	Estimate	49.32	57.59	49.88	64.30	45.04	42.38	42.62
	R^2	0.27	0.10	0.32	0.06	0.25	0.09	0.54
	RMSE	7.58	8.19	6.59	17.38	7.84	8.91	7.44
TCR-2	Estimate	53.34	58.42	56.27	64.85	47.27	43.53	46.77
	R^2	0.26	0.00	0.19	0.02	0.19	0.01	0.40
	RMSE	10.78	10.20	11.74	18.28	10.34	10.06	10.89
2010	Country	EU-27	JPN	USA	KOR	CAN	GBR	Others
	Number	2119	1057	799	265	200	87	121
	Density	5.30E-04	2.90E-03	8.73E-05	2.72E-03	2.28E-05	3.60E-04	5.07E-06
	TOAR	44.06	43.52	48.31	43.13	38.60	34.09	40.30
BME	Estimate	44.09	48.23	48.27	44.43	38.04	33.73	39.33
	R^2	0.57	0.13	0.79	0.14	0.76	0.44	0.57
	RMSE	4.26	6.81	3.30	6.09	2.42	3.88	6.12

NJML	Estimate	55.51	50.45	59.06	46.96	48.53	41.92	51.02
	R^2	0.40	0.01	0.54	0.05	0.56	0.15	0.49
	RMSE	12.59	9.06	11.87	7.20	10.48	9.18	12.81
UKML	Estimate	54.16	58.93	55.80	63.83	46.29	47.68	46.64
	R^2	0.27	0.02	0.43	0.00	0.29	0.26	0.46
	RMSE	11.58	16.08	9.22	21.64	9.15	14.30	9.99
CAMS	Estimate	37.68	43.72	45.81	49.13	38.65	29.04	37.66
	R^2	0.18	0.00	0.43	0.00	0.23	0.05	0.17
	RMSE	8.85	5.19	5.98	9.28	4.24	7.25	9.26
GEOS	Estimate	48.87	55.80	50.48	60.66	46.28	41.62	42.99
	R^2	0.21	0.00	0.26	0.00	0.39	0.06	0.50
	RMSE	7.56	13.17	6.54	18.63	8.57	9.05	7.06
TCR-2	Estimate	51.63	56.58	57.16	60.62	46.53	40.62	44.89
	R^2	0.22	0.00	0.27	0.08	0.44	0.00	0.40
	RMSE	9.79	14.95	11.28	18.95	9.07	8.58	9.61
2011	Country	EU-27	JPN	USA	KOR	CAN	GBR	Others
	Number	2142	822	741	277	205	93	127
	Density	5.36E-04	2.26E-03	8.10E-05	2.84E-03	2.33E-05	3.84E-04	3.16E-06
	TOAR	44.57	41.89	49.27	43.93	38.31	34.76	39.92
BME	Estimate	44.56	46.05	49.10	44.47	38.04	34.69	39.90
	R^2	0.60	0.15	0.86	0.19	0.79	0.38	0.64
	RMSE	4.36	6.24	2.82	5.92	1.98	3.80	5.69
NJML	Estimate	55.86	47.81	59.91	46.71	47.61	43.14	50.90
	R^2	0.43	0.02	0.55	0.04	0.44	0.07	0.55
	RMSE	12.46	8.26	11.83	7.01	9.94	9.60	12.97
UKML	Estimate	53.73	62.96	55.48	65.20	45.66	48.90	45.91
	R^2	0.31	0.00	0.42	0.04	0.12	0.07	0.60
	RMSE	10.84	21.66	8.44	22.19	8.90	14.93	8.93
CAMS	Estimate	41.55	44.45	50.60	47.45	38.45	29.95	39.94
	R^2	0.30	0.02	0.38	0.01	0.21	0.04	0.37
	RMSE	6.98	5.42	6.33	7.34	4.09	6.90	7.60
GEOS	Estimate	48.72	54.45	51.75	59.52	45.27	41.83	42.37
	R^2	0.26	0.01	0.29	0.01	0.23	0.06	0.62
	RMSE	7.24	13.40	6.78	16.86	7.91	8.46	6.39
TCR-2	Estimate	52.46	56.63	56.65	61.01	46.94	42.77	44.52
	R^2	0.27	0.01	0.23	0.06	0.22	0.03	0.57
	RMSE	9.93	16.34	10.22	18.56	10.04	9.35	8.53
2012	Country	EU-27	JPN	KOR	USA	CAN	GBR	Others
	Number	2527	1094	286	262	207	91	129
	Density	6.32E-04	3.00E-03	2.93E-03	2.86E-05	2.36E-05	3.76E-04	3.14E-06
	TOAR	44.30	43.63	47.65	53.11	39.05	33.77	39.36
BME	Estimate	44.52	46.43	48.28	52.68	38.99	33.99	38.97
	R^2	0.63	0.07	0.21	0.83	0.82	0.48	0.62
	RMSE	4.13	5.98	5.87	4.16	2.16	3.18	5.61
NJML	Estimate	54.85	49.44	50.26	62.71	49.42	41.59	49.85
	R^2	0.43	0.01	0.00	0.56	0.55	0.13	0.53
	RMSE	11.76	8.14	7.18	11.81	11.08	8.83	12.45
UKML	Estimate	54.25	61.31	65.08	57.96	45.89	46.96	45.09
	R^2	0.25	0.07	0.00	0.43	0.32	0.07	0.58
	RMSE	11.60	18.31	18.65	9.01	8.09	13.96	8.69
CAMS	Estimate	38.48	43.20	48.55	47.90	38.33	30.19	37.29
	R^2	0.29	0.03	0.01	0.52	0.48	0.08	0.25
	RMSE	8.20	6.10	7.16	8.96	3.92	5.73	8.55

GEOS	Estimate	49.59	56.63	63.73	53.23	46.85	42.57	42.22
	R^2	0.29	0.00	0.00	0.37	0.50	0.11	0.64
	RMSE	7.79	14.03	17.36	7.96	8.62	9.71	6.35
TCR-2	Estimate	52.09	55.53	63.19	56.59	46.95	42.45	44.13
	R^2	0.30	0.00	0.01	0.41	0.48	0.01	0.57
	RMSE	9.76	13.85	17.19	8.45	8.94	9.82	8.58
2013	Country	EU-27	JPN	USA	KOR	CAN	GBR	Others
	Number	2120	1046	866	291	197	94	172
	Density	5.30E-04	2.87E-03	9.47E-05	2.98E-03	2.24E-05	3.89E-04	4.19E-06
	TOAR	44.07	44.37	47.09	49.23	38.14	36.01	39.78
BME	Estimate	45.21	48.59	46.73	49.60	37.85	35.70	40.81
	R^2	0.45	0.11	0.84	0.20	0.73	0.45	0.47
	RMSE	5.19	6.14	2.81	5.67	2.38	3.33	6.92
NJML	Estimate	54.25	50.42	56.60	52.29	47.37	45.22	51.44
	R^2	0.36	0.09	0.55	0.01	0.41	0.03	0.41
	RMSE	11.53	7.85	10.69	6.94	9.93	10.33	13.89
UKML	Estimate	52.83	59.96	55.72	64.72	46.44	46.55	46.94
	R^2	0.24	0.04	0.40	0.01	0.22	0.07	0.51
	RMSE	10.58	16.20	10.19	16.63	9.64	11.52	10.22
CAMS	Estimate	42.93	49.30	49.82	55.17	42.08	33.99	42.04
	R^2	0.28	0.03	0.35	0.01	0.11	0.00	0.27
	RMSE	6.04	6.49	6.38	8.88	5.85	5.39	8.45
GEOS	Estimate	49.32	58.12	51.02	64.31	46.28	43.42	43.98
	R^2	0.21	0.02	0.39	0.00	0.31	0.01	0.54
	RMSE	7.94	14.46	6.71	16.28	8.96	8.69	7.79
TCR-2	Estimate	51.72	59.99	55.76	65.60	47.50	44.61	46.37
	R^2	0.21	0.00	0.19	0.03	0.34	0.00	0.48
	RMSE	9.78	17.16	11.05	17.90	10.56	9.93	10.20
2014	Country	EU-27	JPN	USA	KOR	CAN	GBR	Others
	Number	1787	1127	856	224	204	94	114
	Density	4.47E-04	3.09E-03	9.36E-05	2.30E-03	2.32E-05	3.89E-04	2.76E-06
	TOAR	43.00	45.16	46.44	51.09	37.37	35.51	36.99
BME	Estimate	45.41	49.16	46.65	52.75	38.82	35.16	37.69
	R^2	0.45	0.05	0.86	0.29	0.39	0.34	0.62
	RMSE	5.40	6.46	2.54	6.32	3.81	3.68	5.88
NJML	Estimate	53.42	51.01	55.75	54.87	46.45	43.07	48.33
	R^2	0.40	0.04	0.61	0.01	0.28	0.11	0.38
	RMSE	11.54	7.79	10.30	8.11	10.01	8.69	14.22
UKML	Estimate	53.14	62.07	55.15	67.10	46.29	46.36	41.97
	R^2	0.21	0.07	0.49	0.02	0.17	0.12	0.42
	RMSE	11.65	17.76	9.97	17.75	10.02	11.83	9.23
CAMS	Estimate	42.16	46.48	49.13	56.05	40.62	32.84	40.66
	R^2	0.21	0.01	0.33	0.00	0.01	0.00	0.15
	RMSE	5.87	5.10	6.45	9.88	5.76	5.66	10.70
GEOS	Estimate	49.95	57.55	50.50	65.63	44.76	43.84	40.80
	R^2	0.19	0.00	0.38	0.04	0.23	0.01	0.49
	RMSE	8.97	13.52	6.76	16.16	8.27	9.61	8.09
TCR-2	Estimate	51.78	59.36	55.35	64.89	45.87	43.89	42.19
	R^2	0.17	0.00	0.23	0.09	0.27	0.00	0.41
	RMSE	10.73	16.27	11.03	16.21	9.89	10.13	9.79
2015	Country	EU-27	CHN	JPN	USA	KOR	CAN	Others
	Number	1849	1427	1123	875	312	204	267
	Density	4.63E-04	1.52E-04	3.08E-03	9.57E-05	3.20E-03	2.32E-05	6.10E-06

	TOAR	45.64	50.39	44.03	46.41	50.40	38.58	38.24
BME	Estimate	45.41	48.66	46.34	45.50	50.26	37.28	38.36
	R^2	0.71	0.52	0.02	0.86	0.13	0.50	0.49
	RMSE	3.79	7.73	5.38	2.76	7.91	3.25	6.89
NJML	Estimate	55.88	53.08	49.63	55.51	54.78	47.03	47.10
	R^2	0.52	0.41	0.01	0.61	0.02	0.19	0.31
	RMSE	11.41	8.81	7.49	10.11	9.38	9.52	12.24
UKML	Estimate	53.68	68.02	58.93	52.81	64.40	47.63	47.45
	R^2	0.22	0.21	0.02	0.45	0.00	0.20	0.33
	RMSE	10.17	20.67	15.46	8.22	16.38	9.86	12.44
CAMS	Estimate	44.02	55.71	45.43	49.21	60.94	40.91	38.57
	R^2	0.37	0.07	0.01	0.28	0.04	0.06	0.23
	RMSE	5.92	12.49	4.65	6.73	15.17	4.75	8.92
GEOS	Estimate	50.14	61.94	57.88	50.85	65.42	45.52	43.15
	R^2	0.30	0.20	0.00	0.44	0.00	0.27	0.39
	RMSE	7.39	15.31	14.71	6.83	17.21	7.74	9.12
TCR-2	Estimate	52.27	67.50	59.42	54.73	67.55	46.64	45.51
	R^2	0.39	0.16	0.02	0.24	0.08	0.26	0.38
	RMSE	8.66	20.33	17.55	10.50	19.65	9.35	11.02

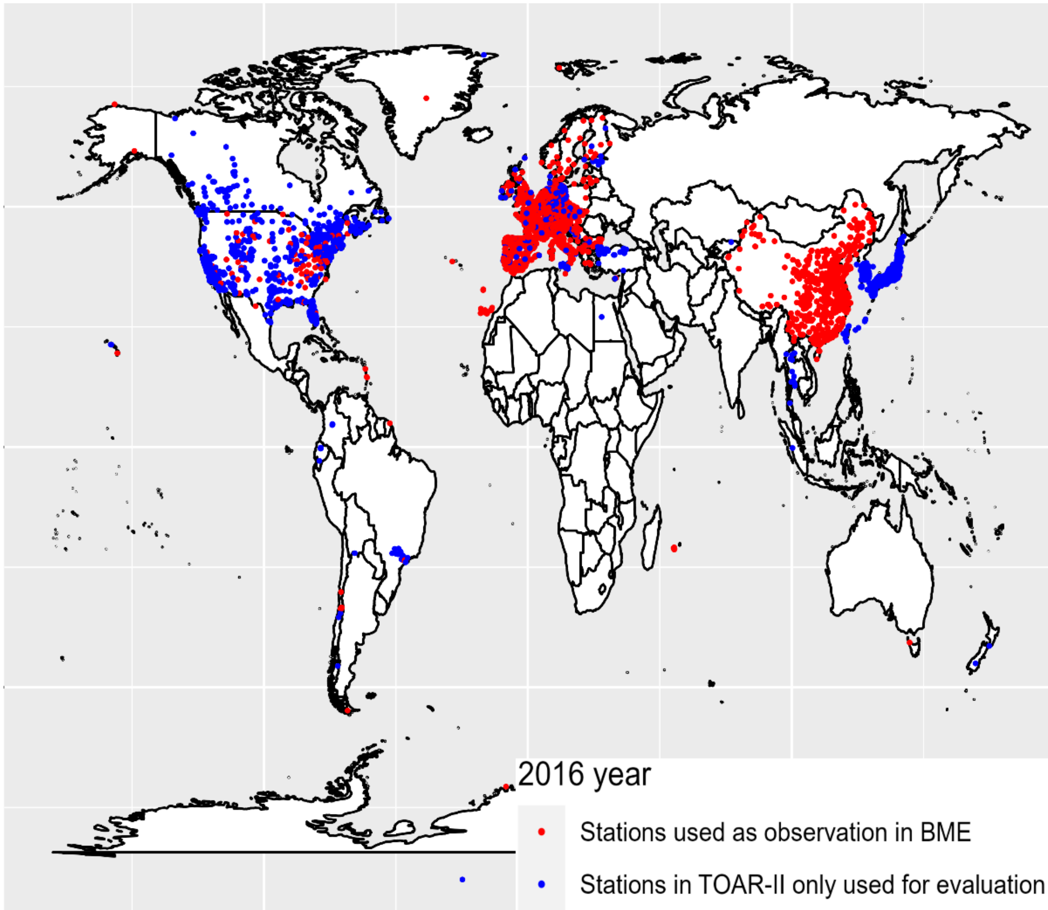

Figure S1. Blue and red dots are TOAR-II January 2016 to March 2017 monitor stations with valid monthly data for more than 11 months (which used for evaluation), red dots are BME inputs from TOAR-I and CNEMC in 2016, blue dots are new TOAR-II stations compared to TOAR-I in 2016 which used for evaluation in Figure S13

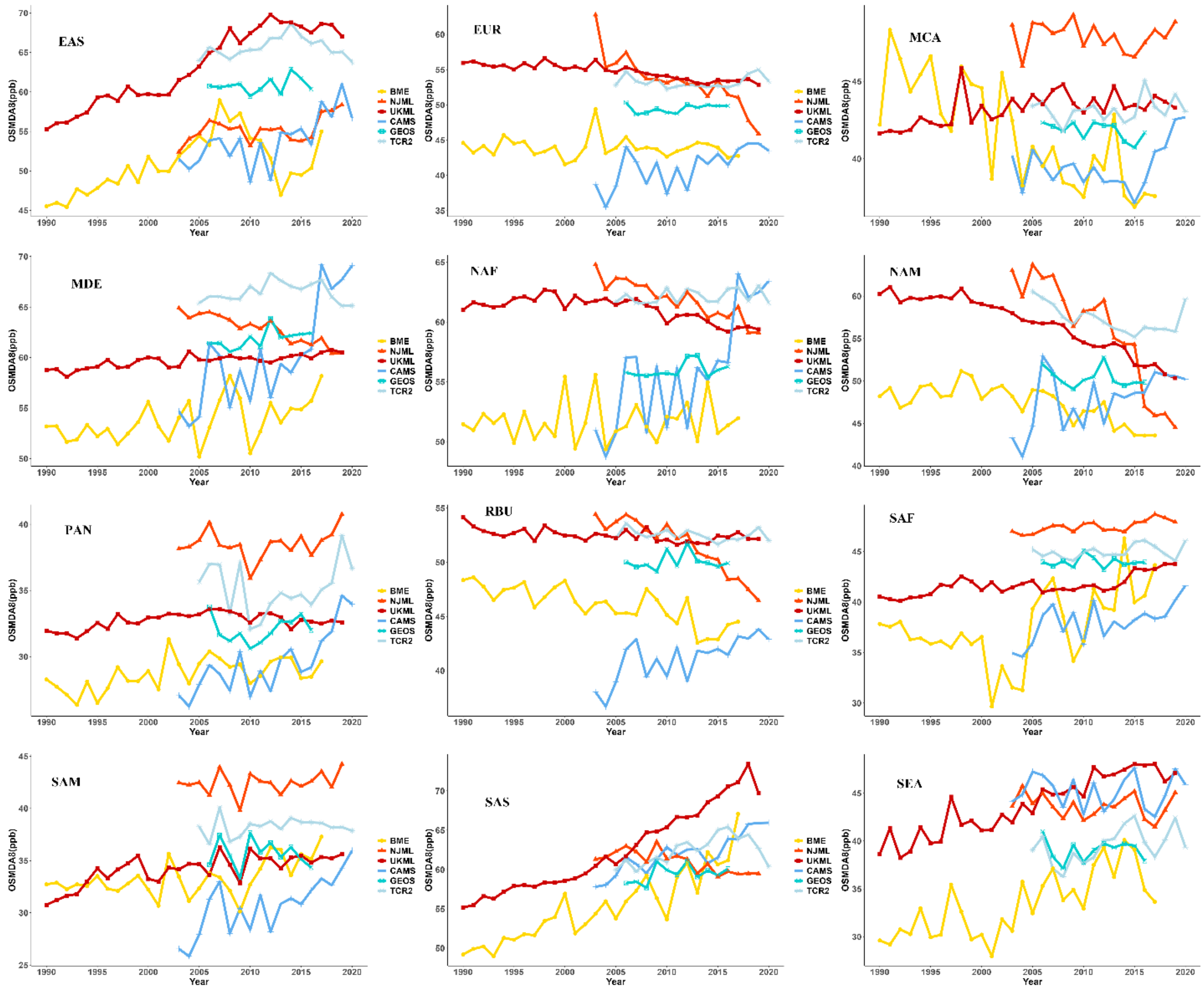

Figure S2. The Yearly trends for six datasets for different regions, where ozone is expressed as population-weighted OSMDA8.

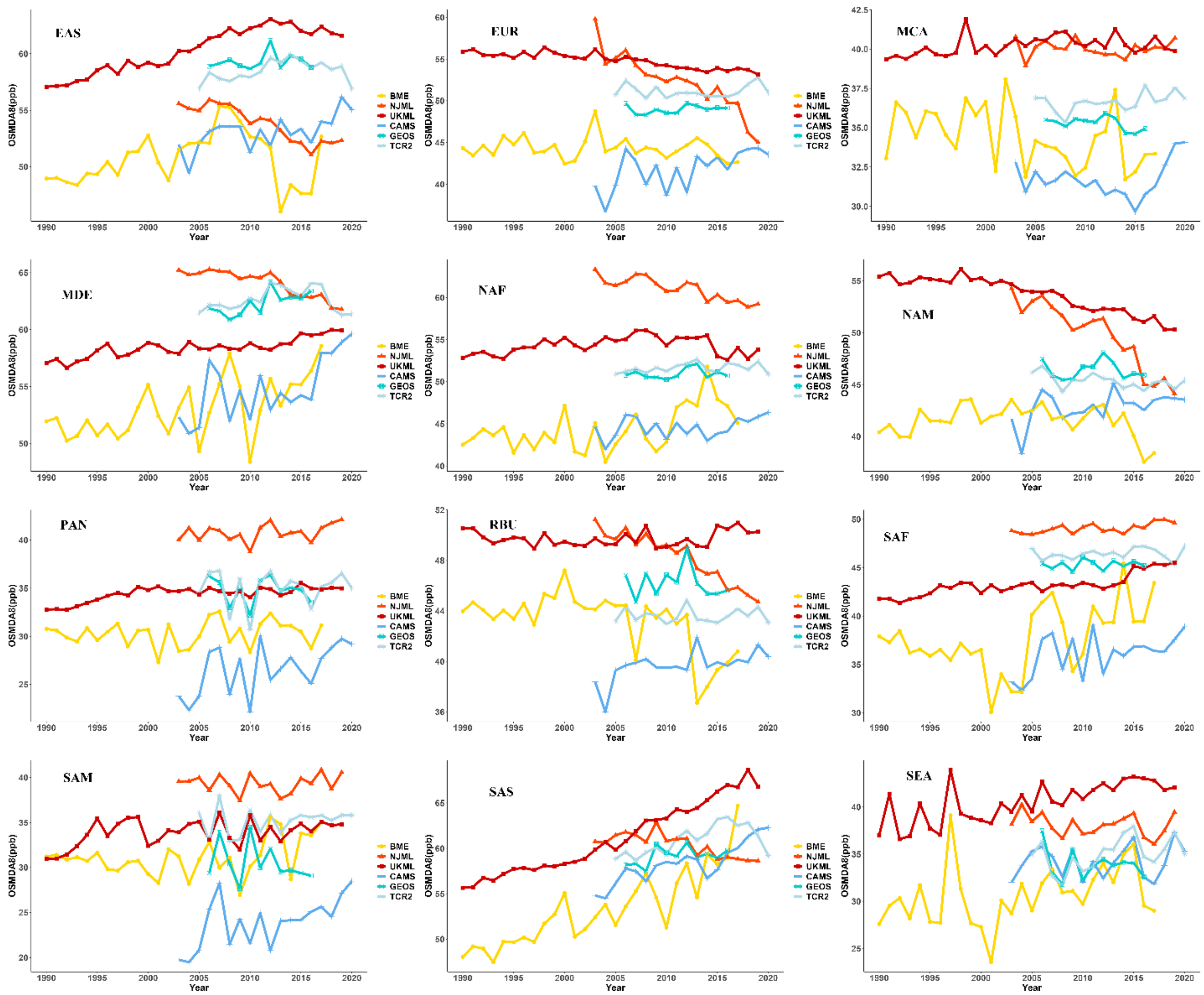

Figure S3. The Yearly trends for six datasets for different regions where ozone is expressed as area-weighted OSMDA8.

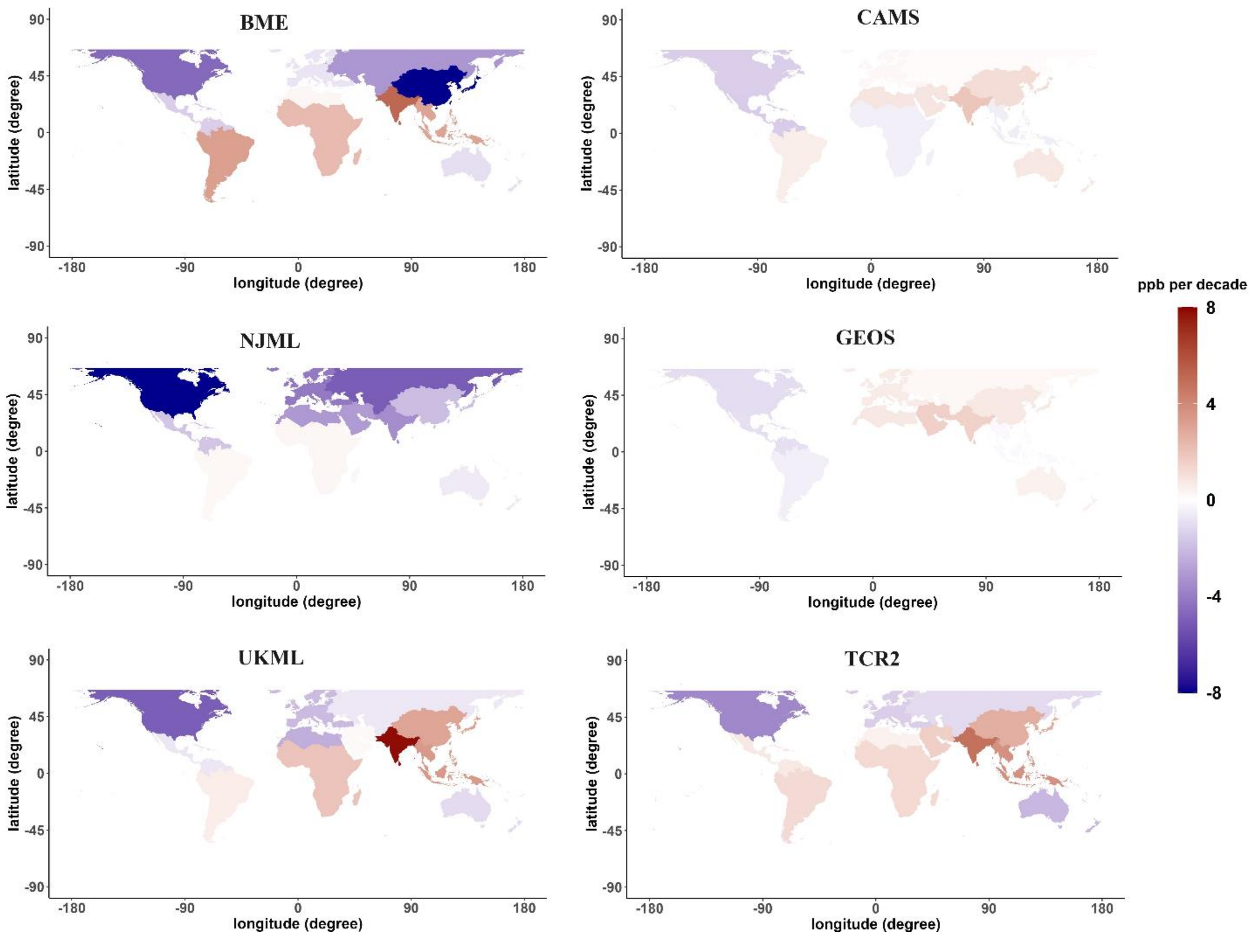

Figure S4. Population weighted ozone (OSMDA8) trends per decade for six datasets, calculated over 2006 to 2016.

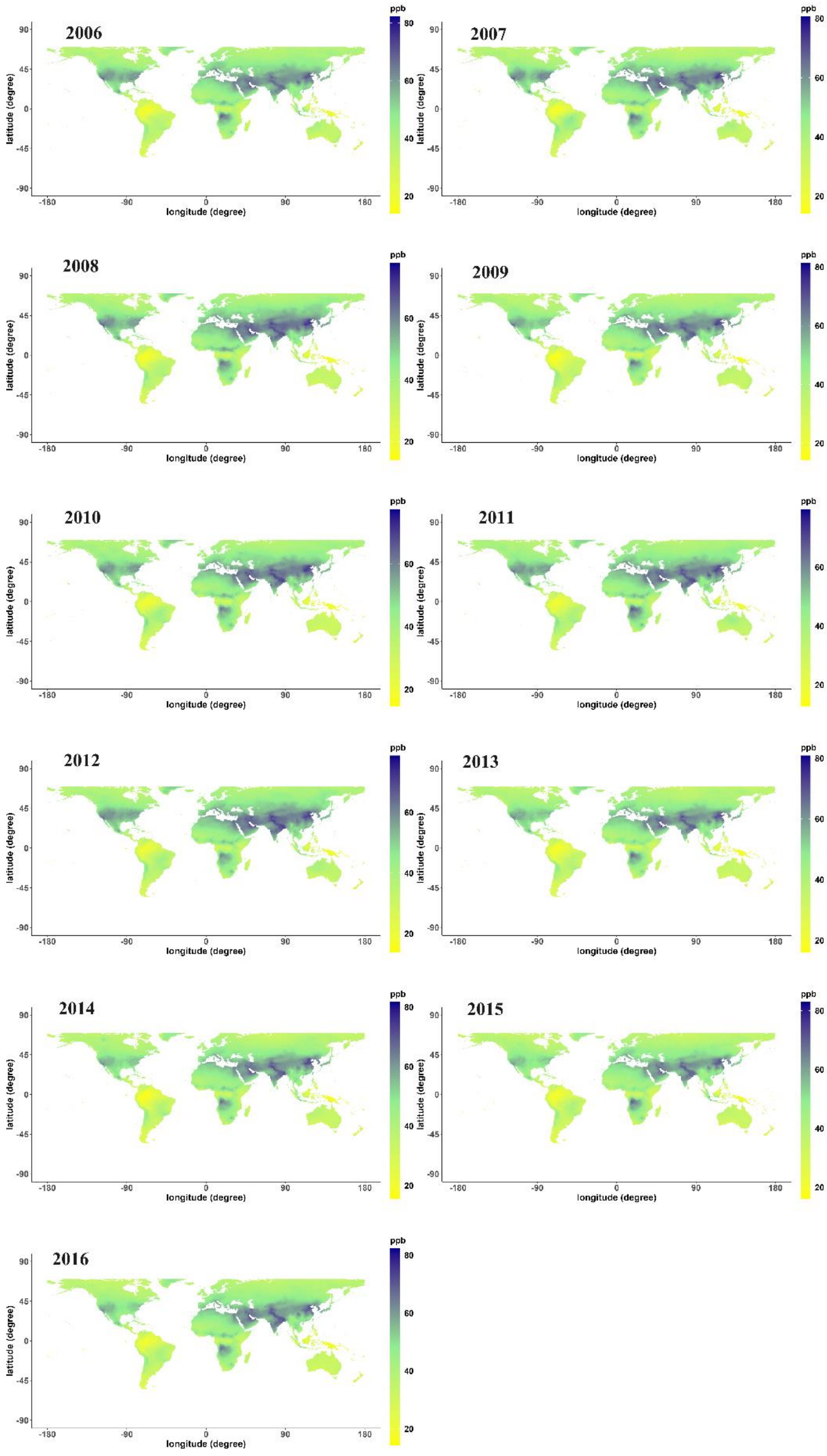

Figure S5. Each year ensemble means of six datasets from 2006 to 2016

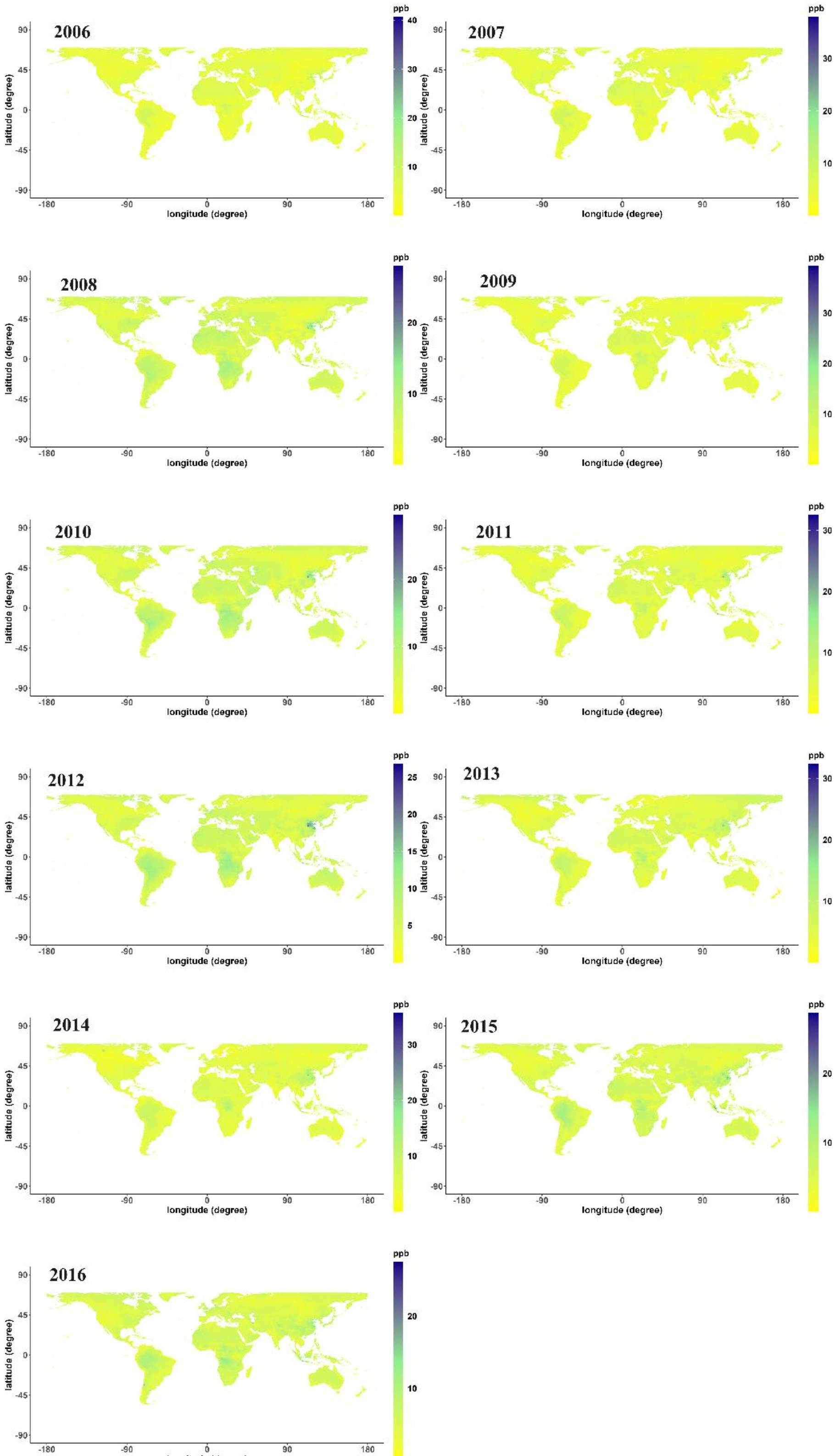

Figure S6. Each year standard deviations of six datasets from 2006 to 2016

Figure S7. Each year the difference in each grid cell between the six datasets and the ensemble mean (Figure S5) from 2006 to 2016. Positive values indicate that the estimate of the dataset is higher than the ensemble mean. Negative values indicate that the estimate of the dataset is lower than the ensemble mean of the six datasets.

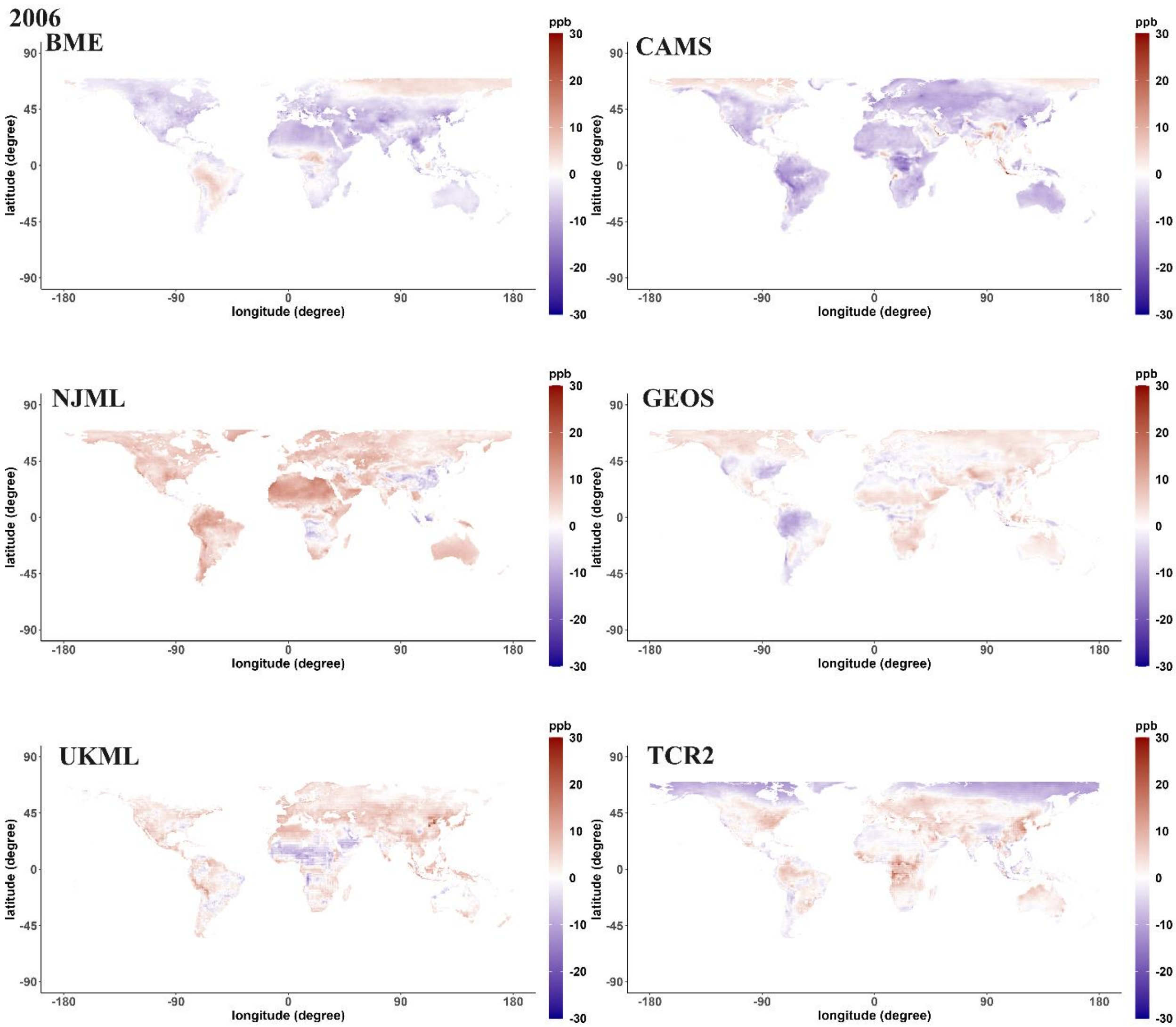

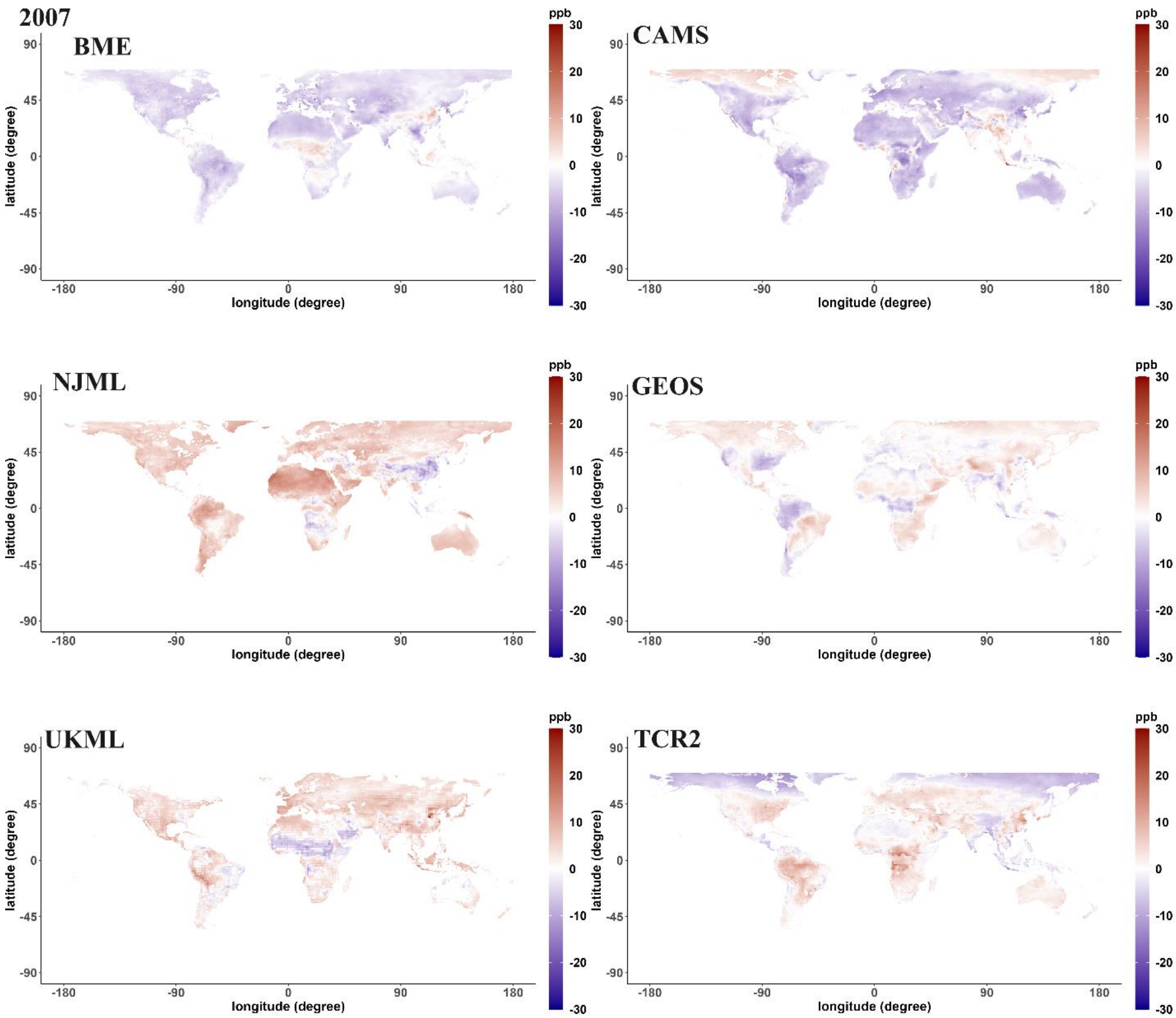
2007
BME
CAMS
NJML
GEOS
UKML
TCR2
ppb
30
20
10
0
-10
-20
-30
90
45
0
-45
-90
latitude (degree)
-180
-90
0
90
180
longitude (degree)

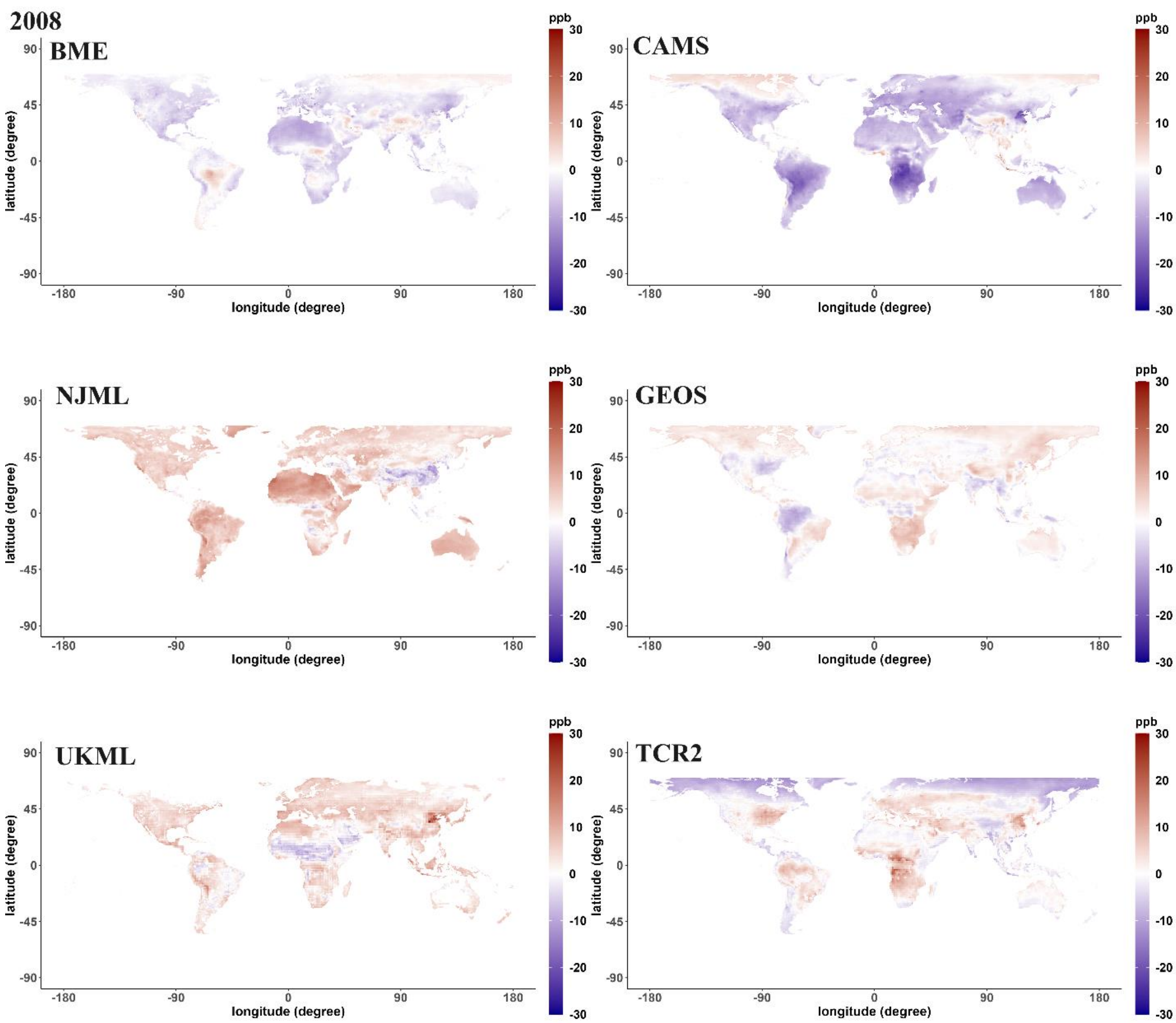
2008
BME
CAMS
NJML
GEOS
UKML
TCR2
ppb
30
20
10
0
-10
-20
-30
latitude (degree)
90
45
0
-45
-90
longitude (degree)
-180
-90
0
90
180

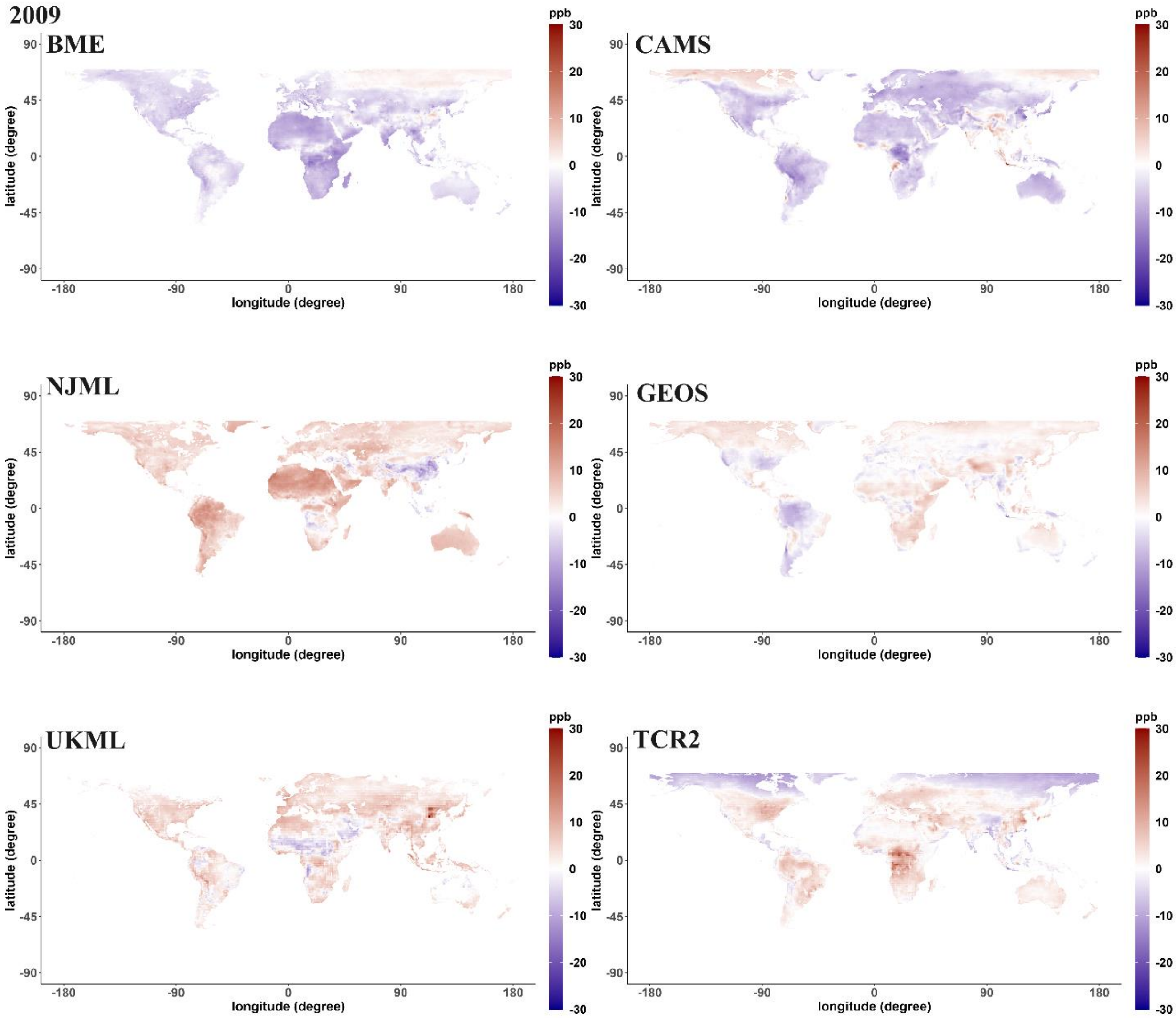
2009
BME
CAMS
NJML
GEOS
UKML
TCR2
ppb
30
20
10
0
-10
-20
-30
latitude (degree)
90
45
0
-45
-90
longitude (degree)
-180
-90
0
90
180

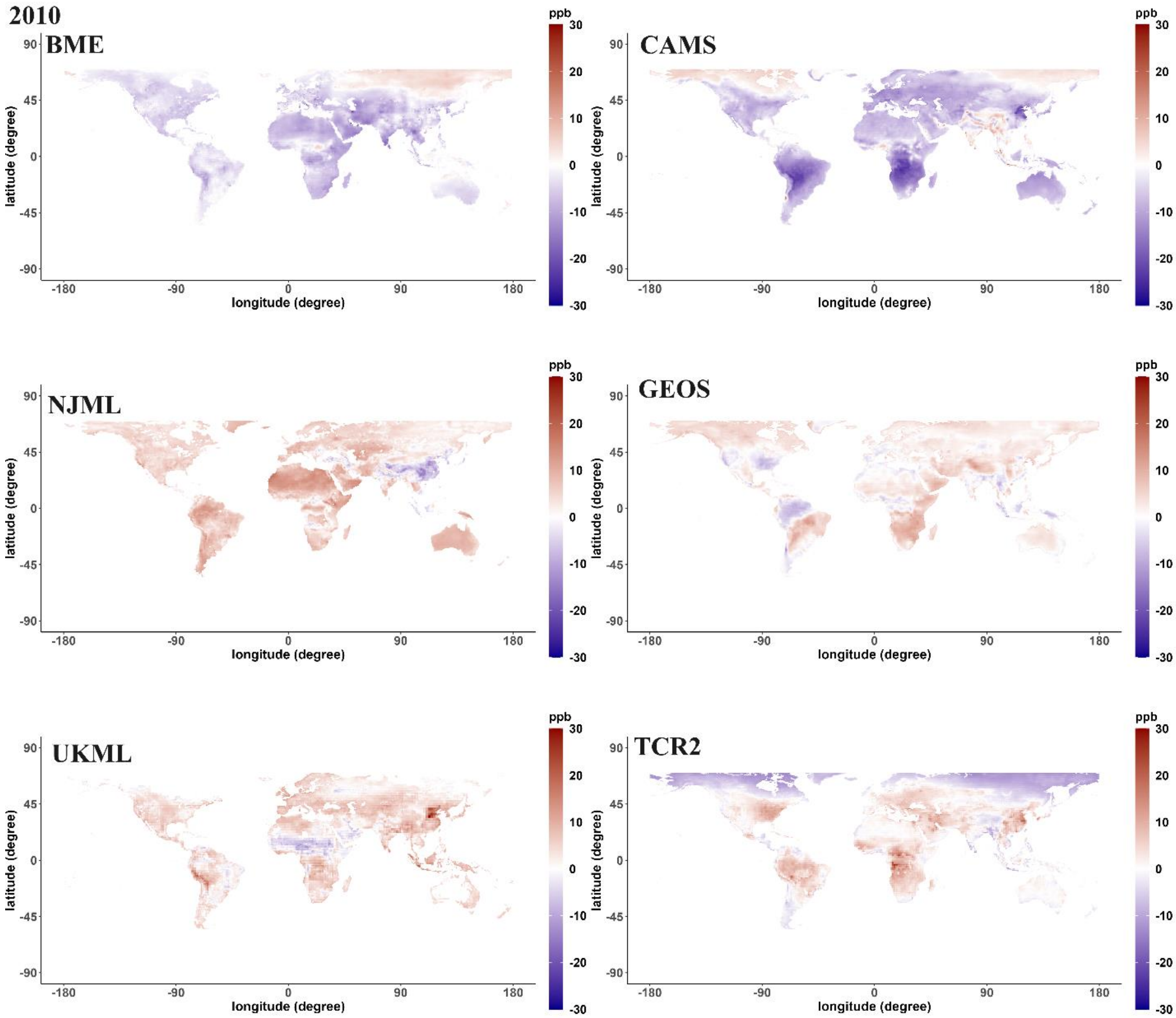
2010
BME
CAMS
NJML
GEOS
UKML
TCR2
ppb
30
20
10
0
-10
-20
-30
latitude (degree)
90
45
0
-45
-90
longitude (degree)
-180
-90
0
90
180

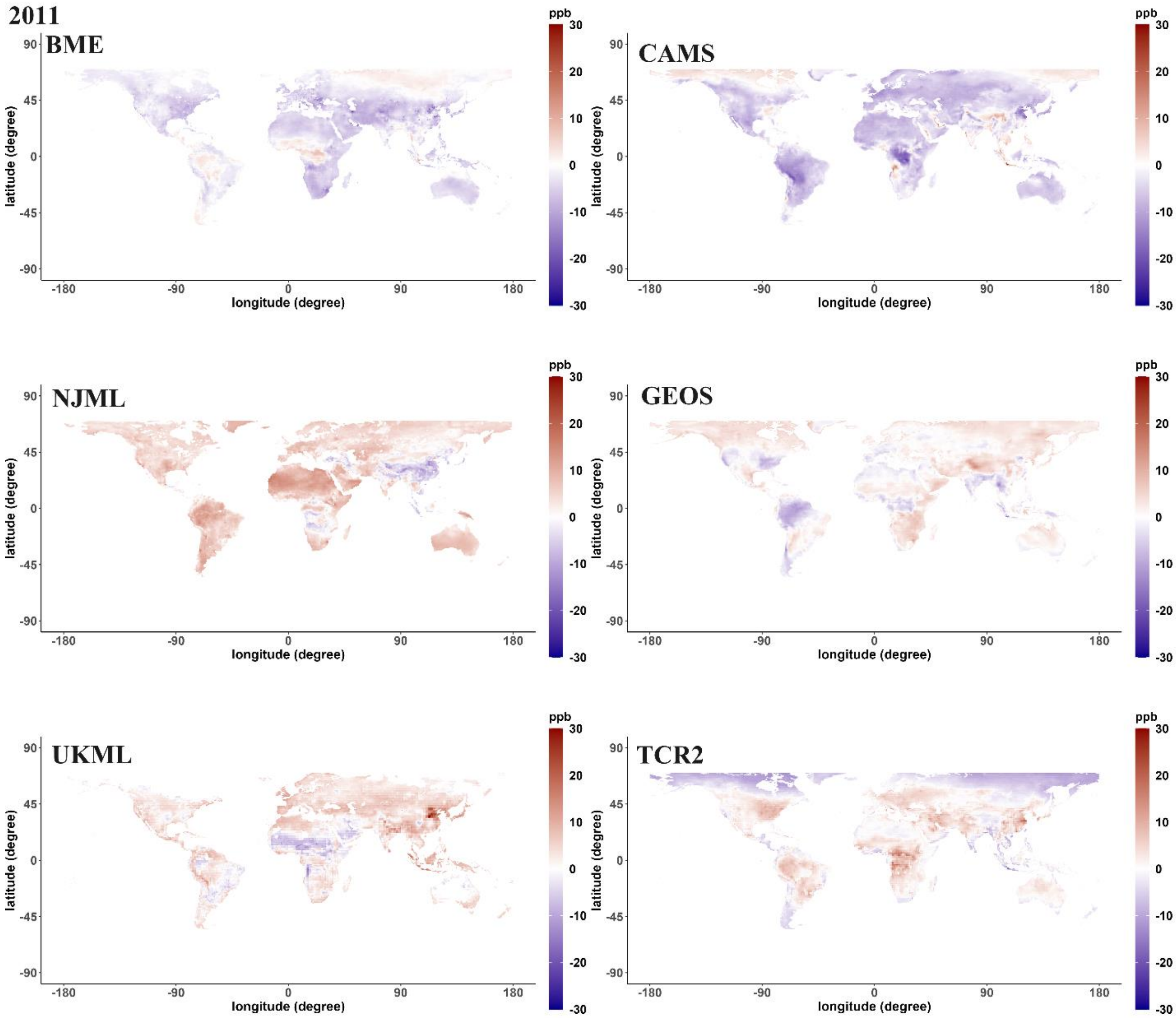

2011
BME
CAMS
NJML
GEOS
UKML
TCR2
ppb
30
20
10
0
-10
-20
-30
latitude (degree)
90
45
0
-45
-90
longitude (degree)
-180
-90
0
90
180

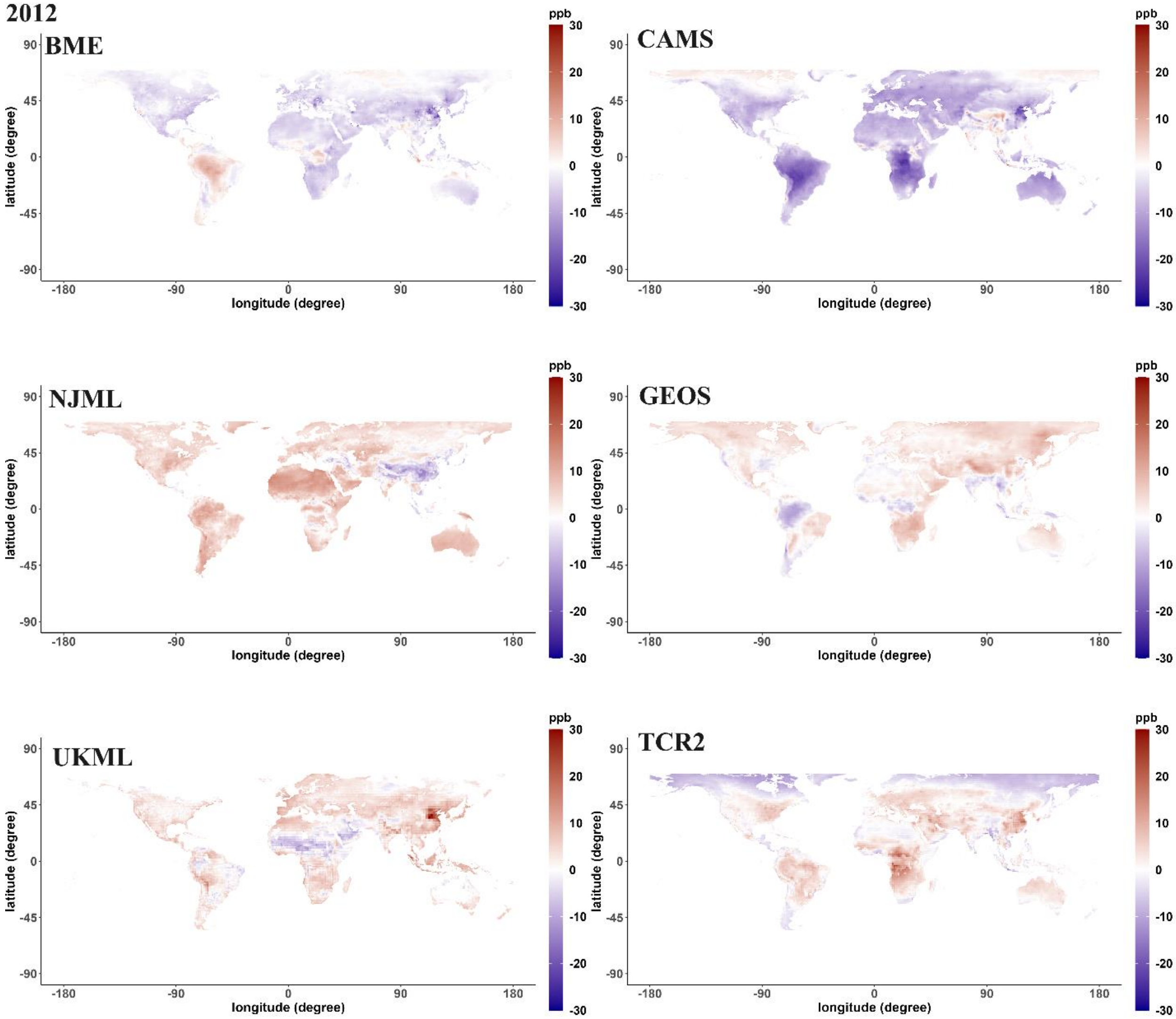
2012
BME
CAMS
NJML
GEOS
UKML
TCR2
ppb
30
20
10
0
-10
-20
-30
90
45
0
-45
-90
latitude (degree)
-180
-90
0
90
180
longitude (degree)

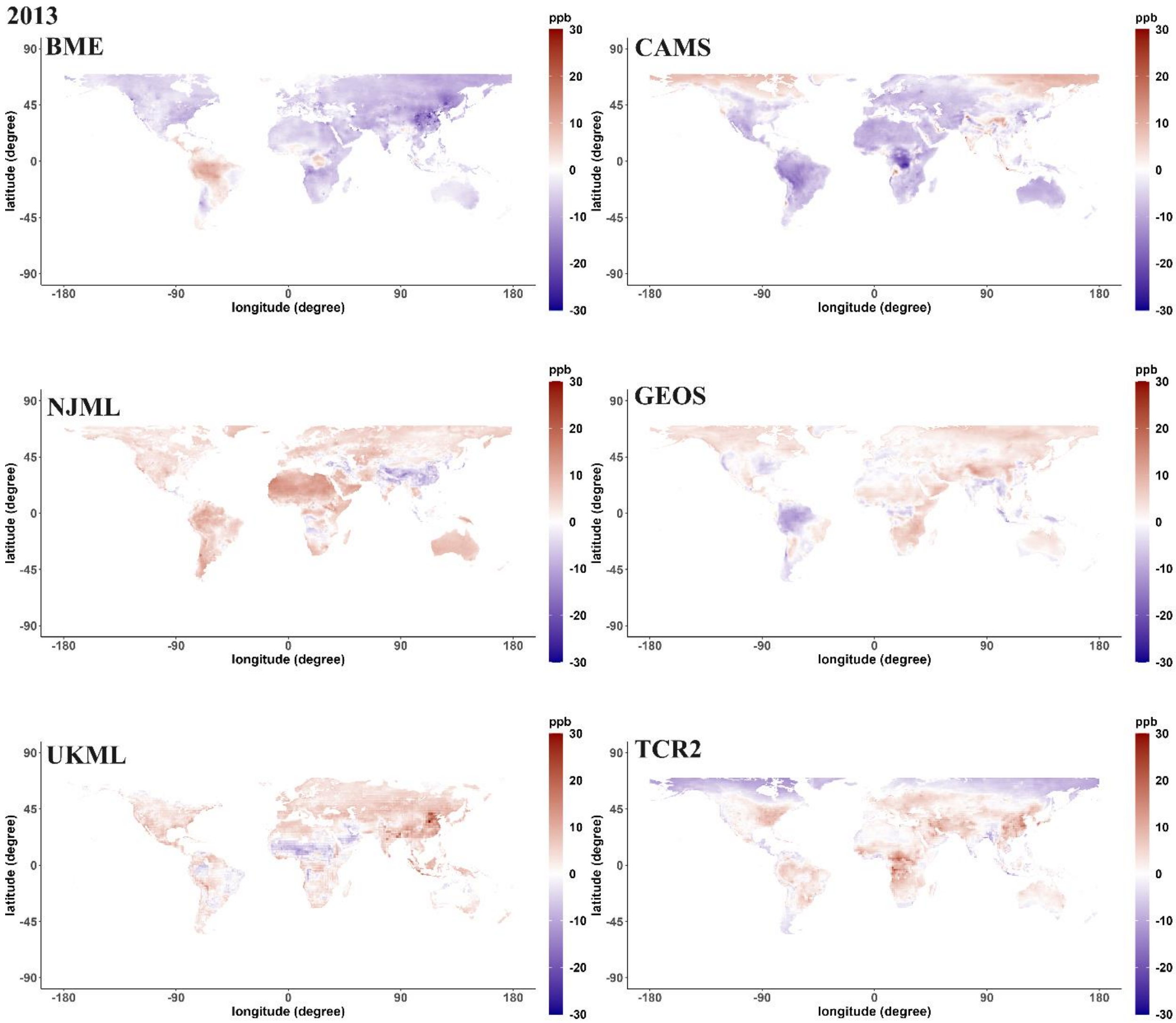
2013
BME
CAMS
NJML
GEOS
UKML
TCR2
ppb
30
20
10
0
-10
-20
-30
latitude (degree)
90
45
0
-45
-90
longitude (degree)
-180
-90
0
90
180

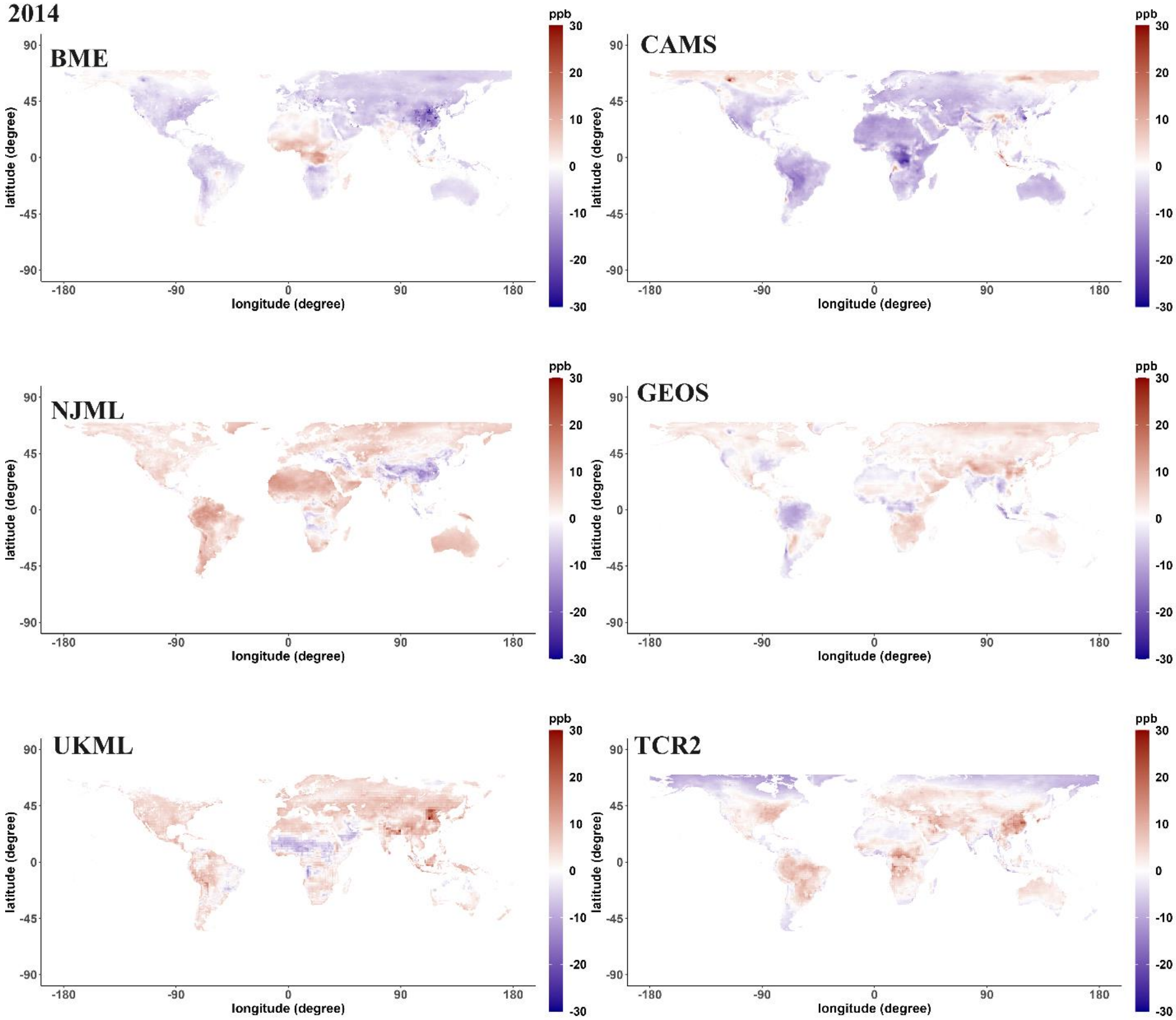
2014
BME
CAMS
NJML
GEOS
UKML
TCR2
latitude (degree)
longitude (degree)
ppb
30
20
10
0
-10
-20
-30
90
45
0
-45
-90
-180
-90
0
90
180

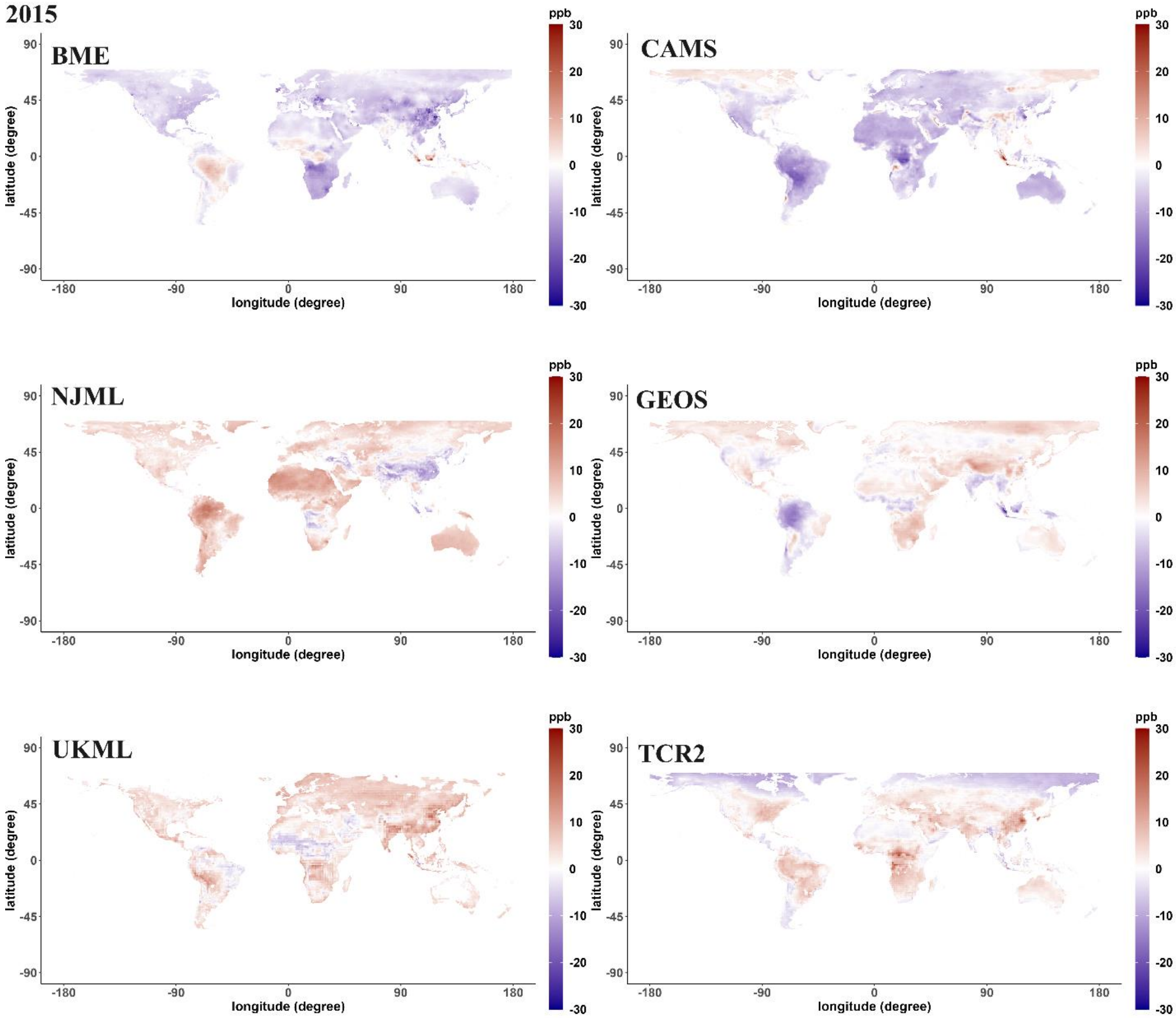
2015
BME
CAMS
NJML
GEOS
UKML
TCR2
latitude (degree)
longitude (degree)
ppb
30
20
10
0
-10
-20
-30
90
45
0
-45
-90
-180
-90
0
90
180

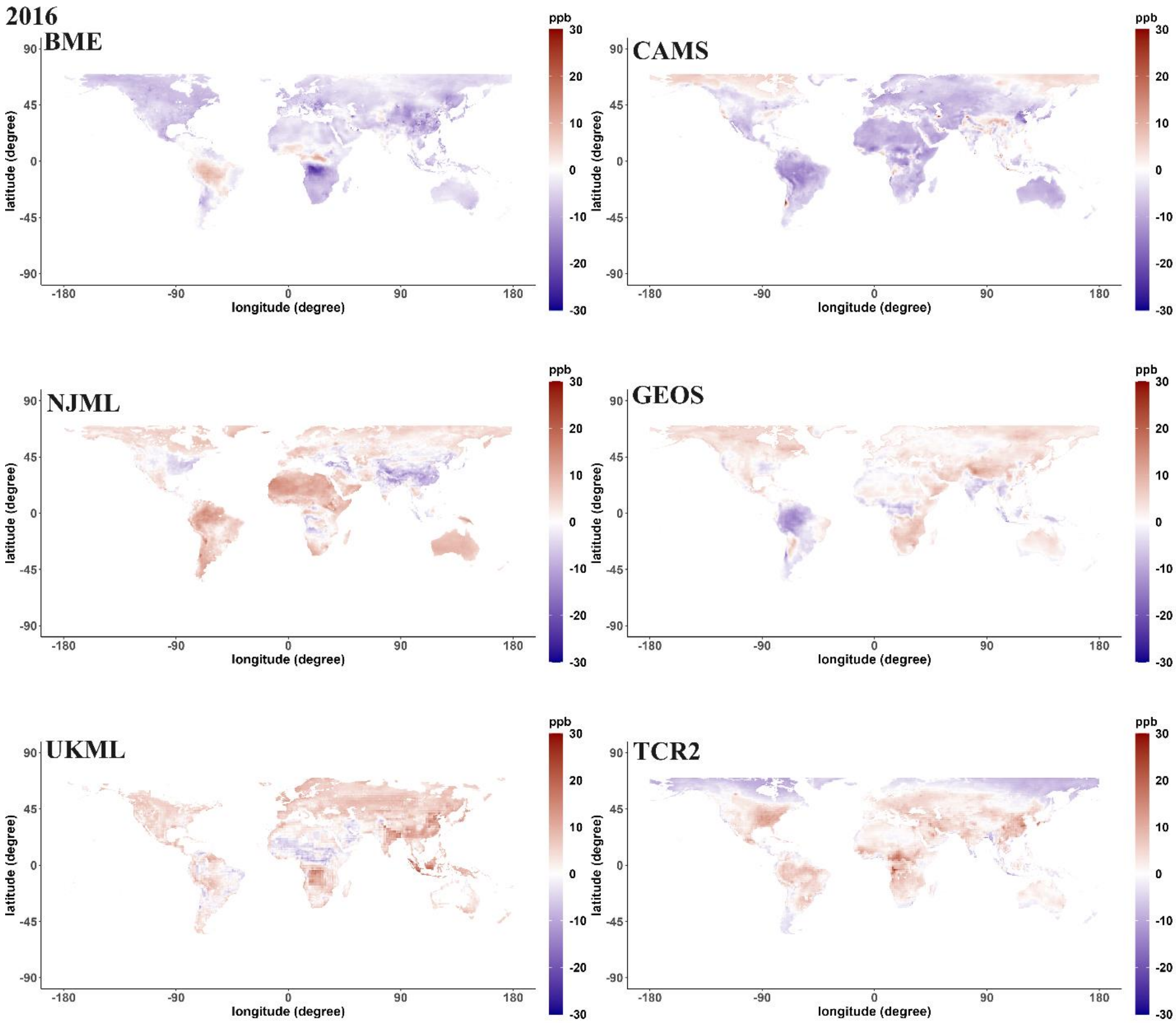
2016
BME
CAMS
NJML
GEOS
UKML
TCR2
ppb
30
20
10
0
-10
-20
-30
latitude (degree)
90
45
0
-45
-90
longitude (degree)
-180
-90
0
90
180

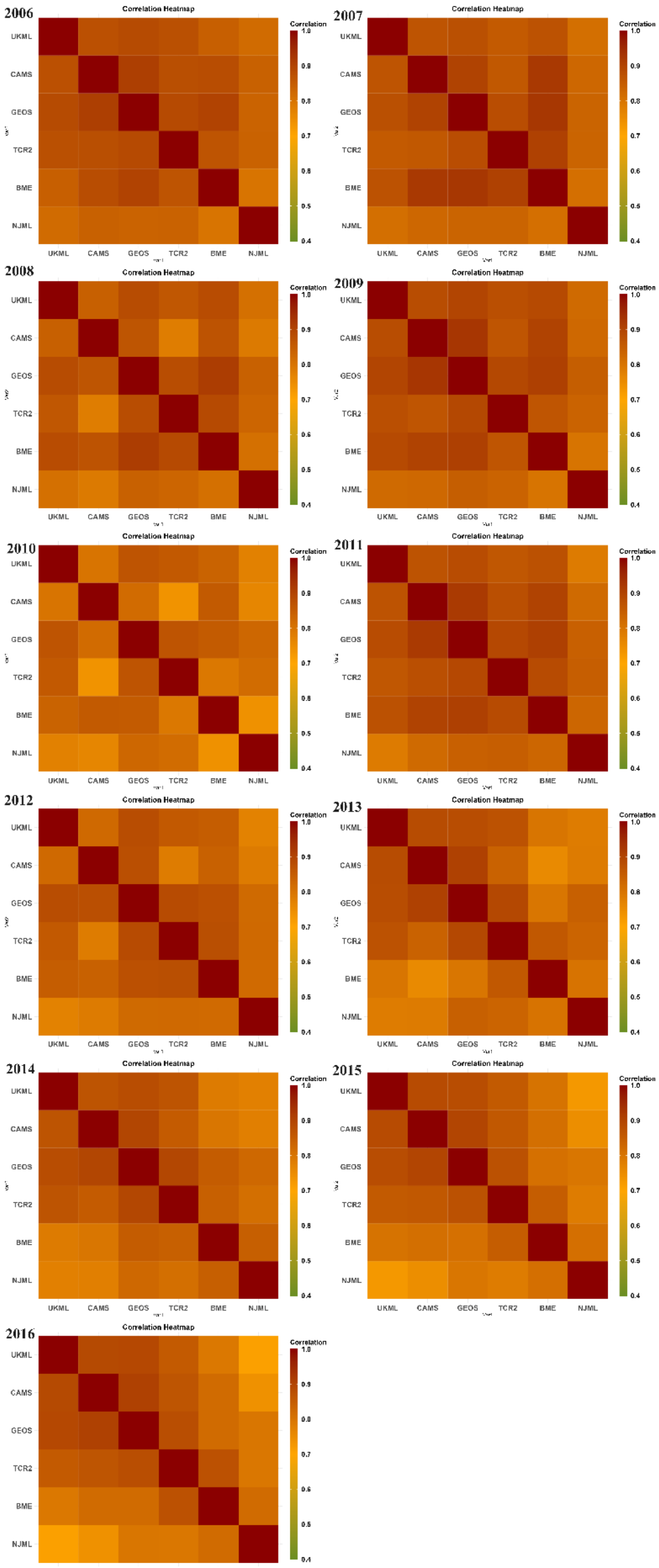

Figure S8. Heatmaps of pairwise correlation (Pearson R) between each dataset from 2006 to 2016.

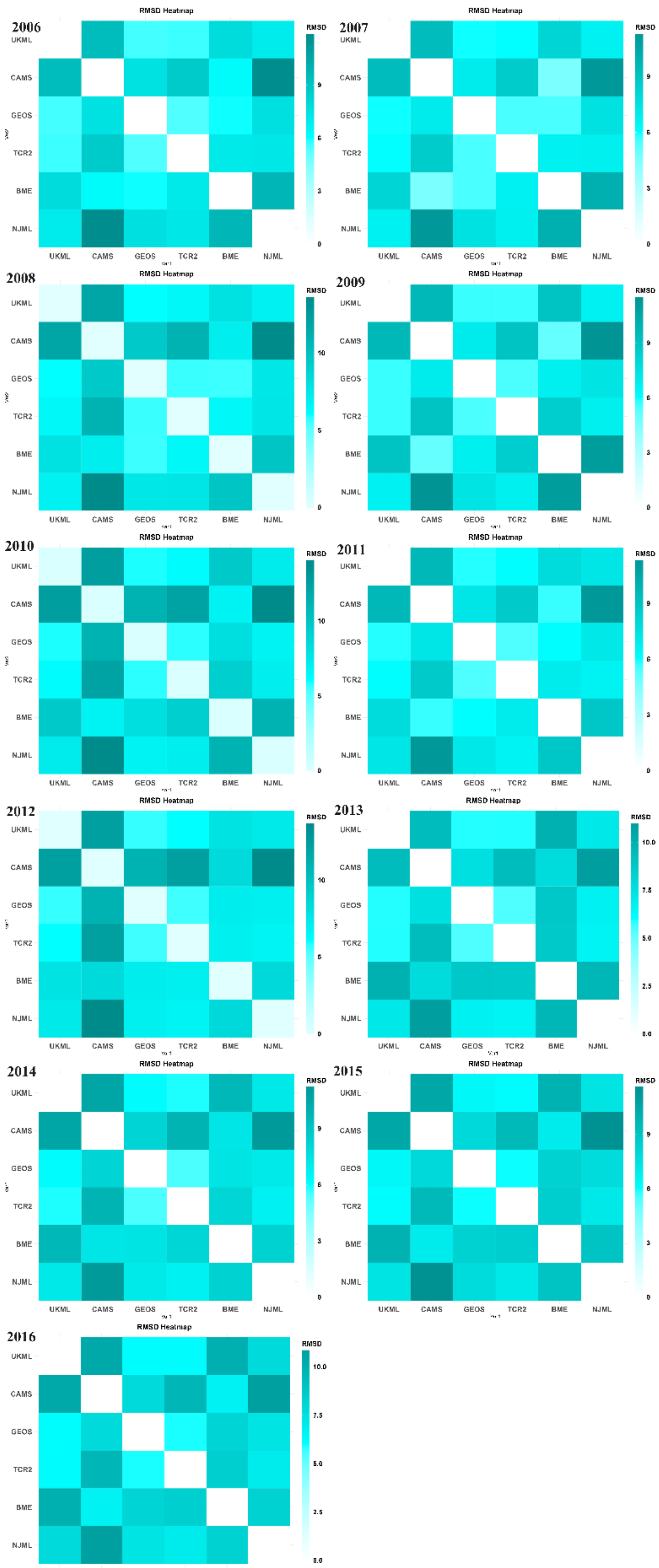

Figure S9. Heatmaps of pairwise Root mean square difference (RMSD) between each dataset from 2006 to 2016.

Figure S10. Population-weighted ozone (OSMDA8) for each year from 2006 to 2016 in different regions. The horizontal axis represents ozone exposure concentrations, and the vertical axis represents population size.

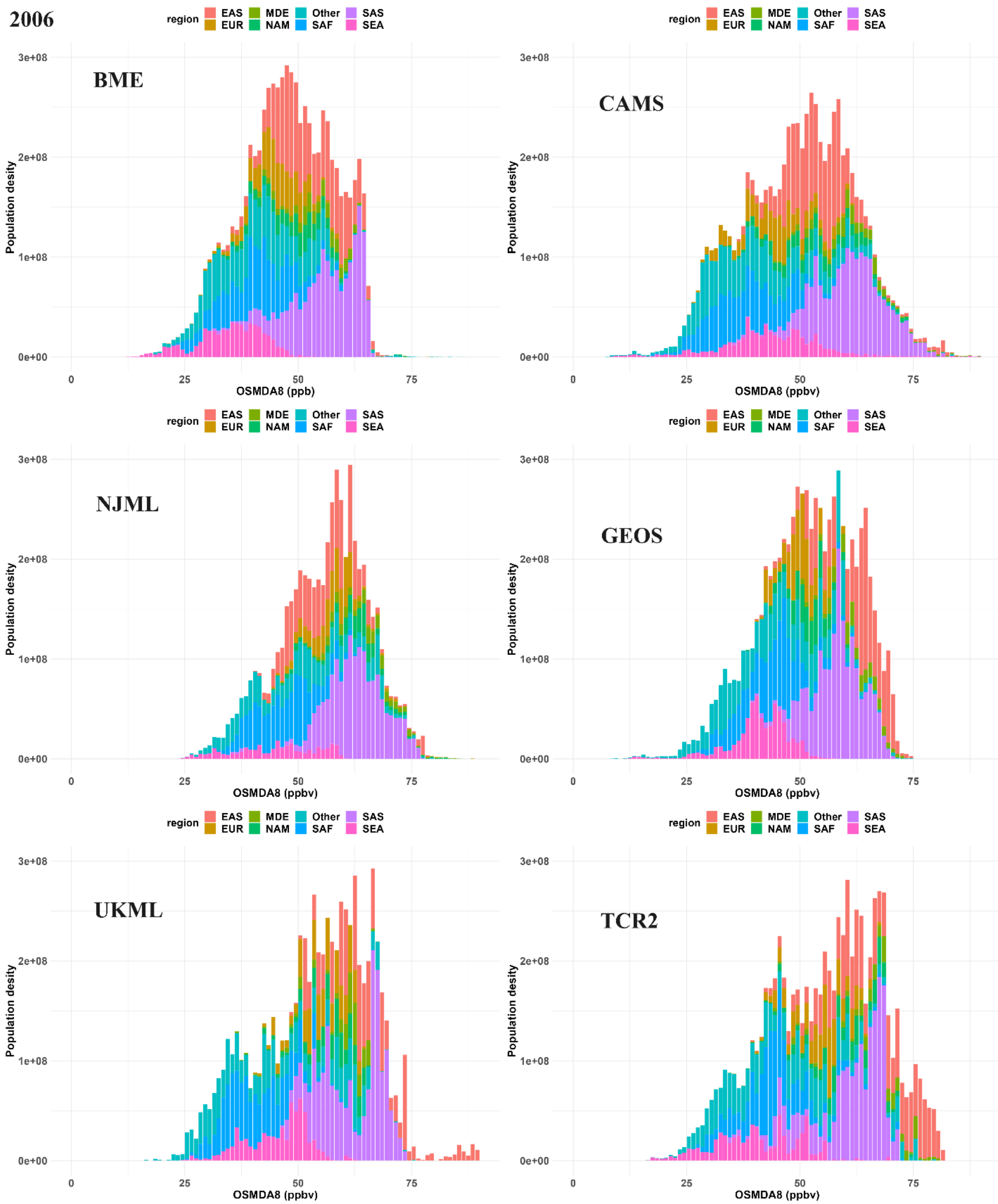

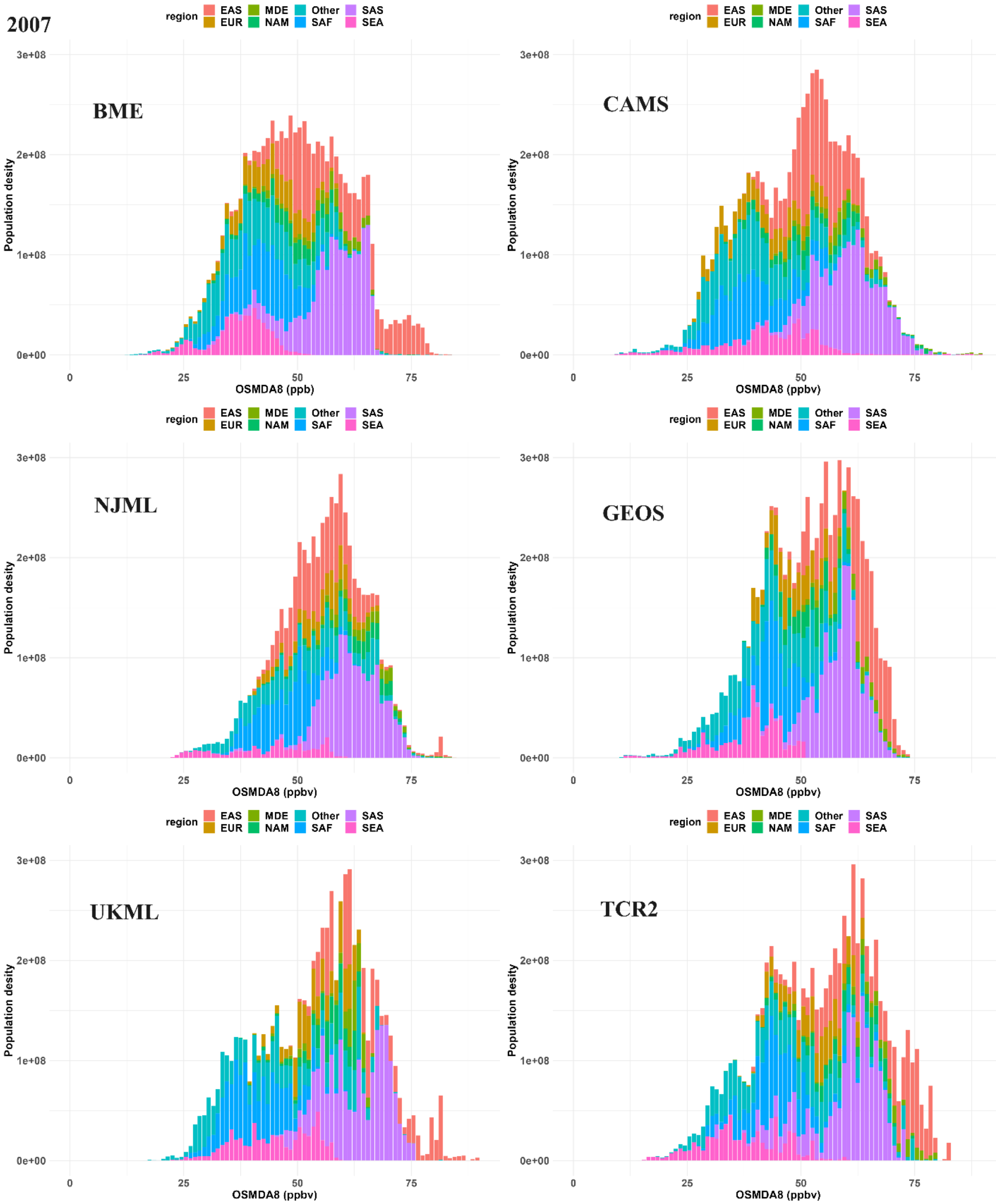
2007
region EAS EUR MDE NAM Other SAF SAS SEA
BME
CAMS
NJML
GEOS
UKML
TCR2
Population desity
OSMDA8 (ppb)
OSMDA8 (ppbv)
3e+08
2e+08
1e+08
0e+00
0
25
50
75

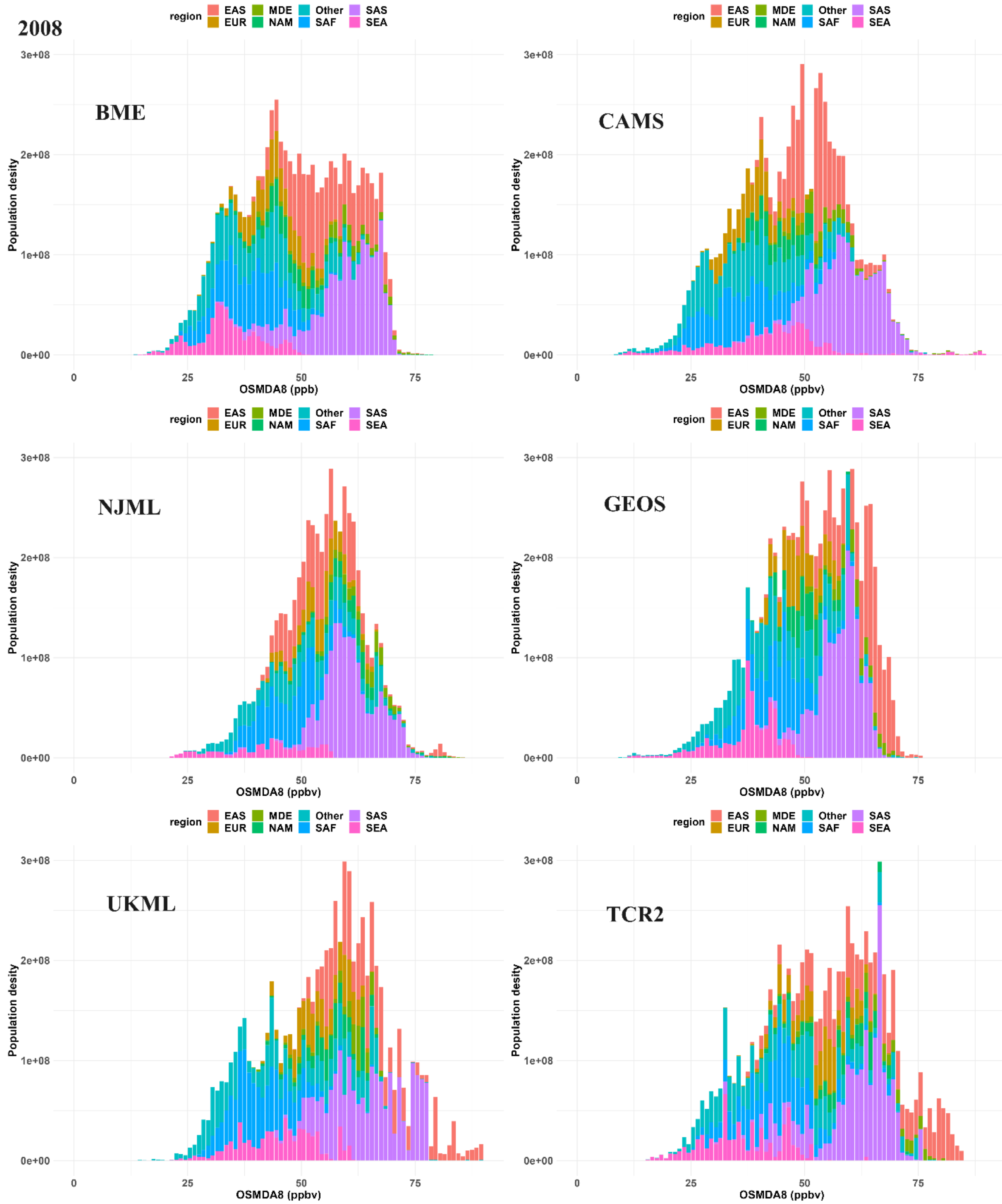
2008
region
EAS
EUR
MDE
NAM
Other
SAF
SAS
SEA
BME
CAMS
NJML
GEOS
UKML
TCR2
Population desity
3e+08
2e+08
1e+08
0e+00
0
25
50
75
OSMDA8 (ppb)
OSMDA8 (ppbv)

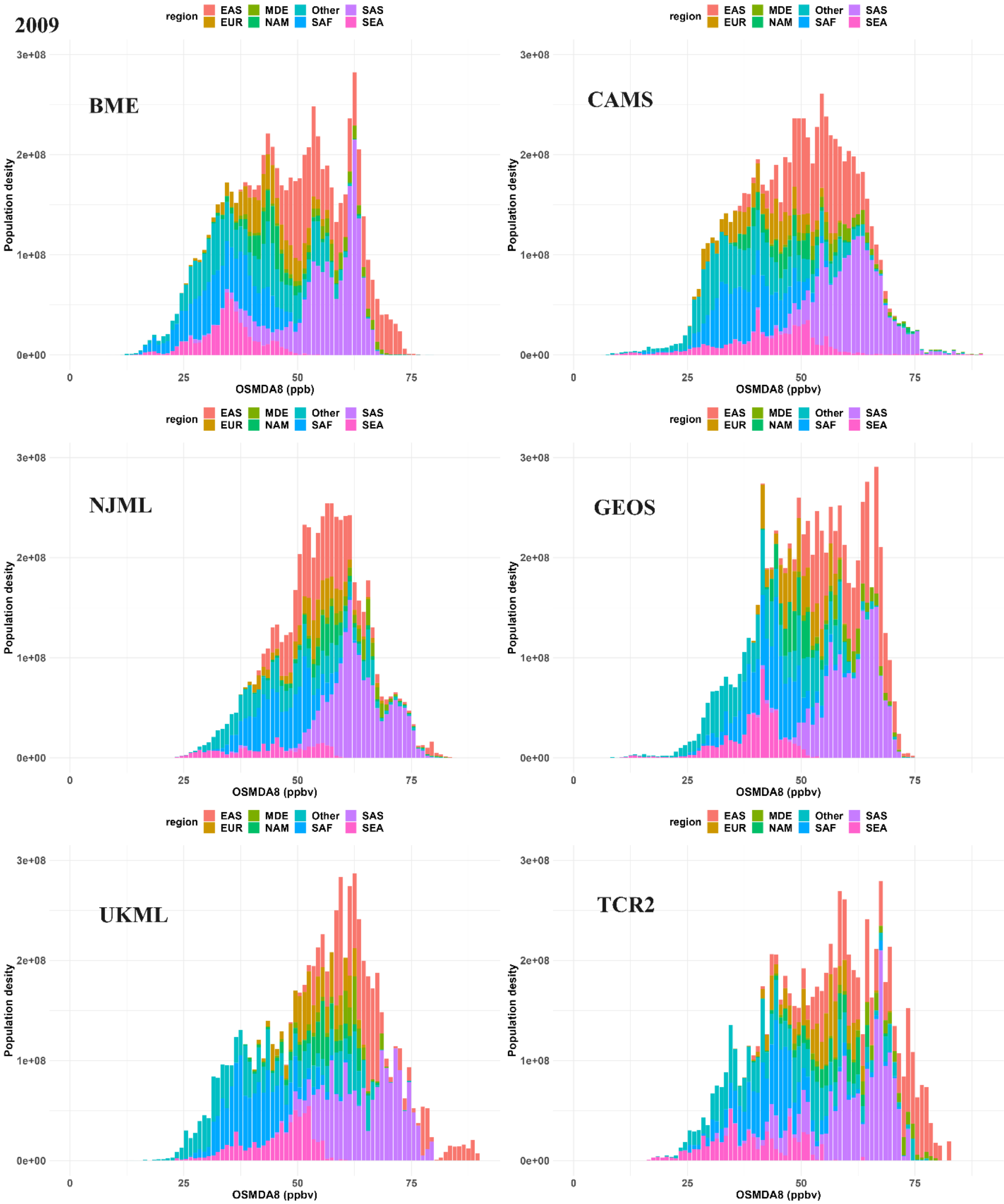
2009
region
EAS
EUR
MDE
NAM
Other
SAF
SAS
SEA
BME
CAMS
NJML
GEOS
UKML
TCR2
Population desity
3e+08
2e+08
1e+08
0e+00
0
25
50
75
OSMDA8 (ppb)
OSMDA8 (ppbv)

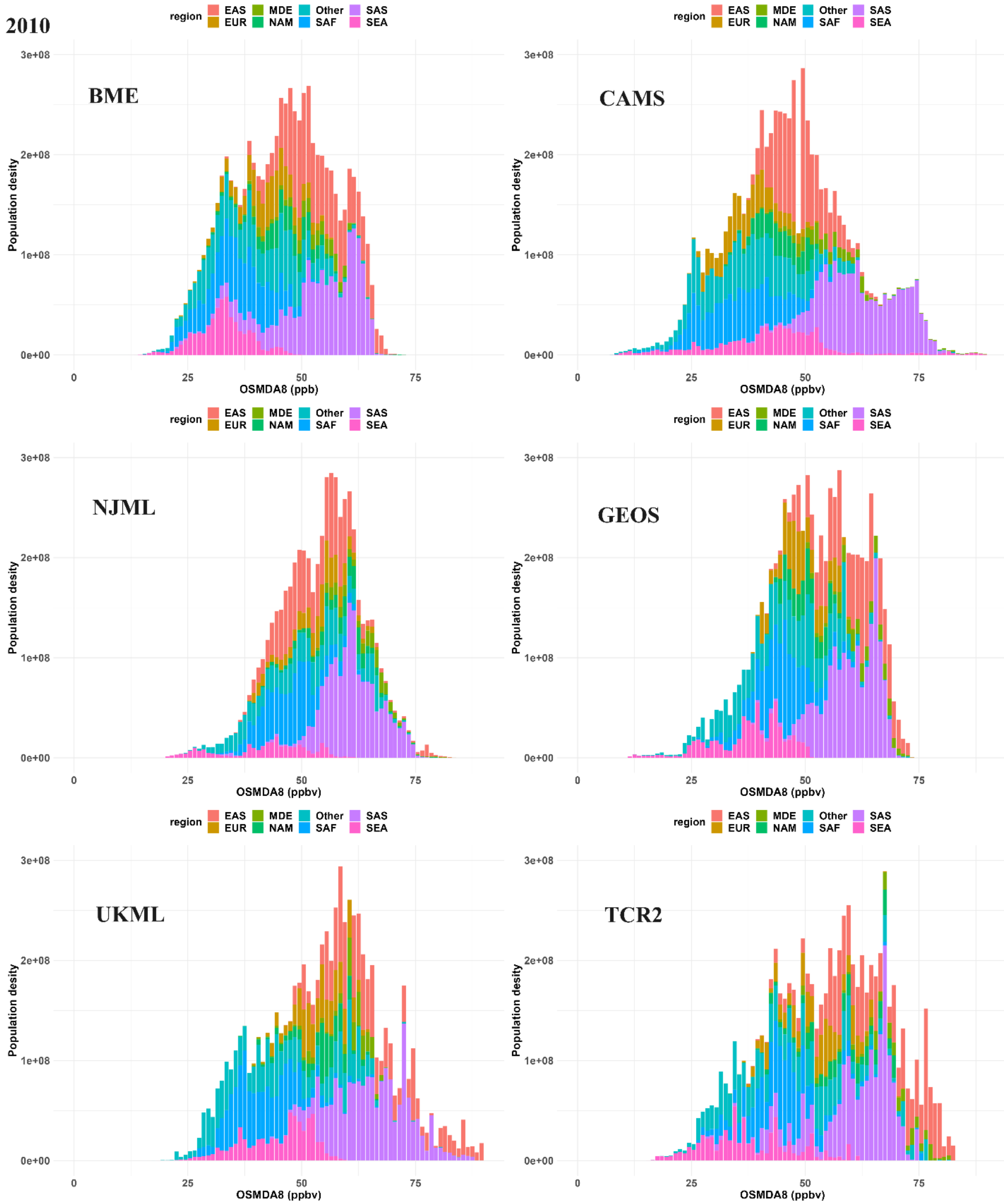
2010
region EAS EUR MDE NAM Other SAF SAS SEA
BME
CAMS
NJML
GEOS
UKML
TCR2
Population desity
3e+08
2e+08
1e+08
0e+00
0
25
50
75
OSMDA8 (ppb)
OSMDA8 (ppbv)

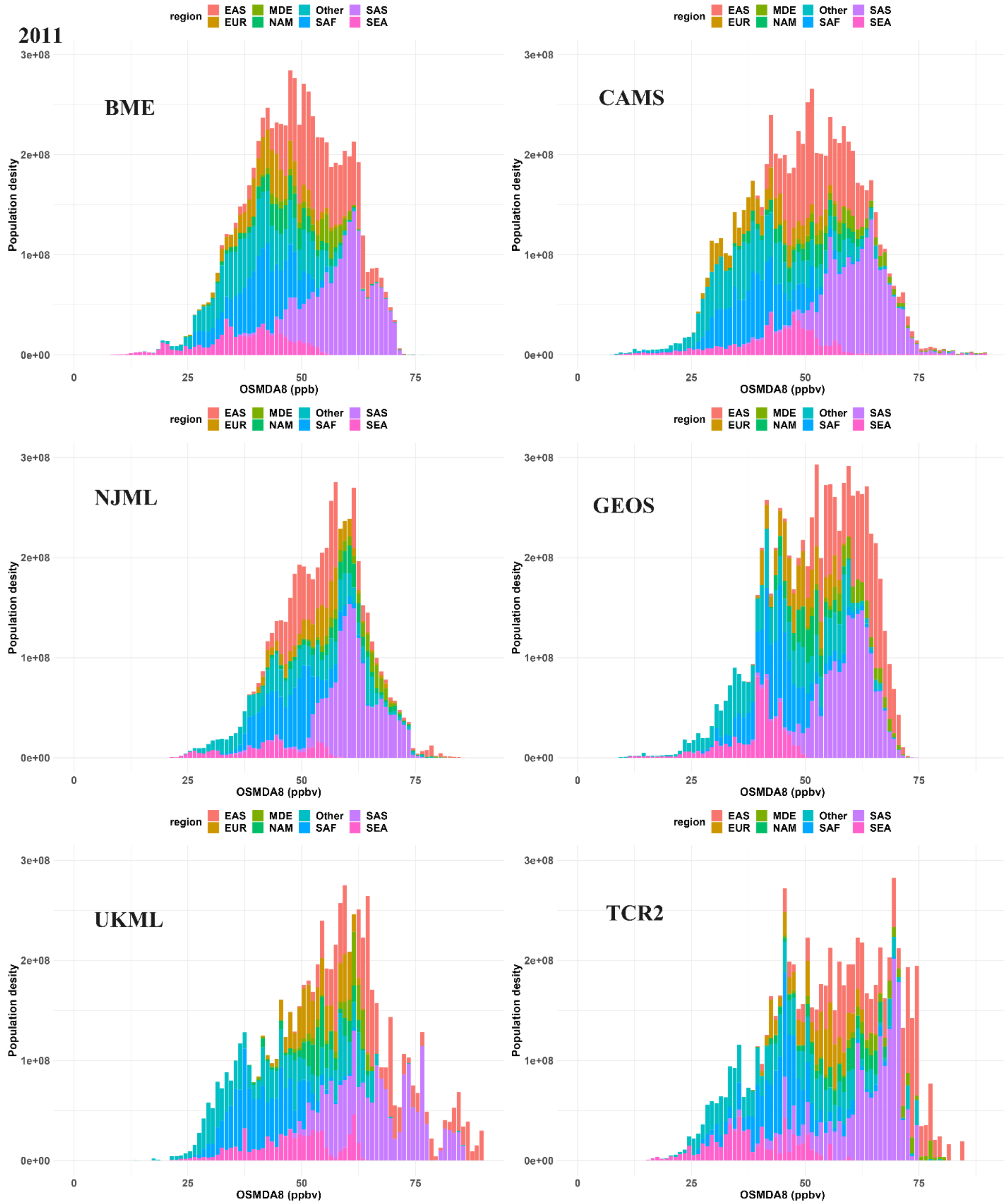
2011
region EAS EUR MDE NAM Other SAF SAS SEA
BME
Population desity
OSMDA8 (ppb)
CAMS
OSMDA8 (ppbv)
NJML
GEOS
UKML
TCR2
3e+08
2e+08
1e+08
0e+00
0
25
50
75

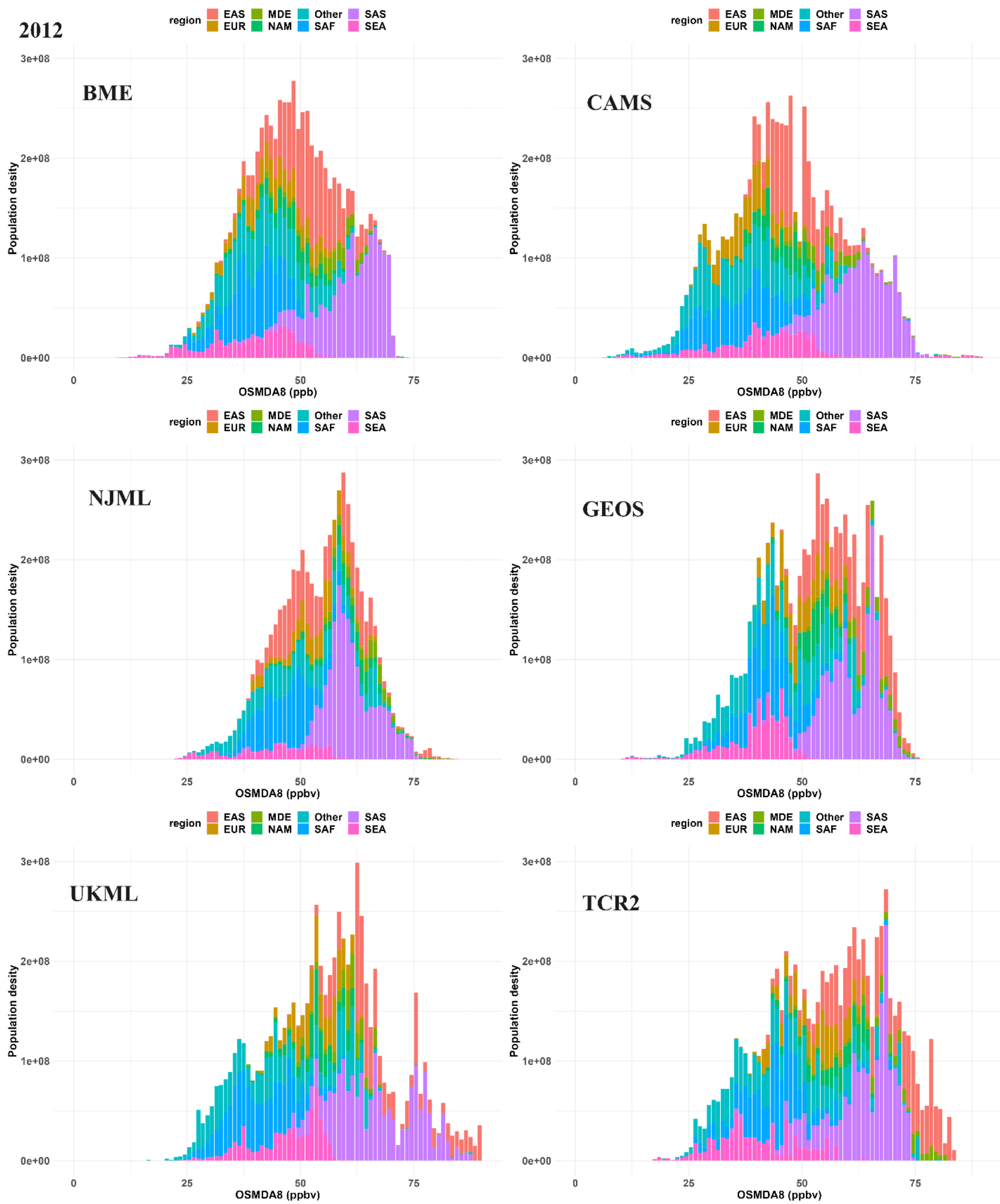
2012
region
EAS EUR MDE NAM Other SAF SAS SEA
BME
CAMS
NJML
GEOS
UKML
TCR2
Population desity
0e+00
1e+08
2e+08
3e+08
0
25
50
75
OSMDA8 (ppb)
OSMDA8 (ppbv)

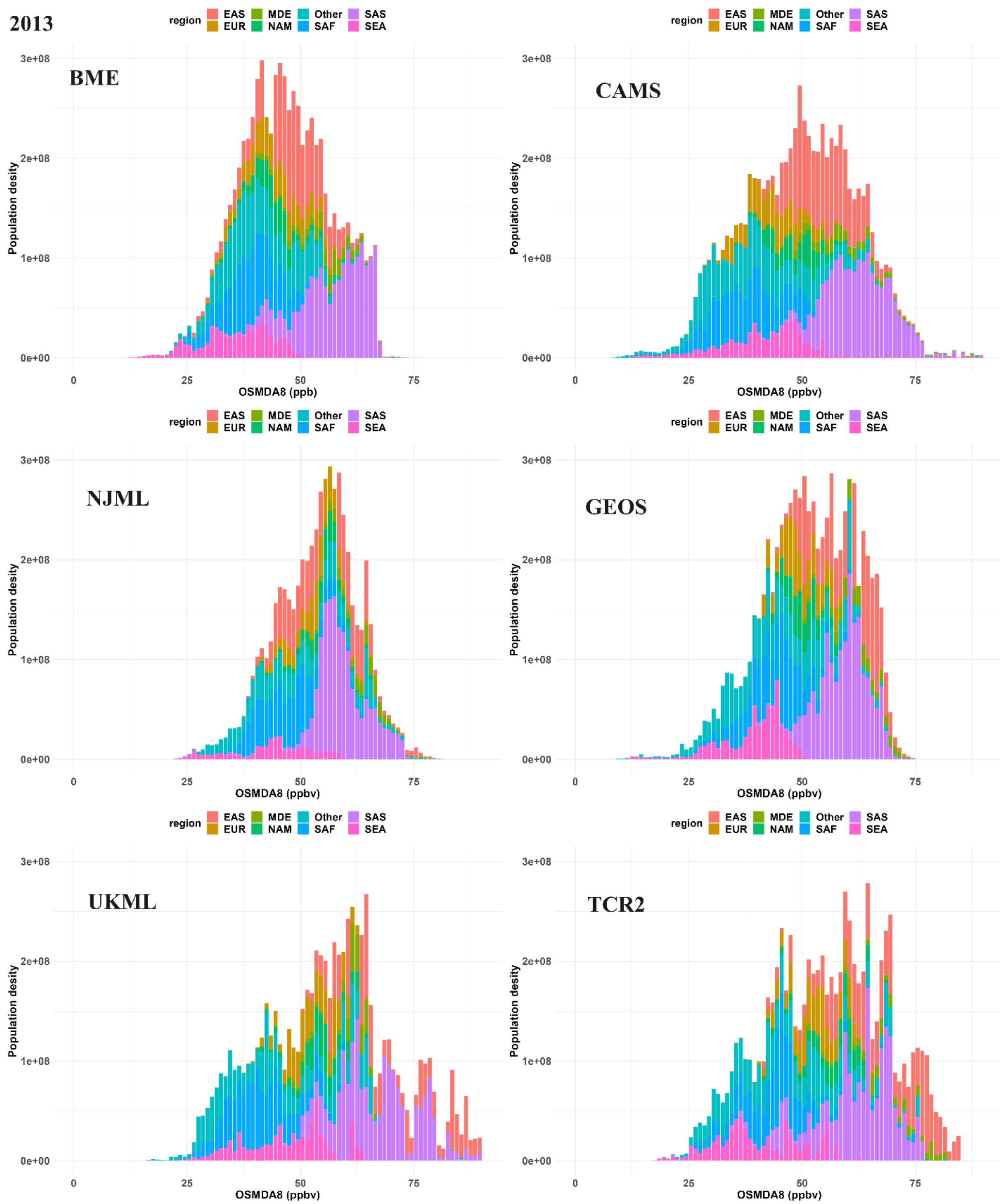
2013
region
EAS EUR MDE NAM Other SAF SAS SEA
BME
CAMS
NJML
GEOS
UKML
TCR2
Population desity
3e+08
2e+08
1e+08
0e+00
0
25
50
75
OSMDA8 (ppb)
OSMDA8 (ppbv)

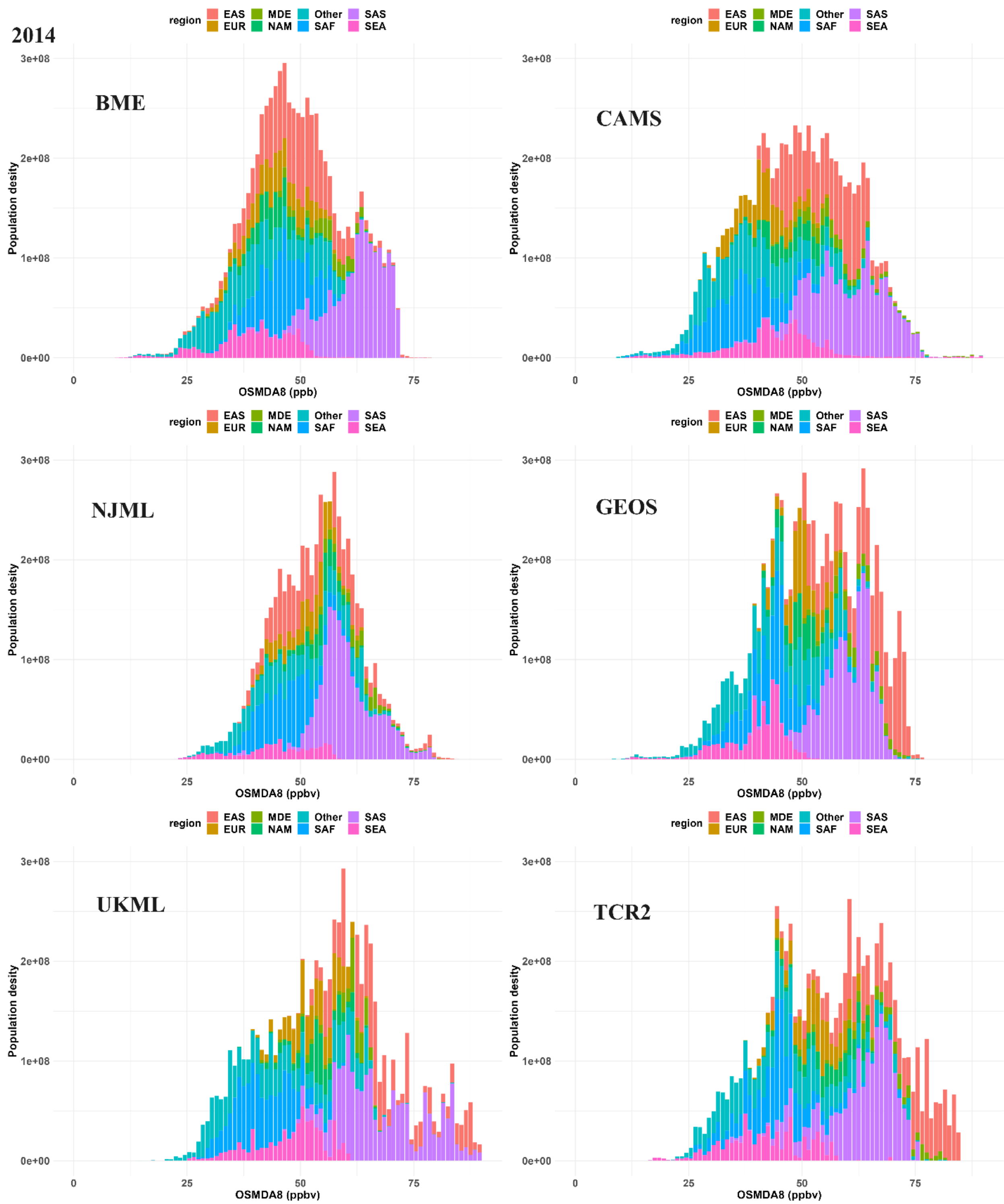
2014
region
EAS
EUR
MDE
NAM
Other
SAF
SAS
SEA
BME
CAMS
NJML
GEOS
UKML
TCR2
Population desity
3e+08
2e+08
1e+08
0e+00
0
25
50
75
OSMDA8 (ppb)
OSMDA8 (ppbv)

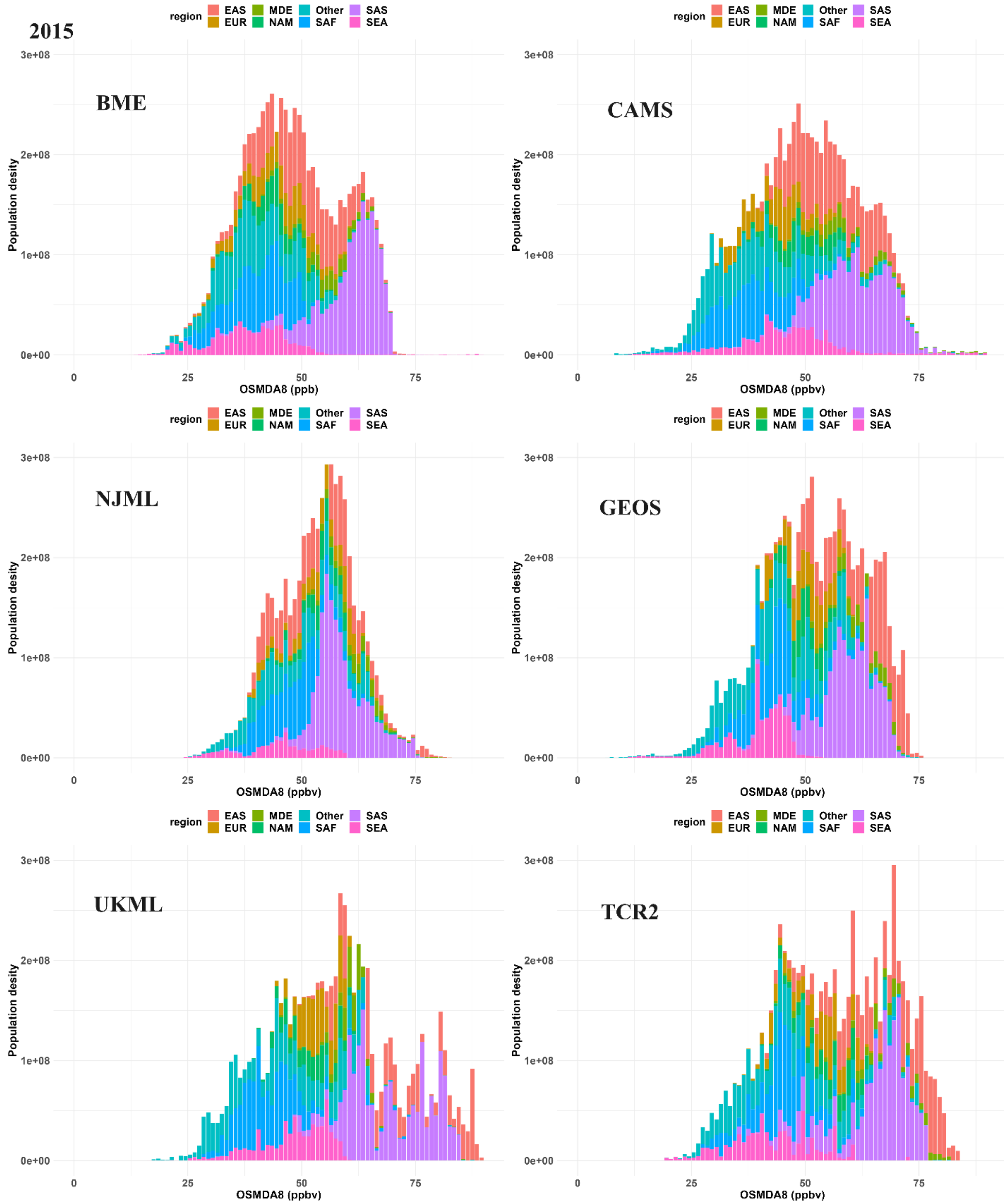
2015
region
EAS
EUR
MDE
NAM
Other
SAF
SAS
SEA
BME
CAMS
NJML
GEOS
UKML
TCR2
Population desity
3e+08
2e+08
1e+08
0e+00
0
25
50
75
OSMDA8 (ppb)
OSMDA8 (ppbv)

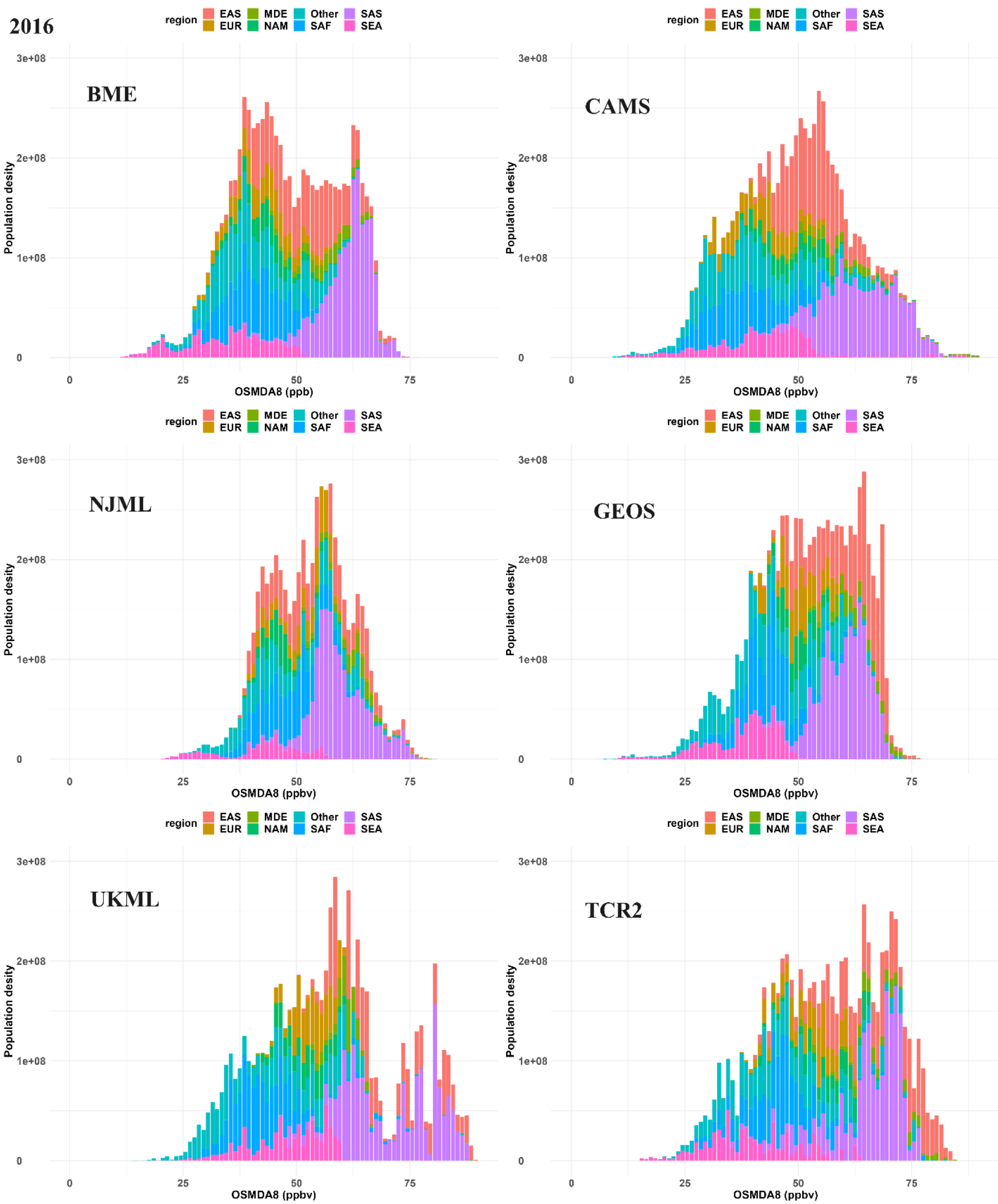
2016
BME
CAMS
NJML
GEOS
UKML
TCR2
region
EAS
EUR
MDE
NAM
Other
SAF
SAS
SEA
Population desity
3e+08
2e+08
1e+08
0
0
25
50
75
OSMDA8 (ppb)
OSMDA8 (ppbv)

Figure S11. Performance evaluations of six datasets with TOAR-II observations for OSDMA8 for each year from 2006 to 2015. The evaluation includes all monitor stations in the TOAR-II network for each year (2006 to 2015).

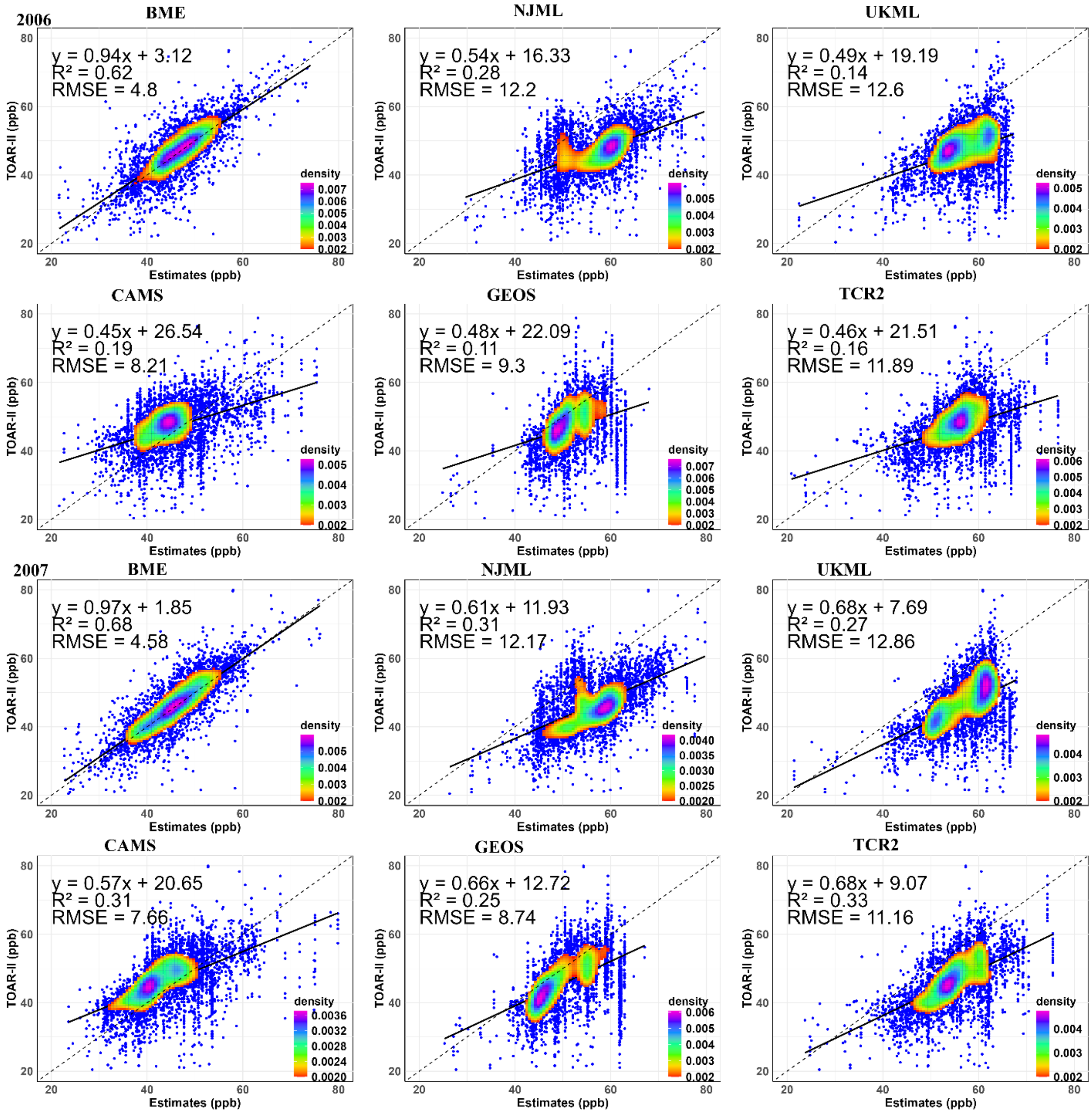

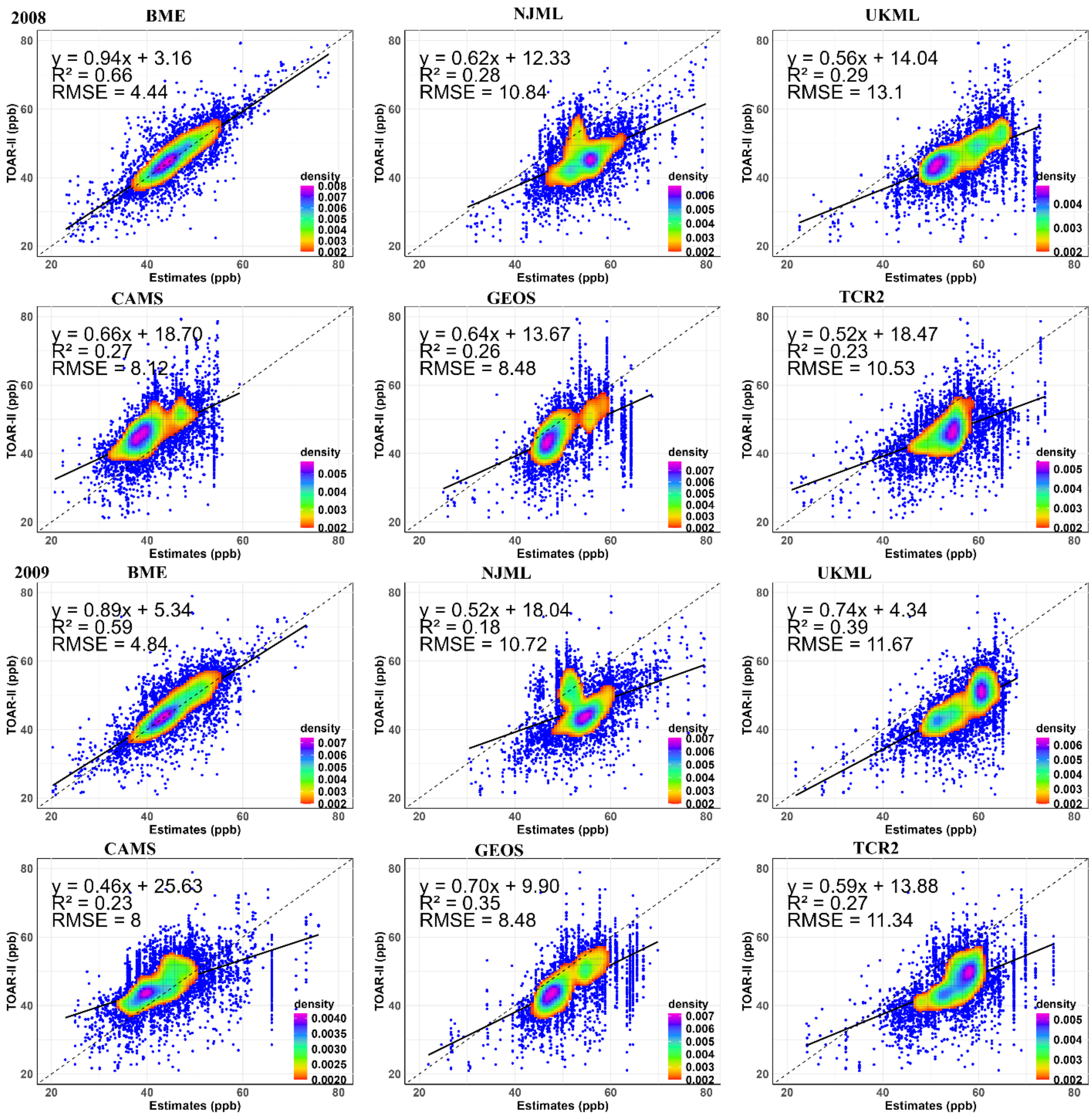
2008
BME
y = 0.94x + 3.16
R² = 0.66
RMSE = 4.44
NJML
y = 0.62x + 12.33
R² = 0.28
RMSE = 10.84
UKML
y = 0.56x + 14.04
R² = 0.29
RMSE = 13.1
CAMS
y = 0.66x + 18.70
R² = 0.27
RMSE = 8.12
GEOS
y = 0.64x + 13.67
R² = 0.26
RMSE = 8.48
TCR2
y = 0.52x + 18.47
R² = 0.23
RMSE = 10.53
2009
BME
y = 0.89x + 5.34
R² = 0.59
RMSE = 4.84
NJML
y = 0.52x + 18.04
R² = 0.18
RMSE = 10.72
UKML
y = 0.74x + 4.34
R² = 0.39
RMSE = 11.67
CAMS
y = 0.46x + 25.63
R² = 0.23
RMSE = 8
GEOS
y = 0.70x + 9.90
R² = 0.35
RMSE = 8.48
TCR2
y = 0.59x + 13.88
R² = 0.27
RMSE = 11.34
TOAR-II (ppb)
Estimates (ppb)
density

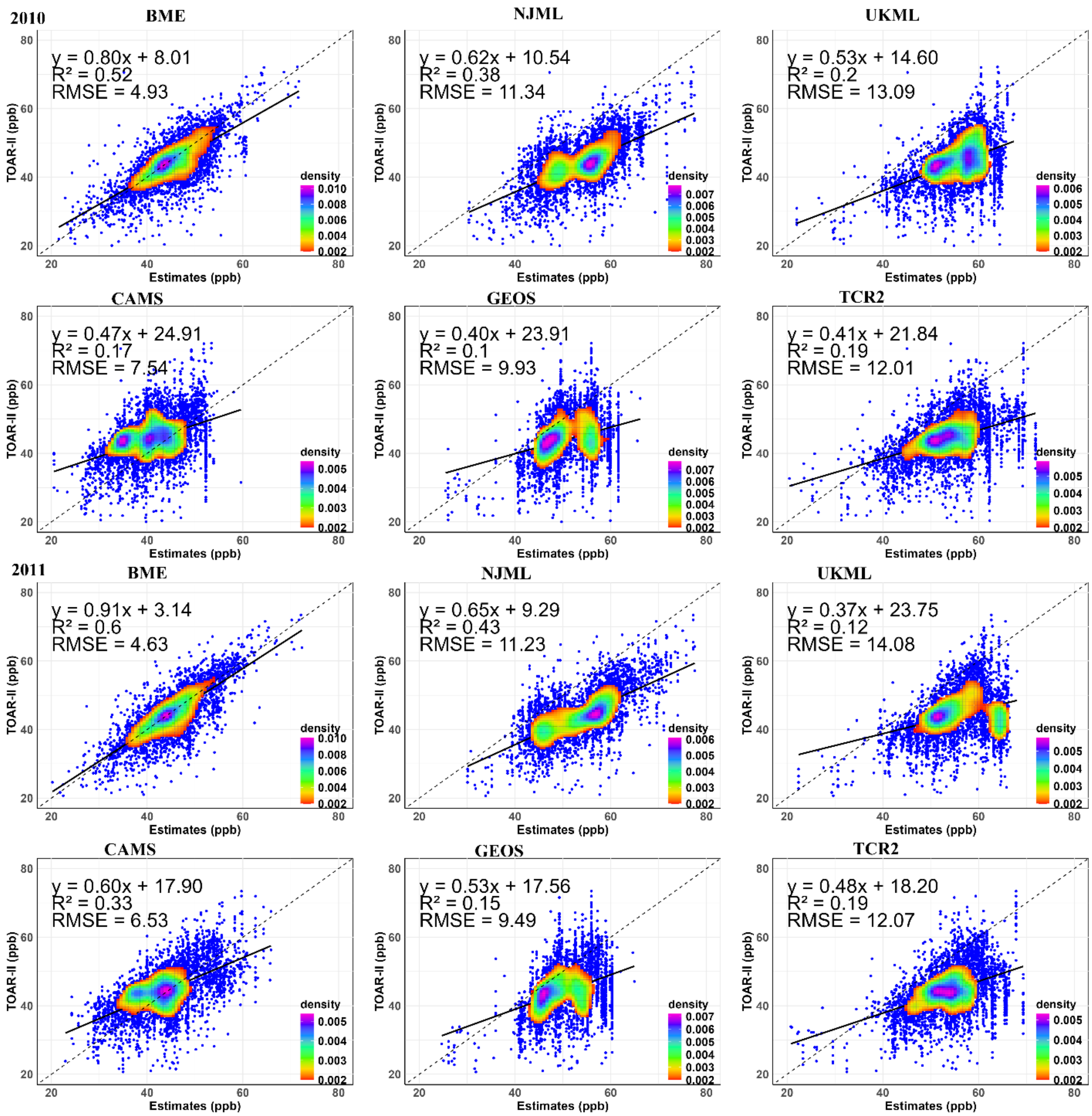

2010
BME
y = 0.80x + 8.01
R² = 0.52
RMSE = 4.93
NJML
y = 0.62x + 10.54
R² = 0.38
RMSE = 11.34
UKML
y = 0.53x + 14.60
R² = 0.2
RMSE = 13.09
CAMS
y = 0.47x + 24.91
R² = 0.17
RMSE = 7.54
GEOS
y = 0.40x + 23.91
R² = 0.1
RMSE = 9.93
TCR2
y = 0.41x + 21.84
R² = 0.19
RMSE = 12.01
2011
BME
y = 0.91x + 3.14
R² = 0.6
RMSE = 4.63
NJML
y = 0.65x + 9.29
R² = 0.43
RMSE = 11.23
UKML
y = 0.37x + 23.75
R² = 0.12
RMSE = 14.08
CAMS
y = 0.60x + 17.90
R² = 0.33
RMSE = 6.53
GEOS
y = 0.53x + 17.56
R² = 0.15
RMSE = 9.49
TCR2
y = 0.48x + 18.20
R² = 0.19
RMSE = 12.07
density
TOAR-II (ppb)
Estimates (ppb)

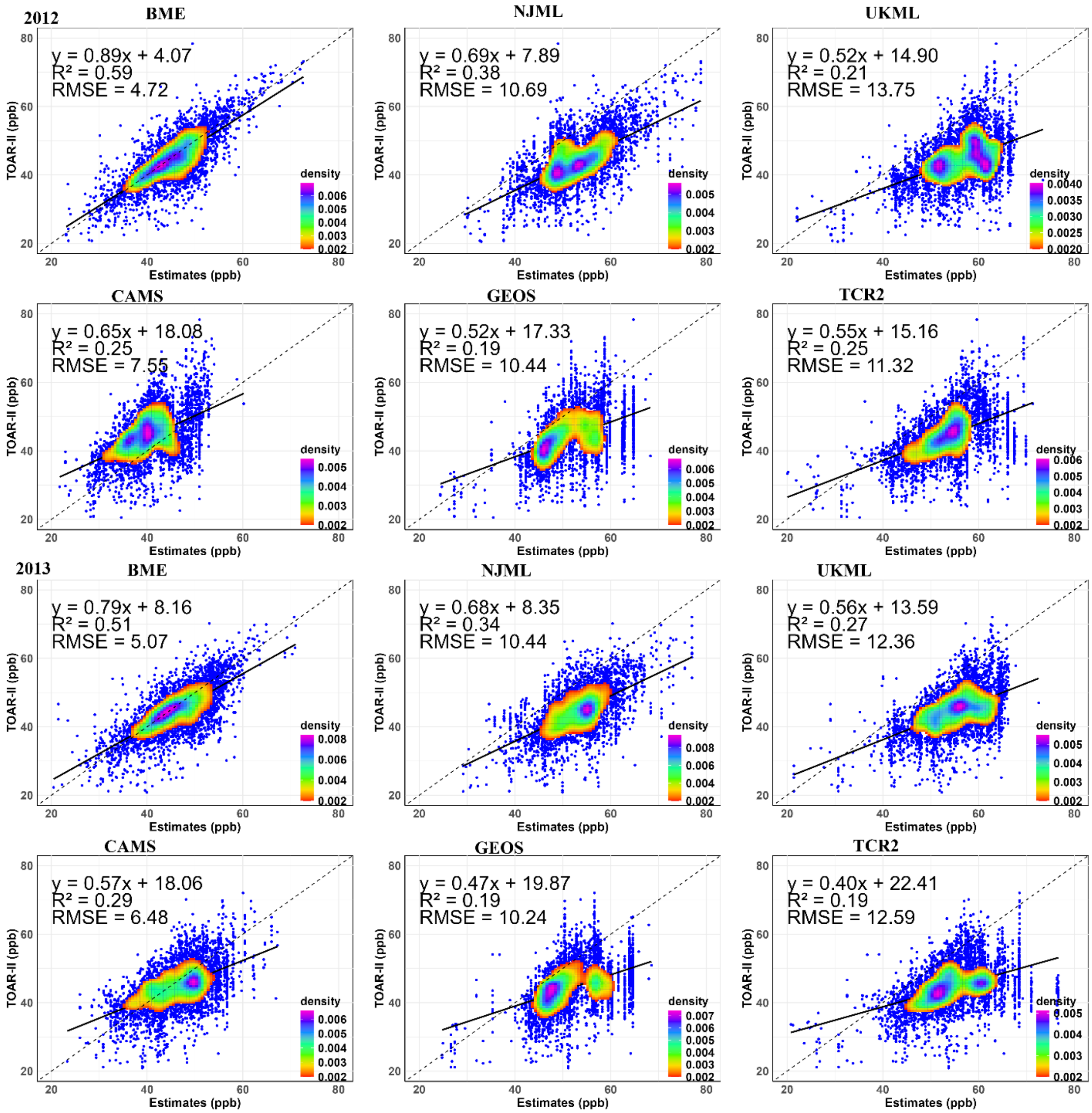
2012
BME
y = 0.89x + 4.07
R² = 0.59
RMSE = 4.72
NJML
y = 0.69x + 7.89
R² = 0.38
RMSE = 10.69
UKML
y = 0.52x + 14.90
R² = 0.21
RMSE = 13.75
CAMS
y = 0.65x + 18.08
R² = 0.25
RMSE = 7.55
GEOS
y = 0.52x + 17.33
R² = 0.19
RMSE = 10.44
TCR2
y = 0.55x + 15.16
R² = 0.25
RMSE = 11.32
2013
BME
y = 0.79x + 8.16
R² = 0.51
RMSE = 5.07
NJML
y = 0.68x + 8.35
R² = 0.34
RMSE = 10.44
UKML
y = 0.56x + 13.59
R² = 0.27
RMSE = 12.36
CAMS
y = 0.57x + 18.06
R² = 0.29
RMSE = 6.48
GEOS
y = 0.47x + 19.87
R² = 0.19
RMSE = 10.24
TCR2
y = 0.40x + 22.41
R² = 0.19
RMSE = 12.59
TOAR-II (ppb)
Estimates (ppb)
density

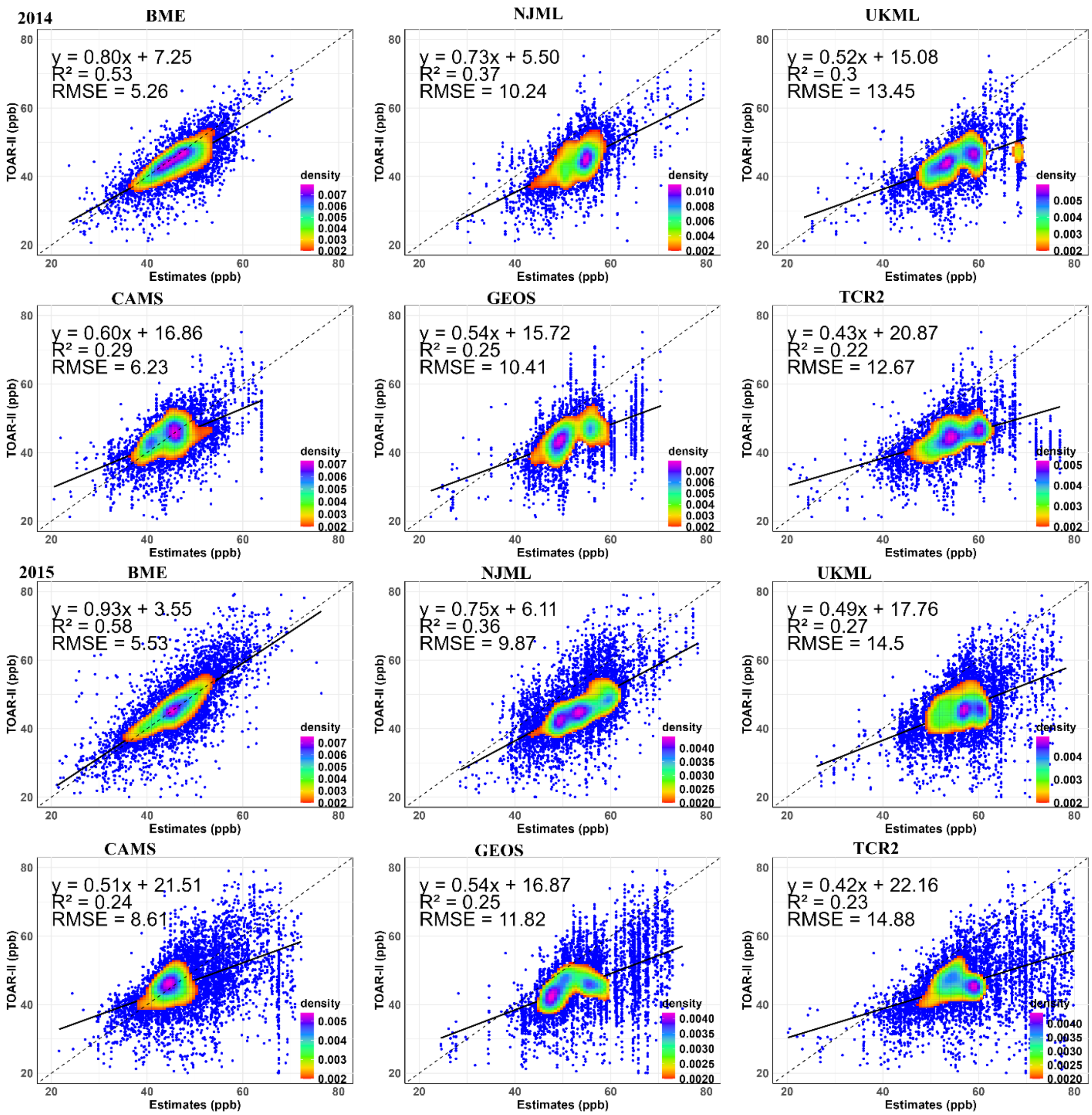
2014
BME
y = 0.80x + 7.25
R² = 0.53
RMSE = 5.26
NJML
y = 0.73x + 5.50
R² = 0.37
RMSE = 10.24
UKML
y = 0.52x + 15.08
R² = 0.3
RMSE = 13.45
CAMS
y = 0.60x + 16.86
R² = 0.29
RMSE = 6.23
GEOS
y = 0.54x + 15.72
R² = 0.25
RMSE = 10.41
TCR2
y = 0.43x + 20.87
R² = 0.22
RMSE = 12.67
2015
BME
y = 0.93x + 3.55
R² = 0.58
RMSE = 5.53
NJML
y = 0.75x + 6.11
R² = 0.36
RMSE = 9.87
UKML
y = 0.49x + 17.76
R² = 0.27
RMSE = 14.5
CAMS
y = 0.51x + 21.51
R² = 0.24
RMSE = 8.61
GEOS
y = 0.54x + 16.87
R² = 0.25
RMSE = 11.82
TCR2
y = 0.42x + 22.16
R² = 0.23
RMSE = 14.88
density
TOAR-II (ppb)
Estimates (ppb)

Figure S12. Performance evaluations of six datasets with TOAR-II observations for OSDMA8 for each year from 2006 to 2015. The evaluation only includes monitor stations above 50ppb in TOAR-II network for each year (2006 to 2015).

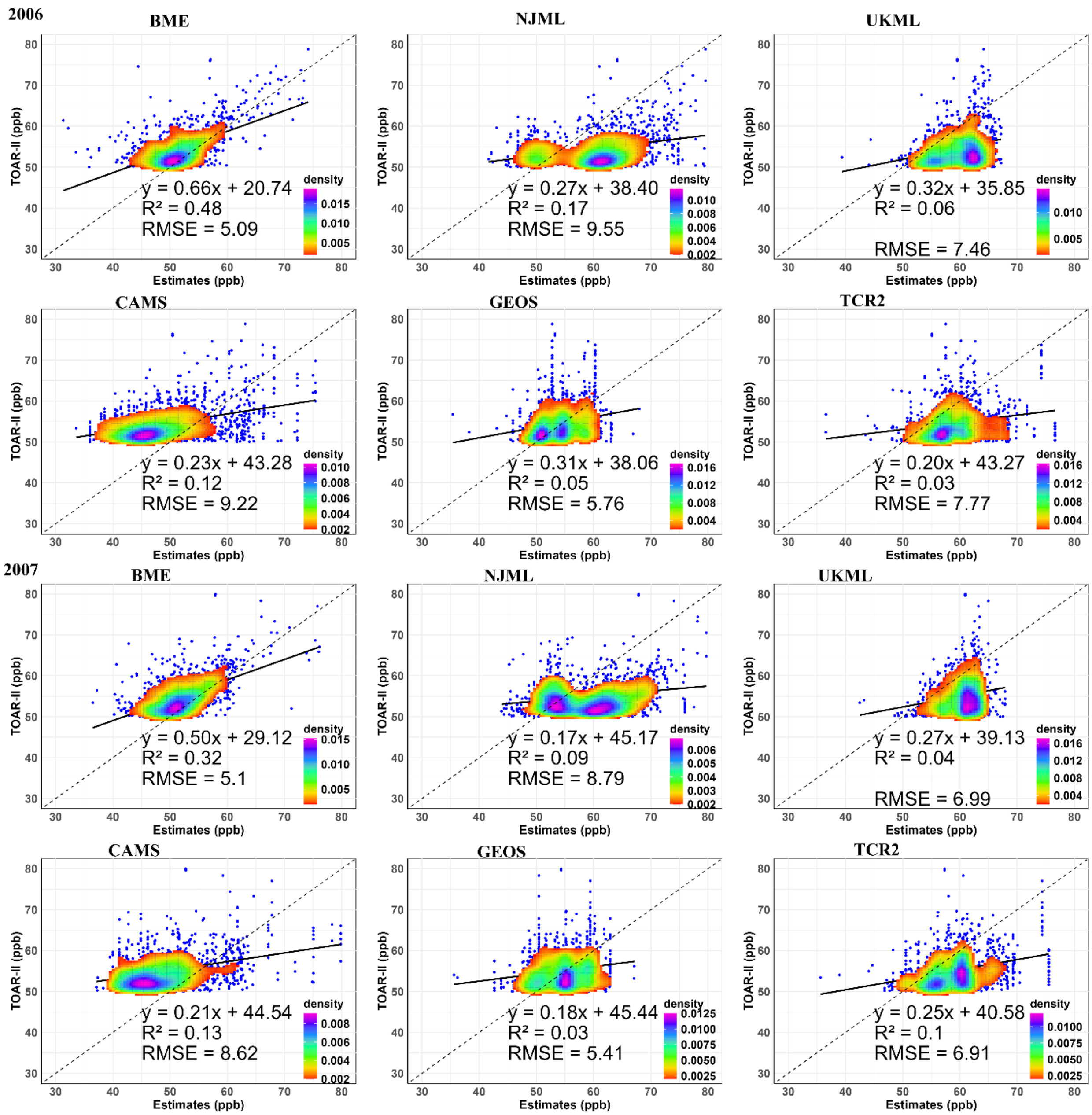

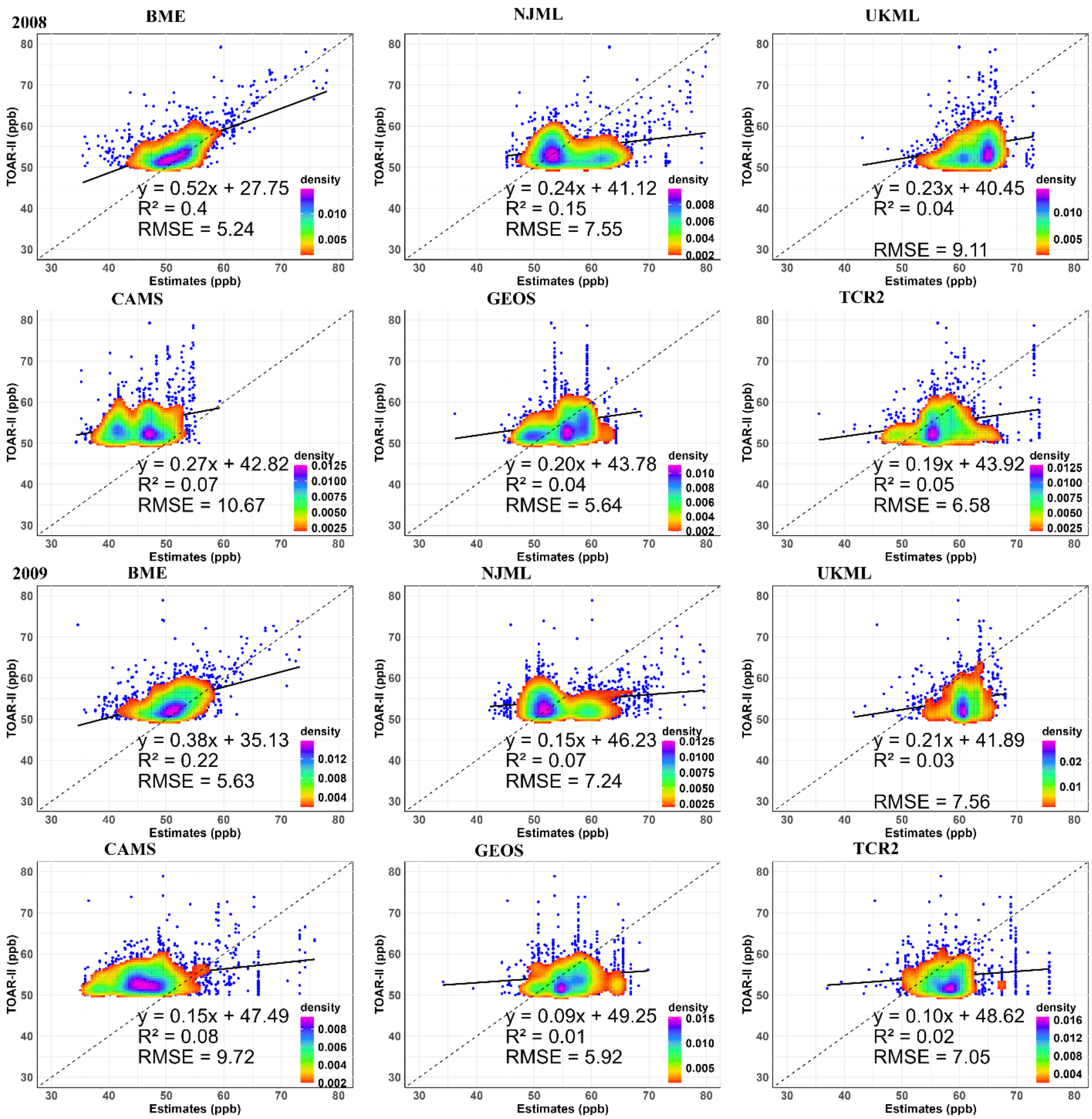
2008
BME
y = 0.52x + 27.75
R² = 0.4
RMSE = 5.24
NJML
y = 0.24x + 41.12
R² = 0.15
RMSE = 7.55
UKML
y = 0.23x + 40.45
R² = 0.04
RMSE = 9.11
CAMS
y = 0.27x + 42.82
R² = 0.07
RMSE = 10.67
GEOS
y = 0.20x + 43.78
R² = 0.04
RMSE = 5.64
TCR2
y = 0.19x + 43.92
R² = 0.05
RMSE = 6.58
2009
BME
y = 0.38x + 35.13
R² = 0.22
RMSE = 5.63
NJML
y = 0.15x + 46.23
R² = 0.07
RMSE = 7.24
UKML
y = 0.21x + 41.89
R² = 0.03
RMSE = 7.56
CAMS
y = 0.15x + 47.49
R² = 0.08
RMSE = 9.72
GEOS
y = 0.09x + 49.25
R² = 0.01
RMSE = 5.92
TCR2
y = 0.10x + 48.62
R² = 0.02
RMSE = 7.05
TOAR-II (ppb)
Estimates (ppb)
density

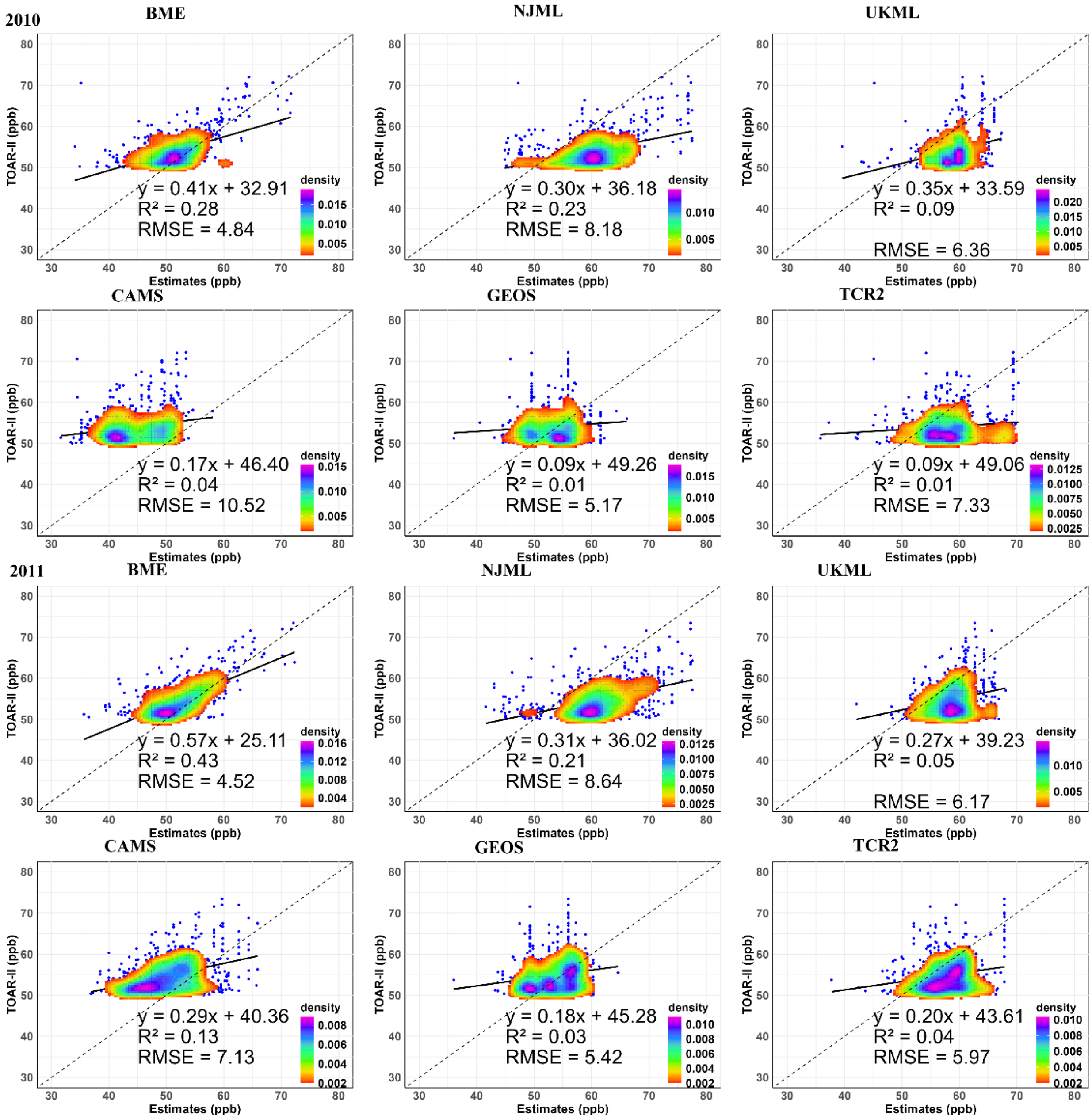
2010
BME
y = 0.41x + 32.91
R² = 0.28
RMSE = 4.84
NJML
y = 0.30x + 36.18
R² = 0.23
RMSE = 8.18
UKML
y = 0.35x + 33.59
R² = 0.09
RMSE = 6.36
CAMS
y = 0.17x + 46.40
R² = 0.04
RMSE = 10.52
GEOS
y = 0.09x + 49.26
R² = 0.01
RMSE = 5.17
TCR2
y = 0.09x + 49.06
R² = 0.01
RMSE = 7.33
2011
BME
y = 0.57x + 25.11
R² = 0.43
RMSE = 4.52
NJML
y = 0.31x + 36.02
R² = 0.21
RMSE = 8.64
UKML
y = 0.27x + 39.23
R² = 0.05
RMSE = 6.17
CAMS
y = 0.29x + 40.36
R² = 0.13
RMSE = 7.13
GEOS
y = 0.18x + 45.28
R² = 0.03
RMSE = 5.42
TCR2
y = 0.20x + 43.61
R² = 0.04
RMSE = 5.97
TOAR-II (ppb)
Estimates (ppb)
density

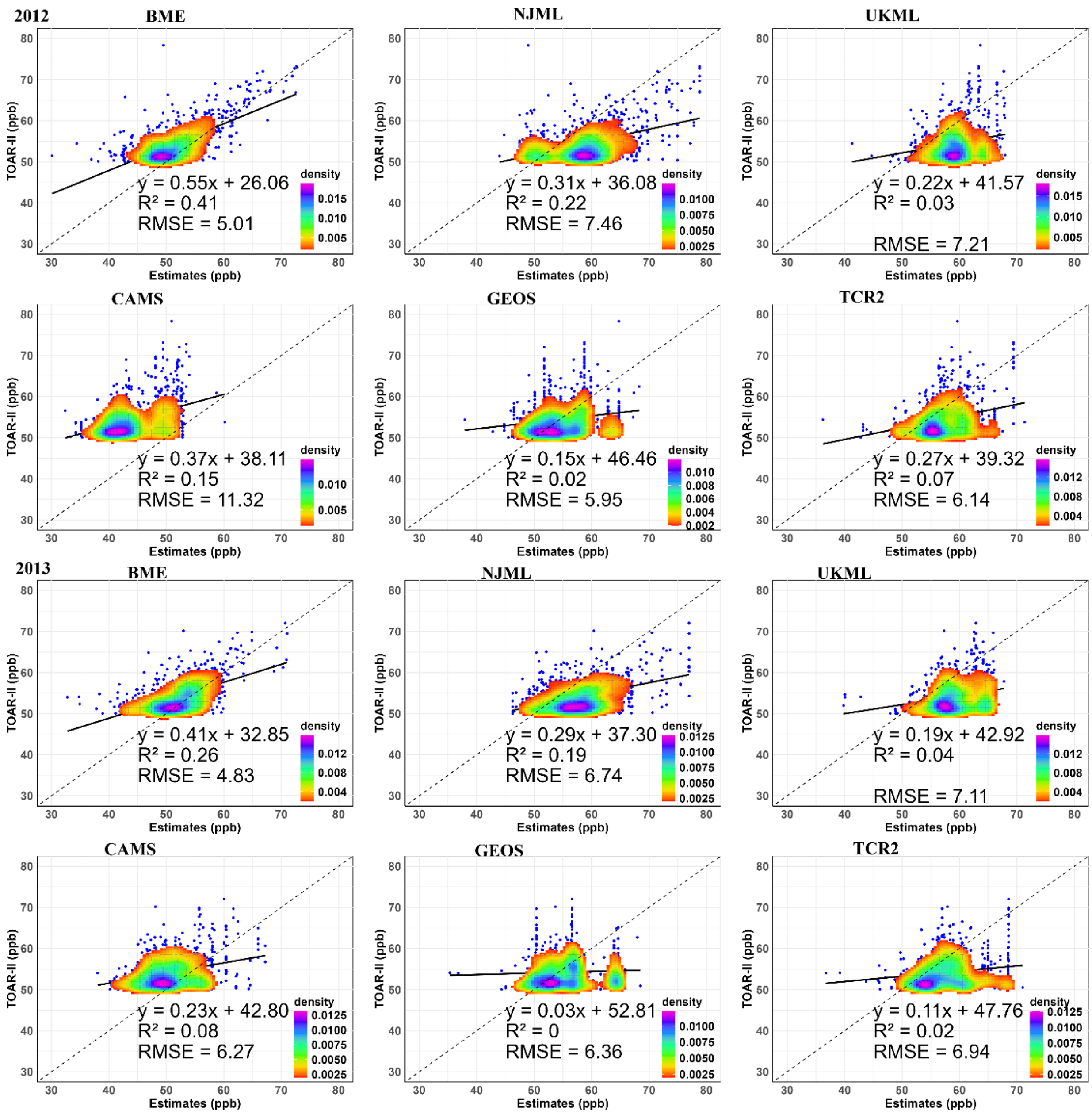

2012
BME
y = 0.55x + 26.06
R² = 0.41
RMSE = 5.01
NJML
y = 0.31x + 36.08
R² = 0.22
RMSE = 7.46
UKML
y = 0.22x + 41.57
R² = 0.03
RMSE = 7.21
CAMS
y = 0.37x + 38.11
R² = 0.15
RMSE = 11.32
GEOS
y = 0.15x + 46.46
R² = 0.02
RMSE = 5.95
TCR2
y = 0.27x + 39.32
R² = 0.07
RMSE = 6.14
2013
BME
y = 0.41x + 32.85
R² = 0.26
RMSE = 4.83
NJML
y = 0.29x + 37.30
R² = 0.19
RMSE = 6.74
UKML
y = 0.19x + 42.92
R² = 0.04
RMSE = 7.11
CAMS
y = 0.23x + 42.80
R² = 0.08
RMSE = 6.27
GEOS
y = 0.03x + 52.81
R² = 0
RMSE = 6.36
TCR2
y = 0.11x + 47.76
R² = 0.02
RMSE = 6.94
density
TOAR-II (ppb)
Estimates (ppb)

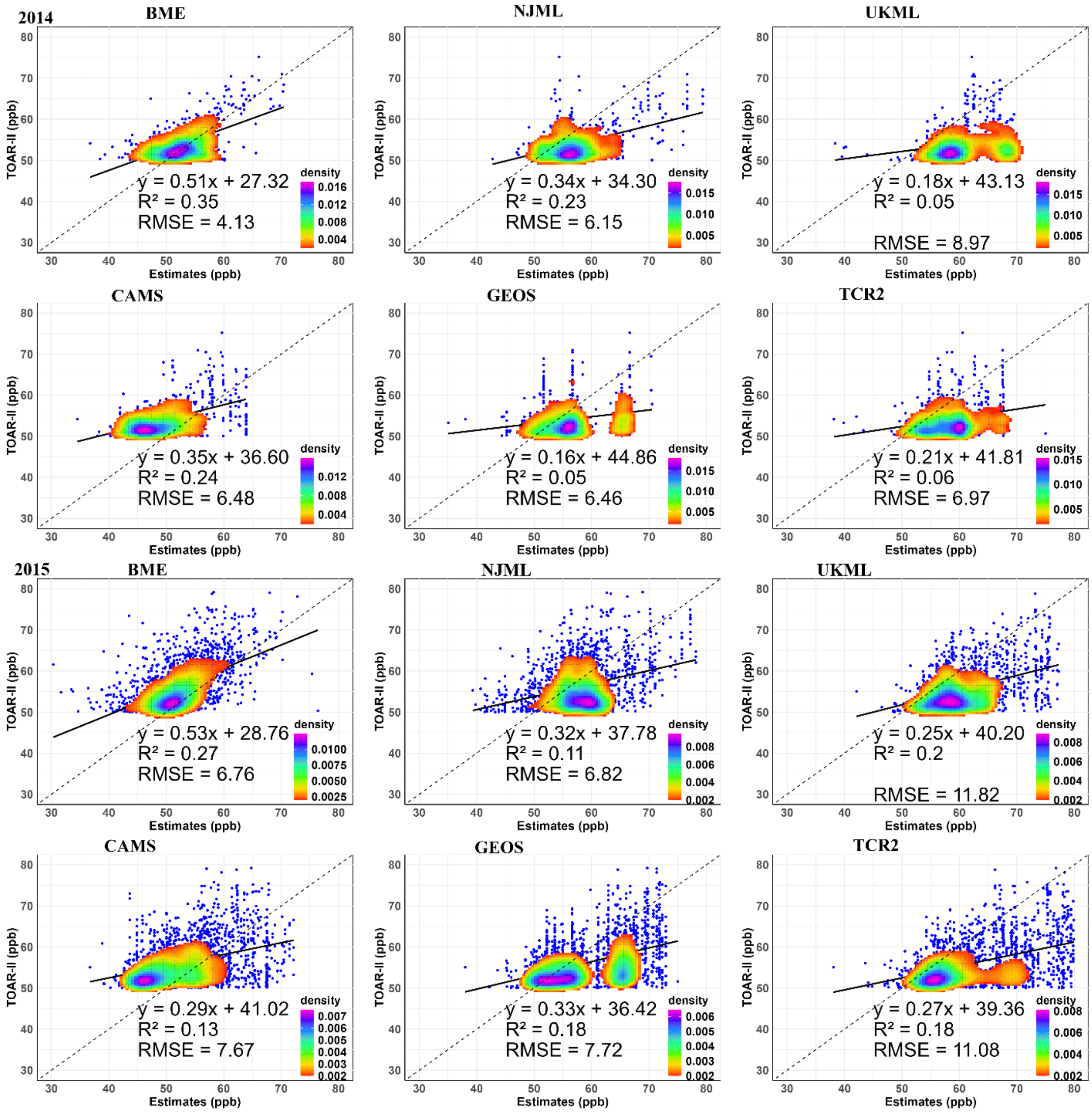
2014
BME
y = 0.51x + 27.32
R² = 0.35
RMSE = 4.13
NJML
y = 0.34x + 34.30
R² = 0.23
RMSE = 6.15
UKML
y = 0.18x + 43.13
R² = 0.05
RMSE = 8.97
CAMS
y = 0.35x + 36.60
R² = 0.24
RMSE = 6.48
GEOS
y = 0.16x + 44.86
R² = 0.05
RMSE = 6.46
TCR2
y = 0.21x + 41.81
R² = 0.06
RMSE = 6.97
2015
BME
y = 0.53x + 28.76
R² = 0.27
RMSE = 6.76
NJML
y = 0.32x + 37.78
R² = 0.11
RMSE = 6.82
UKML
y = 0.25x + 40.20
R² = 0.2
RMSE = 11.82
CAMS
y = 0.29x + 41.02
R² = 0.13
RMSE = 7.67
GEOS
y = 0.33x + 36.42
R² = 0.18
RMSE = 7.72
TCR2
y = 0.27x + 39.36
R² = 0.18
RMSE = 11.08
TOAR-II (ppb)
Estimates (ppb)
density

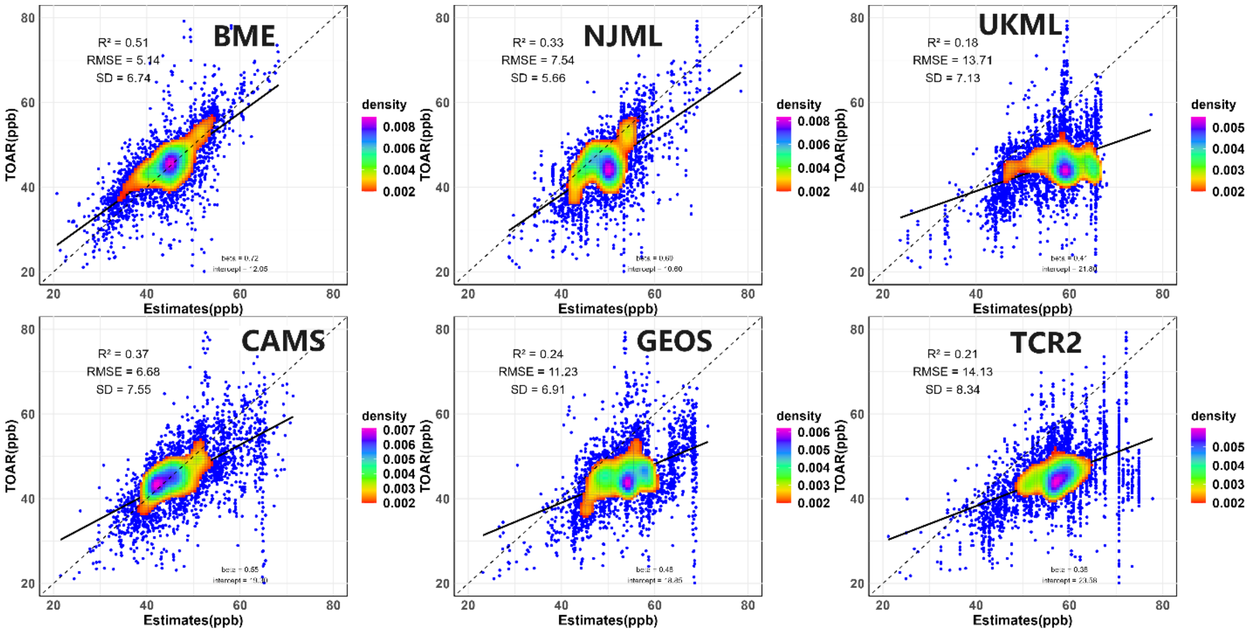

Figure S13. Performance evaluations of six datasets with TOAR-II observations in 2016 for OSDMA8. The evaluation excludes the monitoring stations used as input in BME data fusion in 2016. Location of monitoring stations used as input in BME data fusion in 2016 can be found in Figure S1.

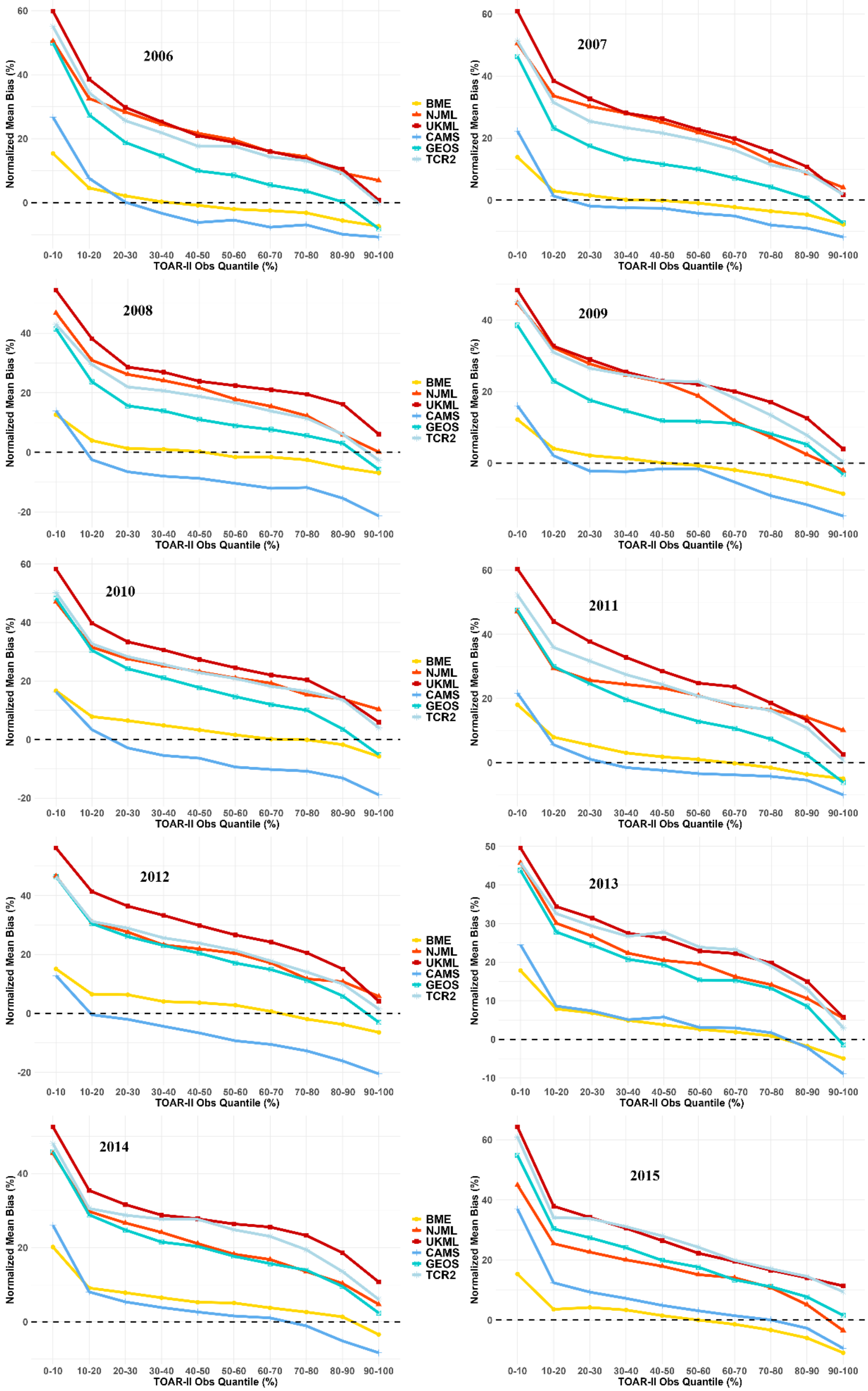
2006
2007
2008
2009
2010
2011
2012
2013
2014
2015
Normalized Mean Bias (%)
TOAR-II Obs Quantile (%)
0-10
10-20
20-30
30-40
40-50
50-60
60-70
70-80
80-90
90-100
BME
NJML
UKML
CAMS
GEOS
TCR2

Figure S14. Normalized mean bias of six databases against TOAR-II observations (OSDMA8) at different quantiles for each year from 2006 to 2015. Different quantiles of TOAR-II observations for each year are shown in Table S9.

References

Global Modeling and Assimilation Office (GMAO) (2015), MERRA-2 instM_2d_gas_Nx: 2d, Monthly mean,Instantaneous, Single-Level, Assimilation, Aerosol Optical Depth Analysis V5.12.4, Greenbelt, MD, USA, Goddard Earth Sciences Data and Information Services Center (GES DISC), Accessed: [*2015*], 10.5067/XOGNBQEPLUC5

Adachi, Y., Yukimoto, S., Deushi, M., Obata, A., Nakano, H., Tanaka, T., Hosaka, M., Sakami, T., Yoshimura, H., Hirabara, M., Shindo, E., Tsujino, H., Mizuta, R., Yabu, S., Koshiro, T., Ose, T., and Kitoh, A.: Basic performance of a new Earth system model of the Meteorological Research Institute (MRI-ESM1), Papers in Meteorology and Geophysics, 64, 1-19, 10.2467/mripapers.64.1, 2013.

Amante, C. and Eakins, B. W.: ETOPO1 Global Relief Model converted to PanMap layer format, PANGAEA [dataset], 10.1594/PANGAEA.769615, 2009.

Archibald, A. T., O'Connor, F. M., Abraham, N. L., Archer-Nicholls, S., Chipperfield, M. P., Dalvi, M., Folberth, G. A., Dennison, F., Dhomse, S. S., Griffiths, P. T., Hardacre, C., Hewitt, A. J., Hill, R. S., Johnson, C. E., Keeble, J., Köhler, M. O., Morgenstern, O., Mulcahy, J. P., Ordóñez, C., Pope, R. J., Rumbold, S. T., Russo, M. R., Savage, N. H., Sellar, A., Stringer, M., Turnock, S. T., Wild, O., and Zeng, G.: Description and evaluation of the UKCA stratosphere–troposphere chemistry scheme (StratTrop vn 1.0) implemented in UKESM1, Geosci. Model Dev., 13, 1223-1266, 10.5194/gmd-13-1223-2020, 2020.

Bentsen, M., Oliviè, D. J. L., Seland, Ø., Toniazzo, T., Gjermundsen, A., Graff, L. S., Debernard, J. B., Gupta, A. K., He, Y., Kirkevåg, A., Schwinger, J., Tjiputra, J., Aas, K. S., Bethke, I., Fan, Y., Griesfeller, J., Grini, A., Guo, C., Ilicak, M., Karset, I. H. H., Landgren, O. A., Liakka, J., Moseid, K. O., Nummelin, A., Spensberger, C., Tang, H., Zhang, Z., Heinze, C., Iversen, T., and Schulz, M.: NCC NorESM2-MM model output prepared for CMIP6 ScenarioMIP ssp245, Earth System Grid Federation [dataset], 10.22033/ESGF/CMIP6.8255, 2019.

Bhartia, P. K., McPeters, R. D., Mateer, C. L., Flynn, L. E., and Wellemeyer, C.: Algorithm for the estimation of vertical ozone profiles from the backscattered ultraviolet technique, Journal of Geophysical Research: Atmospheres, 101, 18793-18806, https://doi.org/10.1029/96JD01165, 1996.

Bishop, C.: Pattern Recognition and Machine Learning, in, 140-155, 10.1117/1.2819119, 2006.

Boersma, K., Eskes, H., Richter, A., De Smedt, I., Lorente, A., Beirle, S., Van Geffen, J., Peters, E., Van Roozendael, M., and Wagner, T.: QA4ECV NO2 tropospheric and stratospheric vertical column data from OMI (Version 1.1)[Data set], Royal Netherlands Meteorological Institute (KNMI), 2017.

Boersma, K. F., Eskes, H. J., and Brinksma, E. J.: Error analysis for tropospheric NO2 retrieval from space, Journal of Geophysical Research: Atmospheres, 109, https://doi.org/10.1029/2003JD003962, 2004.

Boersma, K. F., Eskes, H. J., Dirksen, R. J., van der A, R. J., Veefkind, J. P., Stammes, P., Huijnen, V., Kleipool, Q. L., Sneep, M., Claas, J., Leitão, J., Richter, A., Zhou, Y., and Brunner, D.: An improved tropospheric NO₂ column retrieval algorithm for the Ozone Monitoring Instrument, Atmos. Meas. Tech., 4, 1905-1928, 10.5194/amt-4-1905-2011, 2011.

Bowman, K. W., Rodgers, C. D., Kulawik, S. S., Worden, J., Sarkissian, E., Osterman, G., Steck, T., Ming, L., Eldering, A., Shephard, M., Worden, H., Lampel, M., Clough, S., Brown, P., Rinsland, C., Gunson, M., and Beer, R.: Tropospheric emission spectrometer: retrieval method and error analysis, IEEE Transactions on Geoscience and Remote Sensing, 44, 1297-1307, 10.1109/TGRS.2006.871234, 2006.
Consortium, E. C.-E.: EC-Earth-Consortium EC-Earth3-AerChem model output prepared for CMIP6 CMIP historical, Earth System Grid Federation [dataset], 10.22033/ESGF/CMIP6.4701, 2020.
Atmospheric Chemistry Observations & Modeling, National Center for Atmospheric Research, University Corporation for Atmospheric Research. (2020). CESM2.1 The Community Atmosphere Model with Chemistry (CAM-chem) Outputs as Boundary Conditions. Research Data Archive at the National Center for Atmospheric Research, Computational and Information Systems Laboratory. https://doi.org/10.5065/CKR4-GP38. Accessed 20 November 2024.
Danabasoglu, G.: NCAR CESM2-WACCM model output prepared for CMIP6 CMIP historical, Earth System Grid Federation [dataset], 10.22033/ESGF/CMIP6.10071, 2019.
Deeter, M. N., Edwards, D. P., Francis, G. L., Gille, J. C., Martínez-Alonso, S., Worden, H. M., and Sweeney, C.: A climate-scale satellite record for carbon monoxide: the MOPITT Version 7 product, Atmos. Meas. Tech., 10, 2533-2555, 10.5194/amt-10-2533-2017, 2017.
Deeter, M. N., Martínez-Alonso, S., Edwards, D. P., Emmons, L. K., Gille, J. C., Worden, H. M., Pittman, J. V., Daube, B. C., and Wofsy, S. C.: Validation of MOPITT Version 5 thermal-infrared, near-infrared, and multispectral carbon monoxide profile retrievals for 2000–2011, Journal of Geophysical Research: Atmospheres, 118, 6710-6725, https://doi.org/10.1002/jgrd.50272, 2013.
Deeter, M. N., Martínez-Alonso, S., Edwards, D. P., Emmons, L. K., Gille, J. C., Worden, H. M., Sweeney, C., Pittman, J. V., Daube, B. C., and Wofsy, S. C.: The MOPITT Version 6 product: algorithm enhancements and validation, Atmos. Meas. Tech., 7, 3623-3632, 10.5194/amt-7-3623-2014, 2014.
Doelling, D. R., Sun, M., Nguyen, L. T., Nordeen, M. L., Haney, C. O., Keyes, D. F., and Mlynczak, P. E.: Advances in Geostationary-Derived Longwave Fluxes for the CERES Synoptic (SYN1deg) Product, Journal of Atmospheric and Oceanic Technology, 33, 503-521, https://doi.org/10.1175/JTECH-D-15-0147.1, 2016.
Friedl, M., Sulla-Menashe, D: MCD12C1 MODIS/Terra+Aqua Land Cover Type Yearly L3 Global 0.05Deg CMG V006 [dataset], https://doi.org/10.5067/MODIS/MCD12C1.006, 2015.
Garcia, R. R., Smith, A. K., Kinnison, D. E., Cámara, Á. d. l., and Murphy, D. J.: Modification of the Gravity Wave Parameterization in the Whole Atmosphere Community Climate Model: Motivation and Results, Journal of the Atmospheric Sciences, 74, 275-291, https://doi.org/10.1175/JAS-D-16-0104.1, 2017.
Gettelman, A., Mills, M. J., Kinnison, D. E., Garcia, R. R., Smith, A. K., Marsh, D. R., Tilmes, S., Vitt, F., Bardeen, C. G., McInerny, J., Liu, H.-L., Solomon, S. C., Polvani, L. M., Emmons, L. K., Lamarque, J.-F., Richter, J. H., Glanville, A. S., Bacmeister, J. T., Phillips, A. S., Neale, R. B., Simpson, I. R., DuVivier, A. K., Hodzic, A., and Randel, W. J.: The Whole Atmosphere Community Climate Model Version 6 (WACCM6), Journal of Geophysical Research: Atmospheres, 124, 12380-12403, https://doi.org/10.1029/2019JD030943, 2019.
Good, P., Sellar, A., Tang, Y., Rumbold, S., Ellis, R., Kelley, D., and Kuhlbrodt, T.: MOHC UKESM1.0-LL model output prepared for CMIP6 ScenarioMIP ssp245, Earth System Grid Federation [dataset], 10.22033/ESGF/CMIP6.6339, 2019.

Greg E. Bodeker, S. K., & Jordis S. Tradowsky: BS Filled Total Column Ozone Database V3.4.1 (3.4.1) [dataset], https://doi.org/10.5281/zenodo.7447757, 2022.
Gutjahr, O., Putrasahan, D., Lohmann, K., Jungclaus, J. H., von Storch, J. S., Brüggemann, N., Haak, H., and Stössel, A.: Max Planck Institute Earth System Model (MPI-ESM1.2) for the High-Resolution Model Intercomparison Project (HighResMIP), Geosci. Model Dev., 12, 3241-3281, 10.5194/gmd-12-3241-2019, 2019.
Hao, N., Koukouli, M. E., Inness, A., Valks, P., Loyola, D. G., Zimmer, W., Balis, D. S., Zyrichidou, I., Van Roozendael, M., Lerot, C., and Spurr, R. J. D.: GOME-2 total ozone columns from MetOp-A/MetOp-B and assimilation in the MACC system, Atmos. Meas. Tech., 7, 2937-2951, 10.5194/amt-7-2937-2014, 2014.
Hegglin, M., Kinnison, D., Lamarque, J.-F., and Plummer, D.: CCMI ozone in support of CMIP6 - version 1.0, Earth System Grid Federation [dataset], 10.22033/ESGF/input4MIPs.1115, 2016.
Herman, R. and Kulawik, S.: Tropospheric Emission Spectrometer TES Level 2 (L2) Data User's Guide, D-38042, version 6.0, Jet Propulsion Laboratory, California Institute of Technology, Pasadena, CA, available at: http://tes. jpl. nasa. gov/documents (last access: 30 June 2014), 2013.
Hersbach, H., Bell, B., Berrisford, P., Hirahara, S., Horányi, A., Muñoz Sabater, J., Nicolas, J., Peubey, C., Radu, R., Schepers, D., Simmons, A., Soci, C., Abdalla, S., Abellan, X., Balsamo, G., Bechtold, P., Biavati, G., Bidlot, J., Bonavita, M., and Thépaut, J. N.: The ERA5 global reanalysis, Quarterly Journal of the Royal Meteorological Society, 146, 10.1002/qj.3803, 2020.
Hoesly, R. M., Smith, S. J., Feng, L., Klimont, Z., Janssens-Maenhout, G., Pitkanen, T., Seibert, J. J., Vu, L., Andres, R. J., Bolt, R. M., Bond, T. C., Dawidowski, L., Kholod, N., Kurokawa, J. I., Li, M., Liu, L., Lu, Z., Moura, M. C. P., O'Rourke, P. R., and Zhang, Q.: Historical (1750–2014) anthropogenic emissions of reactive gases and aerosols from the Community Emissions Data System (CEDS), Geosci. Model Dev., 11, 369-408, 10.5194/gmd-11-369-2018, 2018.
Horowitz, L. W., Naik, V., Paulot, F., Ginoux, P. A., Dunne, J. P., Mao, J., Schnell, J., Chen, X., He, J., John, J. G., Lin, M., Lin, P., Malyshev, S., Paynter, D., Shevliakova, E., and Zhao, M.: The GFDL Global Atmospheric Chemistry-Climate Model AM4.1: Model Description and Simulation Characteristics, Journal of Advances in Modeling Earth Systems, 12, e2019MS002032, https://doi.org/10.1029/2019MS002032, 2020.
Horowitz, L. W., Naik, V., Sentman, L., Paulot, F., Blanton, C., McHugh, C., Radhakrishnan, A., Rand, K., Vahlenkamp, H., Zadeh, N. T., Wilson, C., Ginoux, P., He, J., John, J. G., Lin, M., Paynter, D. J., Ploshay, J., Zhang, A., and Zeng, Y.: NOAA-GFDL GFDL-ESM4 model output prepared for CMIP6 AerChemMIP, Earth System Grid Federation [dataset], 10.22033/ESGF/CMIP6.1404, 2018.
Inness, A., Ades, M., Agustí-Panareda, A., Barré, J., Benedictow, A., Blechschmidt, A. M., Dominguez, J. J., Engelen, R., Eskes, H., Flemming, J., Huijnen, V., Jones, L., Kipling, Z., Massart, S., Parrington, M., Peuch, V. H., Razinger, M., Remy, S., Schulz, M., and Suttie, M.: The CAMS reanalysis of atmospheric composition, Atmos. Chem. Phys., 19, 3515-3556, 10.5194/acp-19-3515-2019, 2019.
Janssens-Maenhout, G., Crippa, M., Guizzardi, D., Dentener, F., Muntean, M., Pouliot, G., Keating, T., Zhang, Q., Kurokawa, J., Wankmüller, R., Denier van der Gon, H., Kuenen, J. J. P., Klimont, Z., Frost, G., Darras, S., Koffi, B., and Li, M.: HTAP_v2.2: a mosaic of regional and global emission grid maps for 2008 and 2010 to study hemispheric transport of air pollution, Atmos. Chem. Phys., 15, 11411-11432, 10.5194/acp-15-11411-2015, 2015.
John, J. G., Blanton, C., McHugh, C., Radhakrishnan, A., Rand, K., Vahlenkamp, H., Wilson, C., Zadeh, N. T., Dunne, J. P., Dussin, R., Horowitz, L. W., Krasting, J. P., Lin, P., Malyshev, S.,

Naik, V., Ploshay, J., Shevliakova, E., Silvers, L., Stock, C., Winton, M., and Zeng, Y.: NOAA-GFDL GFDL-ESM4 model output prepared for CMIP6 ScenarioMIP ssp245, Earth System Grid Federation [dataset], 10.22033/ESGF/CMIP6.8686, 2018.
Josse, B., Simon, P., and Peuch, V. H.: Radon global simulations with the multiscale chemistry and transport model MOCAGE, Tellus, Series B: Chemical and Physical Meteorology, 56B, 339-356, 2004.
KOFFI, L. B., DENTENER, F., JANSSENS-MAENHOUT, G., GUIZZARDI, D., CRIPPA, M., DIEHL, T., GALMARINI, S., and SOLAZZO, E.: Hemispheric Transport of Air Pollution (HTAP): Specification of the HTAP2 experiments: Ensuring harmonized modelling, 2016.
Krasting, J. P., John, J. G., Blanton, C., McHugh, C., Nikonov, S., Radhakrishnan, A., Rand, K., Zadeh, N. T., Balaji, V., Durachta, J., Dupuis, C., Menzel, R., Robinson, T., Underwood, S., Vahlenkamp, H., Dunne, K. A., Gauthier, P. P. G., Ginoux, P., Griffies, S. M., Hallberg, R., Harrison, M., Hurlin, W., Malyshev, S., Naik, V., Paulot, F., Paynter, D. J., Ploshay, J., Reichl, B. G., Schwarzkopf, D. M., Seman, C. J., Silvers, L., Wyman, B., Zeng, Y., Adcroft, A., Dunne, J. P., Dussin, R., Guo, H., He, J., Held, I. M., Horowitz, L. W., Lin, P., Milly, P. C. D., Shevliakova, E., Stock, C., Winton, M., Wittenberg, A. T., Xie, Y., and Zhao, M.: NOAA-GFDL GFDL-ESM4 model output prepared for CMIP6 CMIP, Earth System Grid Federation [dataset], 10.22033/ESGF/CMIP6.1407, 2018.
Krotkov, N. A., Lamsal, L. N., Celarier, E. A., Swartz, W. H., Marchenko, S. V., Bucsela, E. J., Chan, K. L., Wenig, M., and Zara, M.: The version 3 OMI NO2 standard product, Atmos. Meas. Tech., 10, 3133-3149, 10.5194/amt-10-3133-2017, 2017.
Krotkov, N. A., McLinden, C. A., Li, C., Lamsal, L. N., Celarier, E. A., Marchenko, S. V., Swartz, W. H., Bucsela, E. J., Joiner, J., and Duncan, B. N.: Aura OMI observations of regional SO 2 and NO 2 pollution changes from 2005 to 2015, Atmospheric Chemistry and Physics, 16, 4605-4629, 2016.
Lerot, C., Van Roozendael, M., van Geffen, J., van Gent, J., Fayt, C., Spurr, R., Lichtenberg, G., and von Bargen, A.: Six years of total ozone column measurements from SCIAMACHY nadir observations, Atmos. Meas. Tech., 2, 87-98, 10.5194/amt-2-87-2009, 2009.
Li, C., Joiner, J., Krotkov, N. A., and Bhartia, P. K.: A fast and sensitive new satellite SO2 retrieval algorithm based on principal component analysis: Application to the ozone monitoring instrument, Geophysical Research Letters, 40, 6314-6318, https://doi.org/10.1002/2013GL058134, 2013.
Lin, M., Horowitz, L., Payton, R., Fiore, A., and Tonnesen, G.: US surface ozone trends and extremes from 1980 to 2014: Quantifying the roles of rising Asian emissions, domestic controls, wildfires, and climate, Atmospheric Chemistry and Physics, 17, 2943-2970, 10.5194/acp-17-2943-2017, 2017.
Lin, W., Yuan, H., Dong, W., Zhang, S., Liu, S., Wei, N., Lu, X., Wei, Z., Hu, Y., and Dai, Y.: Reprocessed MODIS Version 6.1 Leaf Area Index Dataset and Its Evaluation for Land Surface and Climate Modeling, Remote Sensing, 15, 1780, 10.3390/rs15071780, 2023.
Liu, X., Bhartia, P. K., Chance, K., Froidevaux, L., Spurr, R. J. D., and Kurosu, T. P.: Validation of Ozone Monitoring Instrument (OMI) ozone profiles and stratospheric ozone columns with Microwave Limb Sounder (MLS) measurements, Atmos. Chem. Phys., 10, 2539-2549, 10.5194/acp-10-2539-2010, 2010.
Livesey, N., Read, W., Wagner, P., Froidevaux, L., Lambert, A., Manney, G., Valle, L., Pumphrey, H., Santee, M., and Schwartz, M.: Version 4.2 x level 2 data quality and description document, JPL D-33509 Rev, 2017.

Lloyd, C. T., Chamberlain, H., Kerr, D., Yetman, G., Pistolesi, L., Stevens, F. R., Gaughan, A. E., Nieves, J. J., Hornby, G., MacManus, K., Sinha, P., Bondarenko, M., Sorichetta, A., and Tatem, A. J.: Global spatio-temporally harmonised datasets for producing high-resolution gridded population distribution datasets, Big Earth Data, 3, 108-139, 10.1080/20964471.2019.1625151, 2019.
Lu, X., Hong, J., Zhang, L., Cooper, O. R., Schultz, M. G., Xu, X., Wang, T., Gao, M., Zhao, Y., and Zhang, Y.: Severe Surface Ozone Pollution in China: A Global Perspective, Environmental Science & Technology Letters, 5, 487-494, 10.1021/acs.estlett.8b00366, 2018.
Marsh, D. R., Mills, M. J., Kinnison, D. E., Lamarque, J.-F., Calvo, N., and Polvani, L. M.: Climate Change from 1850 to 2005 Simulated in CESM1(WACCM), Journal of Climate, 26, 7372-7391, https://doi.org/10.1175/JCLI-D-12-00558.1, 2013.
McPeters, R. D., Bhartia, P. K., Haffner, D., Labow, G. J., and Flynn, L.: The version 8.6 SBUV ozone data record: An overview, Journal of Geophysical Research: Atmospheres, 118, 8032-8039, https://doi.org/10.1002/jgrd.50597, 2013.
Mulcahy, J. P., Jones, C., Sellar, A., Johnson, B., Boutle, I. A., Jones, A., Andrews, T., Rumbold, S. T., Mollard, J., Bellouin, N., Johnson, C. E., Williams, K. D., Grosvenor, D. P., and McCoy, D. T.: Improved Aerosol Processes and Effective Radiative Forcing in HadGEM3 and UKESM1, Journal of Advances in Modeling Earth Systems, 10, 2786-2805, https://doi.org/10.1029/2018MS001464, 2018.
Neubauer, D., Ferrachat, S., Siegenthaler-Le Drian, C., Stoll, J., Folini, D. S., Tegen, I., Wieners, K.-H., Mauritsen, T., Stemmler, I., Barthel, S., Bey, I., Daskalakis, N., Heinold, B., Kokkola, H., Partridge, D., Rast, S., Schmidt, H., Schutgens, N., Stanelle, T., Stier, P., Watson-Parris, D., and Lohmann, U.: HAMMOZ-Consortium MPI-ESM1.2-HAM model output prepared for CMIP6 CMIP, Earth System Grid Federation [dataset], 10.22033/ESGF/CMIP6.1622, 2019.
Qu, Z., Daven, K. H., Owen, R. C., and Jessica, L. N.: Global (2°x2.5°) top-down NOx emissions from OMI DOMINO product (2005-2016) (V1), Harvard Dataverse [dataset], doi:10.7910/DVN/QBAQZA, 2020a.
Qu, Z., Daven, K. H., Owen, R. C., and Jessica, L. N.: Global (2°x2.5°) top-down NOx emissions from OMI NASA product (2005-2016) (V1), Harvard Dataverse [dataset], doi:10.7910/DVN/HVT1FO, 2020b.
Qu, Z., Henze, D. K., Capps, S. L., Wang, Y., Xu, X., Wang, J., and Keller, M.: Monthly top-down NOx emissions for China (2005–2012): A hybrid inversion method and trend analysis, Journal of Geophysical Research: Atmospheres, 122, 4600-4625, https://doi.org/10.1002/2016JD025852, 2017.
Schultz, M. G., Schröder, S., Lyapina, O., Cooper, O. R., Galbally, I., Petropavlovskikh, I., von Schneidemesser, E., Tanimoto, H., Elshorbany, Y., Naja, M., Seguel, R. J., Dauert, U., Eckhardt, P., Feigenspan, S., Fiebig, M., Hjellbrekke, A.-G., Hong, Y.-D., Kjeld, P. C., Koide, H., Lear, G., Tarasick, D., Ueno, M., Wallasch, M., Baumgardner, D., Chuang, M.-T., Gillett, R., Lee, M., Molloy, S., Moolla, R., Wang, T., Sharps, K., Adame, J. A., Ancellet, G., Apadula, F., Artaxo, P., Barlasina, M. E., Bogucka, M., Bonasoni, P., Chang, L., Colomb, A., Cuevas-Agulló, E., Cupeiro, M., Degorska, A., Ding, A., Fröhlich, M., Frolova, M., Gadhavi, H., Gheusi, F., Gilge, S., Gonzalez, M. Y., Gros, V., Hamad, S. H., Helmig, D., Henriques, D., Hermansen, O., Holla, R., Hueber, J., Im, U., Jaffe, D. A., Komala, N., Kubistin, D., Lam, K.-S., Laurila, T., Lee, H., Levy, I., Mazzoleni, C., Mazzoleni, L. R., McClure-Begley, A., Mohamad, M., Murovec, M., Navarro-Comas, M., Nicodim, F., Parrish, D., Read, K. A., Reid, N., Ries, L., Saxena, P., Schwab, J. J., Scorgie, Y., Senik, I., Simmonds, P., Sinha, V., Skorokhod, A. I., Spain, G., Spangl,

W., Spoor, R., Springston, S. R., Steer, K., Steinbacher, M., Suharguniyawan, E., Torre, P., Trickl, T., Weili, L., Weller, R., Xiaobin, X., Xue, L., and Zhiqiang, M.: Tropospheric Ozone Assessment Report: Database and metrics data of global surface ozone observations, Elementa: Science of the Anthropocene, 5, 10.1525/elementa.244, 2017.
Schupfner, M., Wieners, K.-H., Wachsmann, F., Steger, C., Bittner, M., Jungclaus, J., Früh, B., Pankatz, K., Giorgetta, M., Reick, C., Legutke, S., Esch, M., Gayler, V., Haak, H., de Vrese, P., Raddatz, T., Mauritsen, T., von Storch, J.-S., Behrens, J., Brovkin, V., Claussen, M., Crueger, T., Fast, I., Fiedler, S., Hagemann, S., Hohenegger, C., Jahns, T., Kloster, S., Kinne, S., Lasslop, G., Kornblueh, L., Marotzke, J., Matei, D., Meraner, K., Mikolajewicz, U., Modali, K., Müller, W., Nabel, J., Notz, D., Peters-von Gehlen, K., Pincus, R., Pohlmann, H., Pongratz, J., Rast, S., Schmidt, H., Schnur, R., Schulzweida, U., Six, K., Stevens, B., Voigt, A., and Roeckner, E.: DKRZ MPI-ESM1.2-HR model output prepared for CMIP6 ScenarioMIP ssp245, Earth System Grid Federation [dataset], 10.22033/ESGF/CMIP6.4398, 2019.
Schwartz, M., Froidevaux, L., Livesey, N. and Read, W: MLS/Aura Level 2 Ozone (O3) Mixing Ratio V004 [dataset], 10.5067/Aura/MLS/DATA2017, 2015.
Seland, Ø., Bentsen, M., Olivié, D. J. L., Toniazzo, T., Gjermundsen, A., Graff, L. S., Debernard, J. B., Gupta, A. K., He, Y., Kirkevåg, A., Schwinger, J., Tjiputra, J., Aas, K. S., Bethke, I., Fan, Y., Griesfeller, J., Grini, A., Guo, C., Ilicak, M., Karset, I. H. H., Landgren, O. A., Liakka, J., Moseid, K. O., Nummelin, A., Spensberger, C., Tang, H., Zhang, Z., Heinze, C., Iversen, T., and Schulz, M.: NCC NorESM2-LM model output prepared for CMIP6 CMIP historical, Earth System Grid Federation [dataset], 10.22033/ESGF/CMIP6.8036, 2019.
Sellar, A. A., Jones, C. G., Mulcahy, J. P., Tang, Y., Yool, A., Wiltshire, A., O'Connor, F. M., Stringer, M., Hill, R., Palmieri, J., Woodward, S., de Mora, L., Kuhlbrodt, T., Rumbold, S. T., Kelley, D. I., Ellis, R., Johnson, C. E., Walton, J., Abraham, N. L., Andrews, M. B., Andrews, T., Archibald, A. T., Berthou, S., Burke, E., Blockley, E., Carslaw, K., Dalvi, M., Edwards, J., Folberth, G. A., Gedney, N., Griffiths, P. T., Harper, A. B., Hendry, M. A., Hewitt, A. J., Johnson, B., Jones, A., Jones, C. D., Keeble, J., Liddicoat, S., Morgenstern, O., Parker, R. J., Predoi, V., Robertson, E., Siahaan, A., Smith, R. S., Swaminathan, R., Woodhouse, M. T., Zeng, G., and Zerroukat, M.: UKESM1: Description and Evaluation of the U.K. Earth System Model, Journal of Advances in Modeling Earth Systems, 11, 4513-4558, https://doi.org/10.1029/2019MS001739, 2019.
Sellar, A. A., Walton, J., Jones, C. G., Wood, R., Abraham, N. L., Andrejczuk, M., Andrews, M. B., Andrews, T., Archibald, A. T., de Mora, L., Dyson, H., Elkington, M., Ellis, R., Florek, P., Good, P., Gohar, L., Haddad, S., Hardiman, S. C., Hogan, E., Iwi, A., Jones, C. D., Johnson, B., Kelley, D. I., Kettleborough, J., Knight, J. R., Köhler, M. O., Kuhlbrodt, T., Liddicoat, S., Linova-Pavlova, I., Mizielinski, M. S., Morgenstern, O., Mulcahy, J., Neininger, E., O'Connor, F. M., Petrie, R., Ridley, J., Rioual, J.-C., Roberts, M., Robertson, E., Rumbold, S., Seddon, J., Shepherd, H., Shim, S., Stephens, A., Teixiera, J. C., Tang, Y., Williams, J., Wiltshire, A., and Griffiths, P. T.: Implementation of U.K. Earth System Models for CMIP6, Journal of Advances in Modeling Earth Systems, 12, e2019MS001946, https://doi.org/10.1029/2019MS001946, 2020.
Shindell, D. T., Pechony, O., Voulgarakis, A., Faluvegi, G., Nazarenko, L., Lamarque, J. F., Bowman, K., Milly, G., Kovari, B., Ruedy, R., and Schmidt, G. A.: Interactive ozone and methane chemistry in GISS-E2 historical and future climate simulations, Atmos. Chem. Phys., 13, 2653-2689, 10.5194/acp-13-2653-2013, 2013.

Strode, S. A., Ziemke, J. R., Oman, L. D., Lamsal, L. N., Olsen, M. A., and Liu, J.: Global changes in the diurnal cycle of surface ozone, Atmospheric Environment, 199, 323-333, https://doi.org/10.1016/j.atmosenv.2018.11.028, 2019.
Studies, N. G. I. f. S.: NASA-GISS GISS-E2.1H model output prepared for CMIP6 CMIP, Earth System Grid Federation [dataset], 10.22033/ESGF/CMIP6.1421, 2018a.
Studies, N. G. I. f. S.: NASA-GISS GISS-E2.1G model output prepared for CMIP6 CMIP, Earth System Grid Federation [dataset], 10.22033/ESGF/CMIP6.1400, 2018b.
Studies, N. G. I. f. S.: NASA-GISS GISS-E2.1G model output prepared for CMIP6 ScenarioMIP ssp245, Earth System Grid Federation [dataset], 10.22033/ESGF/CMIP6.7415, 2020.
Sudo, K., Takahashi, M., and Akimoto, H.: CHASER: A global chemical model of the troposphere 2. Model results and evaluation, Journal of Geophysical Research: Atmospheres, 107, ACH 9-1-ACH 9-39, https://doi.org/10.1029/2001JD001114, 2002.
Tang, Y., Rumbold, S., Ellis, R., Kelley, D., Mulcahy, J., Sellar, A., Walton, J., and Jones, C.: MOHC UKESM1.0-LL model output prepared for CMIP6 CMIP historical, Earth System Grid Federation [dataset], 10.22033/ESGF/CMIP6.6113, 2019.
Teyssèdre, H., Michou, M., Clark, H. L., Josse, B., Karcher, F., Olivié, D., Peuch, V. H., Saint-Martin, D., Cariolle, D., Attié, J. L., Nédélec, P., Ricaud, P., Thouret, V., van der A, R. J., Volz-Thomas, A., and Chéroux, F.: A new tropospheric and stratospheric Chemistry and Transport Model MOCAGE-Climat for multi-year studies: evaluation of the present-day climatology and sensitivity to surface processes, Atmos. Chem. Phys., 7, 5815-5860, 10.5194/acp-7-5815-2007, 2007.
Tilmes, S., Lamarque, J. F., Emmons, L. K., Kinnison, D. E., Ma, P. L., Liu, X., Ghan, S., Bardeen, C., Arnold, S., Deeter, M., Vitt, F., Ryerson, T., Elkins, J. W., Moore, F., Spackman, J. R., and Val Martin, M.: Description and evaluation of tropospheric chemistry and aerosols in the Community Earth System Model (CESM1.2), Geosci. Model Dev., 8, 1395-1426, 10.5194/gmd-8-1395-2015, 2015.
von Clarmann, T., Höpfner, M., Kellmann, S., Linden, A., Chauhan, S., Funke, B., Grabowski, U., Glatthor, N., Kiefer, M., Schieferdecker, T., Stiller, G. P., and Versick, S.: Retrieval of temperature, H₂O, O₃, HNO₃, CH₄, N₂O, ClONO₂ and ClO from MIPAS reduced resolution nominal mode limb emission measurements, Atmos. Meas. Tech., 2, 159-175, 10.5194/amt-2-159-2009, 2009.
von Storch, J.-S., Putrasahan, D., Lohmann, K., Gutjahr, O., Jungclaus, J., Bittner, M., Haak, H., Wieners, K.-H., Giorgetta, M., Reick, C., Esch, M., Gayler, V., de Vrese, P., Raddatz, T., Mauritsen, T., Behrens, J., Brovkin, V., Claussen, M., Crueger, T., Fast, I., Fiedler, S., Hagemann, S., Hohenegger, C., Jahns, T., Kloster, S., Kinne, S., Lasslop, G., Kornblueh, L., Marotzke, J., Matei, D., Meraner, K., Mikolajewicz, U., Modali, K., Müller, W., Nabel, J., Notz, D., Peters-von Gehlen, K., Pincus, R., Pohlmann, H., Pongratz, J., Rast, S., Schmidt, H., Schnur, R., Schulzweida, U., Six, K., Stevens, B., Voigt, A., and Roeckner, E.: MPI-M MPIESM1.2-HR model output prepared for CMIP6 HighResMIP, Earth System Grid Federation [dataset], 10.22033/ESGF/CMIP6.762, 2017.
Watanabe, S., Hajima, T., Sudo, K., Nagashima, T., Takemura, T., Okajima, H., Nozawa, T., Kawase, H., Abe, M., Yokohata, T., Ise, T., Sato, H., Kato, E., Takata, K., Emori, S., and Kawamiya, M.: MIROC-ESM 2010: model description and basic results of CMIP5-20c3m experiments, Geosci. Model Dev., 4, 845-872, 10.5194/gmd-4-845-2011, 2011.

Wu, T., Zhang, F., Zhang, J., Jie, W., Zhang, Y., Wu, F., Li, L., Yan, J., Liu, X., Lu, X., Tan, H., Zhang, L., Wang, J., and Hu, A.: Beijing Climate Center Earth System Model version 1 (BCC-ESM1): model description and evaluation of aerosol simulations, Geosci. Model Dev., 13, 977-1005, 10.5194/gmd-13-977-2020, 2020.
Wu, T., Yu, R., Lu, Y., Jie, W., Fang, Y., Zhang, J., Zhang, L., Xin, X., Li, L., Wang, Z., Liu, Y., Zhang, F., Wu, F., Chu, M., Li, J., Li, W., Zhang, Y., Shi, X., Zhou, W., Yao, J., Liu, X., Zhao, H., Yan, J., Wei, M., Xue, W., Huang, A., Zhang, Y., Zhang, Y., Shu, Q., and Hu, A.: BCC-CSM2-HR: a high-resolution version of the Beijing Climate Center Climate System Model, Geosci. Model Dev., 14, 2977-3006, 10.5194/gmd-14-2977-2021, 2021.
Yool, A., Palmiéri, J., Jones, C. G., Sellar, A. A., de Mora, L., Kuhlbrodt, T., Popova, E. E., Mulcahy, J. P., Wiltshire, A., Rumbold, S. T., Stringer, M., Hill, R. S. R., Tang, Y., Walton, J., Blaker, A., Nurser, A. J. G., Coward, A. C., Hirschi, J., Woodward, S., Kelley, D. I., Ellis, R., and Rumbold-Jones, S.: Spin-up of UK Earth System Model 1 (UKESM1) for CMIP6, Journal of Advances in Modeling Earth Systems, 12, e2019MS001933, https://doi.org/10.1029/2019MS001933, 2020.
Yukimoto, S., Koshiro, T., Kawai, H., Oshima, N., Yoshida, K., Urakawa, S., Tsujino, H., Deushi, M., Tanaka, T., Hosaka, M., Yoshimura, H., Shindo, E., Mizuta, R., Ishii, M., Obata, A., and Adachi, Y.: MRI MRI-ESM2.0 model output prepared for CMIP6 ScenarioMIP ssp245, Earth System Grid Federation [dataset], 10.22033/ESGF/CMIP6.6910, 2019a.
Yukimoto, S., Adachi, Y., Hosaka, M., Sakami, T., Yoshimura, H., Hirabara, M., Tanaka, T. Y., Shindo, E., Tsujino, H., Deushi, M., Mizuta, R., Yabu, S., Obata, A., Nakano, H., Koshiro, T., Ose, T., and Kitoh, A.: A New Global Climate Model of the Meteorological Research Institute: MRI-CGCM3 —Model Description and Basic Performance&mdash, Journal of the Meteorological Society of Japan. Ser. II, 90A, 23-64, 10.2151/jmsj.2012-A02, 2012.
Yukimoto, S., Kawai, H., Koshiro, T., Oshima, N., Yoshida, K., Urakawa, S., Tsujino, H., Deushi, M., Tanaka, T., Hosaka, M., Yabu, S., Yoshimura, H., Shindo, E., Mizuta, R., Obata, A., Adachi, Y., and Ishii, M.: The Meteorological Research Institute Earth System Model Version 2.0, MRI-ESM2.0: Description and Basic Evaluation of the Physical Component, Journal of the Meteorological Society of Japan. Ser. II, 97, 931-965, 10.2151/jmsj.2019-051, 2019b.
Yukimoto, S., Kawai, H., Koshiro, T., Oshima, N., Yoshida, K., Urakawa, S., Tsujino, H., Deushi, M., Tanaka, T., Hosaka, M., Yabu, S., Yoshimura, H., Shindo, E., Mizuta, R., Obata, A., Adachi, Y., and Ishii, M.: The Meteorological Research Institute Earth System Model Version 2.0, MRI-ESM2.0: Description and Basic Evaluation of the Physical Component, Journal of the Meteorological Society of Japan, 97, 10.2151/jmsj.2019-051, 2019c.
Zhang, J., Wu, T., Shi, X., Zhang, F., Li, J., Chu, M., Liu, Q., Yan, J., Ma, Q., and Wei, M.: BCC BCC-ESM1 model output prepared for CMIP6 CMIP, Earth System Grid Federation [dataset], 10.22033/ESGF/CMIP6.1734, 2018.
Zhang, L., Lin, M., Langford, A. O., Horowitz, L. W., Senff, C. J., Klovenski, E., Wang, Y., Alvarez Ii, R. J., Petropavlovskikh, I., Cullis, P., Sterling, C. W., Peischl, J., Ryerson, T. B., Brown, S. S., Decker, Z. C. J., Kirgis, G., and Conley, S.: Characterizing sources of high surface ozone events in the southwestern US with intensive field measurements and two global models, Atmos. Chem. Phys., 20, 10379-10400, 10.5194/acp-20-10379-2020, 2020.
Ziemke, J. R., Oman, L. D., Strode, S. A., Douglass, A. R., Olsen, M. A., McPeters, R. D., Bhartia, P. K., Froidevaux, L., Labow, G. J., Witte, J. C., Thompson, A. M., Haffner, D. P., Kramarova, N. A., Frith, S. M., Huang, L. K., Jaross, G. R., Seftor, C. J., Deland, M. T., and Taylor, S. L.: Trends in global tropospheric ozone inferred from a composite record of

TOMS/OMI/MLS/OMPS satellite measurements and the MERRA-2 GMI simulation, Atmos. Chem. Phys., 19, 3257-3269, 10.5194/acp-19-3257-2019, 2019.